TITLE:

Sedimentary Environment and Basin Analyses of the Miocene Kumano Group in the Kii Peninsula, Southwest Japan

AUTHOR(S):

Hisatomi, Kunihiko

CITATION:

Hisatomi, Kunihiko. Sedimentary Environment and Basin Analyses of the Miocene Kumano Group in the Kii Peninsula, Southwest Japan. Memoirs of the Faculty of Science, Kyoto University. Series of geology and mineralogy 1984, 50(1-2): 1-65

ISSUE DATE:

1984-03-25

URL:

http://hdl.handle.net/2433/186653

RIGHT:

京都大学学術情報リポジトリ
KURENAI 紅
Kyoto University Research Information Repository

MEMOIRS OF THE FACULTY OF SCIENCE, KYOTO UNIVERSITY, SERIES OF GEOL. & MINERAL.,
Vol. L, Nos. 1 & 2, pp. 1-65, Pls. 1-4, 1984

Sedimentary Environment and Basin Analyses of the Miocene Kumano Group in the Kii Peninsula, Southwest Japan

By

Kunihiko HISATOMI*

(Received January 11, 1984)

Contents

* Present address: Institute of Earth Science, Faculty of Education, Wakayama Univ., Wakayama City.

Abstract

The Lower to Middle Miocene Kumano Group in the southeastern part of the Kii Peninsula makes a thick sedimentary pile, consisting of mudstone and muddy alternation of sandstone and mudstone. A special attention was paid to the genesis of such fine-grained clastic rock piles and the reconstruction of the sedimentary basin.

The Kumano Group is lithologically divided into three formations, namely, the Shimosato, the Shikiya and the Mitsuno Formations in ascending order. The sedimentological analyses were made on the former two formations which are predominant in fine-grained clastic materials.

First, based on the analyses on the various sedimentary features of muddy alternation and bedded mudstone, such as thickness distribution, mud-sand ratio, bedding type, internal sedimentary structures and combination of sedimentary divisions, it is concluded that most of these fine-grained materials have been transported and deposited by a low-density current and partly by a tractional current.

A morphological reconstruction of the Kumano basin was attempted by paleocurrent analysis through various kinds of current marks, cross lamination and grain-orientation and by paleoslope analysis through slump structure and debris flow deposits. As the results, the Kumano basin in the study area which occupies a southern part of the basin is revealed to have located on the southward inclining slope and slope-basin bordered by the upheaval zone related to magmatism to the south. On the other hand, the Kumano Group in the northern part is known to be of the shallow marine origin and that of the central part in between is much thinner in thickness than in the other two areas suggesting a topographic high of this region. Thus the whole Kumano basin is concluded to have comprised topographically the shelf, the shelf edge high, the slope, the slope-basin, and the outer upheaval zone (the outer ridge), from north to south. Such a situation is very similar to that of the present forearc region in Southwest Japan, though it was located more northward than the latter.

Introduction

The Lower to Middle Miocene Kumano Group crops out extensively in the southeastern part of the Kii Peninsula, overlying the Cretaceous to Lowest Miocene Shimanto Supergroup with a remarkable clino-unconformity (Fig. 1). It consists dominantly of mudstone and muddy alternation of sandstone and mudstone.

The general stratigraphy of the Kumano Group was first established by TANAI and MIZUNO (1954) and MIZUNO (1957). The present author has been engaged in the stratigraphic and sedimentological studies on the Kumano Group in the southern part of its distribution.

The group in the study area is characterized by the predominance of muddy materials. However, on the formation processes of thick sequence of fine-grained clastics, the detailed studies have been few in comparison with the energetic studies on the sandy or gravelly submarine fan deposits in the world (e.g. WALKER and MUTTI, 1973). The Kumano Group offers a good example to study thick sequence of muddy materials. Therefore, the sedimentological study on the Kumano Group will contribute to the consideration on the origin of such thick, muddy sedimentary piles.

Adding to this, it is important to reconstruct the sedimentary environments of

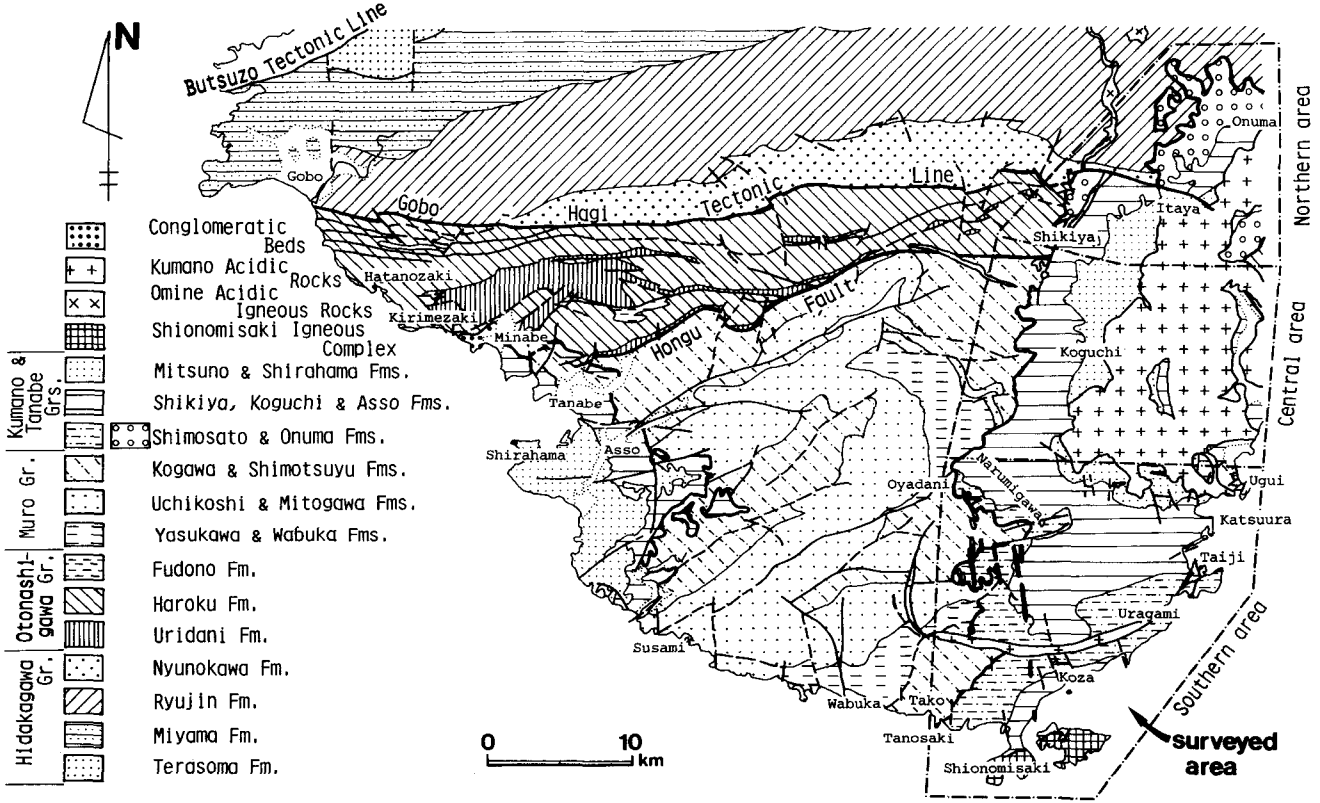

Fig. 1. Generalized geological map of the Shimanto Terrain in the Kii Peninsula. Compiled from HATENASHI RESEARCH GROUP (1980), HISATOMI (1981), SAEKI and KOTO (1972), SUZUKI *et al.* (1979), TATEISHI *et al.* (1979) and TOKUOKA *et al.* (1981).

the Kumano Group in detail to consider the geologic development of the Outer Zone of Southwest Japan in Miocene age, because no sedimentological studies have been made on the Neogene basins in the Outer Zone of Southwest Japan.

In this paper, the sedimentological analyses and the discussions will be made on muddy alternation of sandstone and mudstone, bedded mudstone and angular clast-bearing mudstone, all of which comprise the most part of the group in the area.

The main purposes of this paper are (1) to clarify the transportation and sedimentation mechanisms of the fine-grained clastic materials, and (2) to reconstruct the sedimentary evnironments of the Kumano sedimentary basin in detail.

I. General Geology

In the Kii Peninsula, the Shimanto Supergroup is widely distributed in the Shimanto Terrain situated on the south of the Butsuzo Tectonic Line (Fig. 1). The Shimanto Supergroup is divided into three groups, namely, the Cretaceous Hidakagawa, the Eocene? Otonashigawa and the Oligocene to earliest Miocene Muro Groups (KISHU SHIMANTO RESEARCH GROUP, 1975).

The Hidakagawa Group, more than 13,000 m in cumulative thickness, is composed of shale, sandstone, basaltic lava, hyaloclastite, chert and acidic tuff. The Otonashigawa Group, 1,950 m thick, is composed of mudstone, alternation of sandstone and mudstone, sandstone and conglomerate. The Muro Group, 7,500–9,000 m in cumulative thickness, consists of sandstone, alternation of sandstone and mudstone, mudstone, conglomerate and angular clast-bearing mudstone.

The strata of the Shimanto Supergroup are severely deformed by many E–W trending faults and folds.

With a remarkable clino-unconformity, the Lower to Middle Miocene strata overlie the Shimanto Supergroup. The strata in the southeastern part of the Kii Peninsula are called the Kumano Group (TANAI and MIZUNO, 1954), and those in the southwestern part of the peninsula the Tanabe Group (SHINAGAWA, 1958MS, MATSUHITA, 1971).

The Kumano Group is composed of mudstone, sandstone and a small amount of conglomerate and angular clast-bearing mudstone, attaining to 1,500 to 4,000 m in total thickness. The group partly interfingers with the Shionomisaki Igneous Complex at the southernmost part of its distribution, and is intruded by the Kumano Acidic Rocks and the Omine Acidic Igneous Rocks (Fig. 1). The detailed descriptions on the geology of the Kumano Group will be made in the next chapter.

The Tanabe Group, correlative to the Kumano Group, is about 1,400 m in total thickness. It is composed of mudstone, muddy alternation of sandstone and mudstone, massive sandstone, breccia and conglomerate (TERAI and TANABE RESEARCH GROUP, 1982). The group is lithologically divided into two formations, namely, the

Asso (lower) and the Shirahama (upper) Formations.

The geological age of the group is in the upper part of Blow's N8 based on the planktonic foraminifers (SASAKI, 1981MS). The E–W trending gentle folds are developed in the group. The gentle dip of the strata shows a distinctive contrast to the steeply dipping, severely folded Shimanto Supergroup.

The Shionomisaki Igneous Complex (MIYAKE, 1981) is a volcano-plutonic igneous complex comprising both acidic and basic rocks. The effusive rocks of the complex are rhyolitic pyroclastic rocks and basaltic lava, and the intrusive rocks are gabbro, dolerite, granophyre, quartz porphyry and hypersthene rhyolite. The interbedded relation between the effusive rocks and mudstone of the Shikiya Formation is observed at the northeastern coast of the Shionomisaki. Therefore, the activity of the complex is safely assigned to the latest Early Miocene (HISATOMI and MIYAKE, 1981).

In the southeastern and the central part of the Kii Peninsula, aicdic ingeous rocks are distributed. They are the Kumano Acidic Rocks (ARAMAKI and HADA, 1965) and the Omine Acidic Igneous Rokcs (SAEKI and KOTO, 1972), both of which are the constituents of the "Southwest Outer Zone Petrologic Province" (SHIBATA, 1962). The Kumano Acidic Rocks consist of granite porphyry, rhyolite and acidic pyroclastic dykes. They intruded into the Kumano Group. The K–Ar age of them is 14.1±0.3 my (KAWANO and UEDA, 1969). The Omine Acidic Igneous Rocks are composed of quartz porphyry and granite, and also intruded into the Kumano Group (Report of METAL MINING AGENCY, 1979).

II. Geology of the Kumano Group

The Kumano Group was first defined by TANAI and MIZUNO (1954) in the central part of its distribution. The general stratigraphy of the group was established by A. MIZUNO and his colleagues (MIZUNO, 1957; MURAYAMA, 1954; MIZUNO and IMAI, 1964; HIROKAWA and MIZUNO, 1965). In these studies, it was pointed out that the lithology and the thickness of the group vary from north to south. Therefore, the stratigraphy will be described separately in three areas, that is, the northern, the central and the southern areas (Fig. 1). The stratigraphic relation among these areas are summarized in Table 1.

Table 1. Stratigraphic relation of the Kumano Group in three areas.

	Northern area	Central area	Southern area
Kumano Group	Mitsuno Formation		
	Koguchi Formation		Shikiya Formation
	Onuma Formation		Shimosato Formation

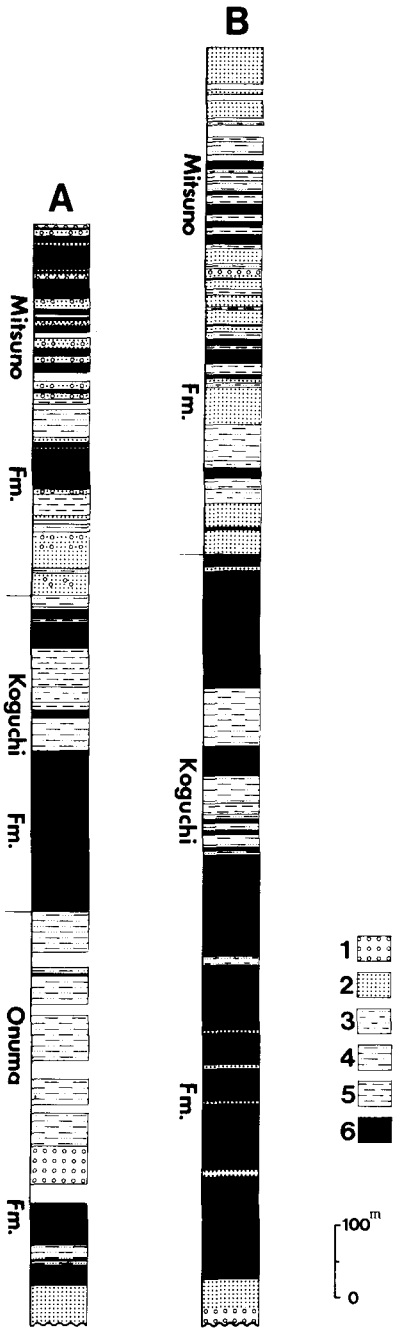

Fig. 2. Columnar sections of the Kumano Group in the northern area (A) and in the central area (B). Modified from CHIJIWA and TOMITA (1981). 1: conglomerate, 2: sandstone, 3: sandy alternation, 4: normal alternation, 5: muddy alternation, 6: mudstone.

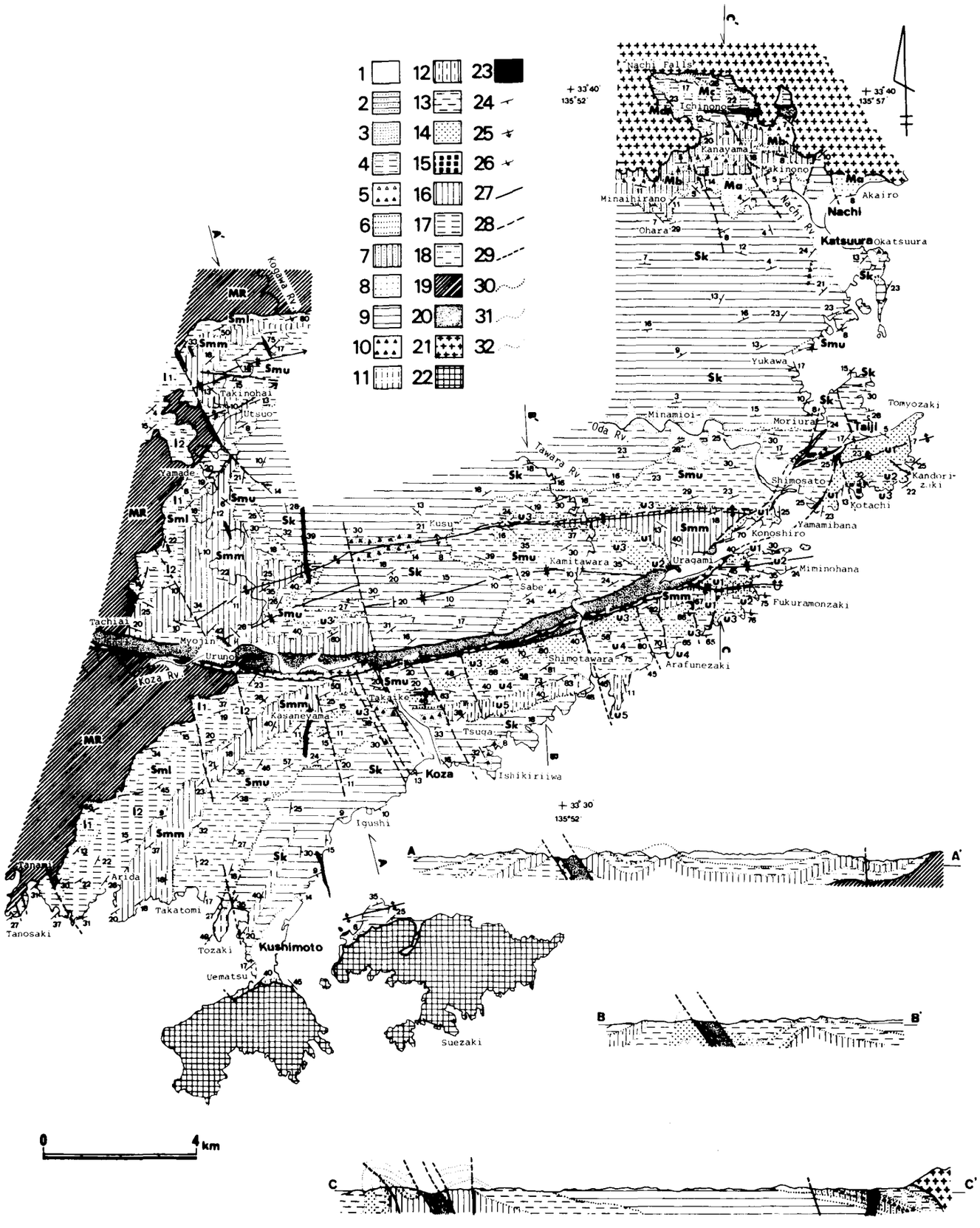

Fig. 3. Geologic map of the Kumano Group in the southern area. 1: alluvium, 2–8: Mitsuno Formation, 2: Member Md, 3 & 4: Member Mc (3: sandstone, 4: sandy alternation), 5–7: Member Mb (5: angular clast-bearing mudstone, 6: sandstone, 7: muddy alternation), 8: Member Ma, 9–11: Shikiya Formation (9: mudstone, 10: angular clast-bearing mudstone, 11: muddy alternation), 12–18: Shimosato Formation, 12–15: Member Smu (12: mudstone, 13: muddy alternation, 14: sandstone and muddy alternation, 15: angular clast-bearing mudstone), 16: Member Smm, 17 & 18: Member Sml (17: muddy alternation, 18: sandstone and muddy alternation), 19: Muro Group, 20: acidic pyroclastic rocks, 21: granite porphyry, 22: Shionomisaki Igneous Complex, 23: quartz prophyry, 24–26: dips and strikes (24: normal, 25: vertical, 26: overturned), 27: fault, 28: inferred fault, 29: concealed fault, 30: formation boundary, 31: member boundary, 32: unit boundary. After Hisatomi (1981).

1. Kumano Group in the northern area

In the northern area, the Kumano Group attains to 1,500 m in thickness, and was lithologically divided into the Onuma, the Koguchi and the Mitsuno Formations in ascending order by CHIJIWA and TOMITA (1981). According to them, the stratigraphy is as follows:

The Onuma Formation, about 600 m thick, consists of normal alternation*, mudstone, pebble to cobble conglomerate and sandstone (Fig. 2A). The thickness and the grain-size of deposits of the formation decreases toward the south. It is correlated to the Shimosato Formation in the southern area based on its stratigraphic position (HISATOMI, 1981).

The Koguchi Formation, about 450 m thick, is composed of mudstone in the lower half and muddy to normal alternation and mudstone in the upper half (Fig. 2A). It is characterized by the stable lithology, and is safely correlated to the Shikiya Formation in the southern area. The thickness of the formation increases toward the south.

The Mitsuno Formation, 400 m thick, consists of thick-bedded sandstone, alternation of sandstone and mudstone, and mudstone (CHIJIWA and TOMITA, 1981).

2. Kumano Group in the central area

In the central area, the Kumano Group is about 1,750 m thick, and was divided into the Koguchi Formation, below, and the Mitsuno Formation, above, by TANAI and MIZUNO (1954), and lacks in the lower formation in other areas. The basal part of the group is composed of conglomerate-sandstone beds, 20–50 m thick, and is directly overlain by mudstone of the Koguchi Formation (Fig. 2B). The basal conglomerate-sandstone beds becomes finer in grain-size toward the south.

The Koguchi Formation ranges from 700 m to 1,000 m in thickness, increasing the thickness toward the south. The formation is composed of massive or bedded mudstone in the lower part, and muddy alternation in the upper. In the southern part of this area, thick angular clast-bearing mudstone body is developed in the lower part of the formation (MURAYAMA, 1954).

The Mitsuno Formation, 650 m thick, consists of thick-bedded sandstone with frequent intercalations of muddy alternation. It also intercalates several coal-beds (20–70 cm thick) in the lowest part (TANAI and MIZUNO, 1954).

3. Kumano Group in the southern area

The stratigraphy of the Kumano Group in the southern area has been reported

* In this study, normal alternation is defined as the alternation of sandstone and mudstone, of which mud-sand ratio is between 0.67 and 1.5. Sandy alternation is less than 0.67, and muddy alternation is more than 1.5 in mud-sand ratio.

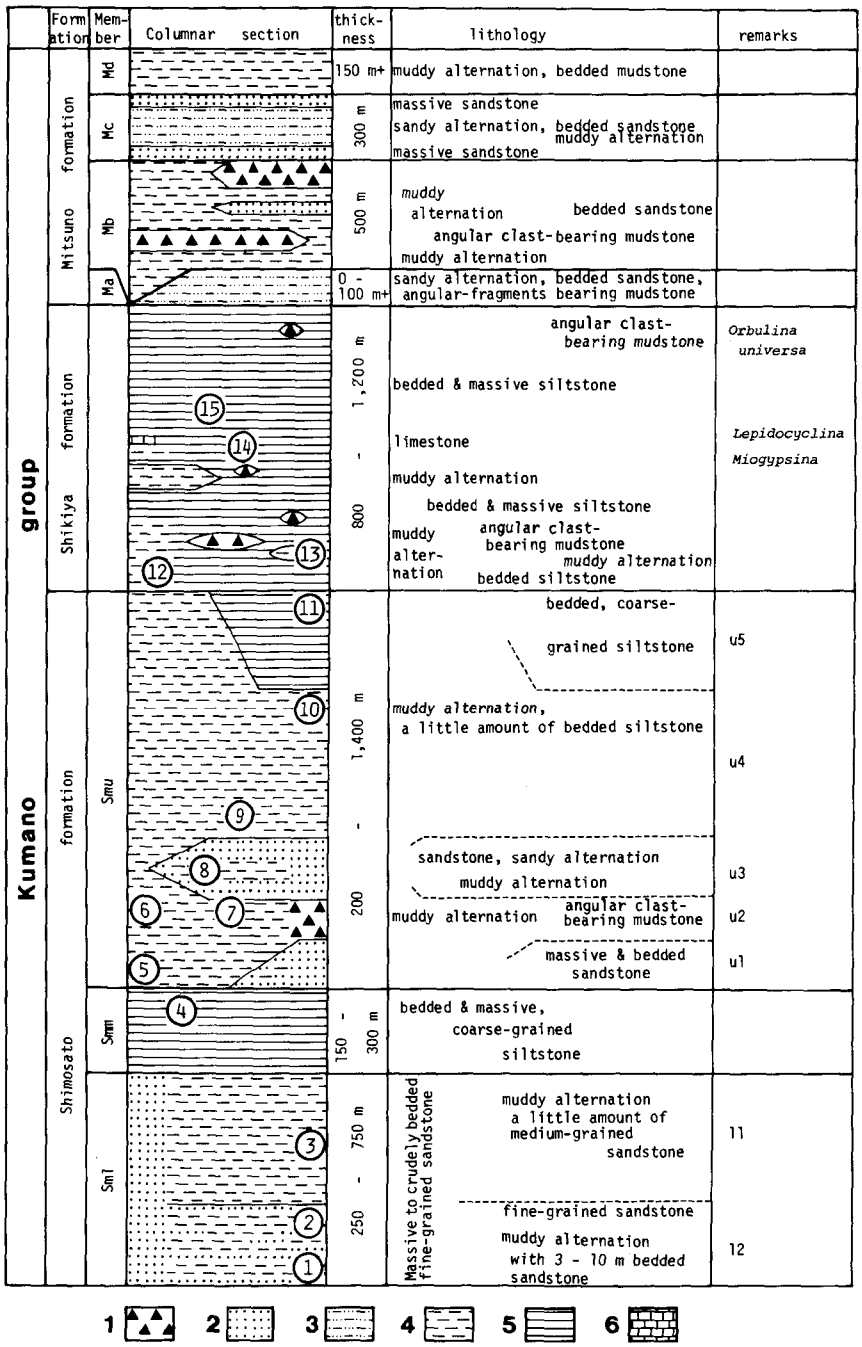

Fig. 4. Stratigraphy and lithology of the Kumano Group in the southern area. 1: angular clast-bearing mudstone, 2: sandstone, 3: sandy alternation, 4: muddy alternation, 5: mudstone, 6: limestone. Numerals in circles indicate the horizon of fifteen localities for the sedimentological analyses. Modified from HISATOMI (1981).

by the author (HISATOMI, 1981). The group varies from 2,500 m to 4,000 m in thickness. It is divided into three formations, namely, the Shimosato, the Shikiya and the Mitsuno Formations in ascending order (Figs. 3 and 4). The stratigraphy and lithology are summarized in Fig. 4.

The Shimosato Formation, 600 m to 1,800 m thick, is composed mainly of mudstone and muddy alternation, and is subdivided into the Lower (Sml), the Middle (Smm) and the Upper (Smu) Members. The formation increases its thickness and the grain-size of sediments toward the south, and pinches out at the northern end of this area.

The Lower Member (max. 750 m thick) consists mostly of muddy alternation, and can be subdivided into two lithologic units (units Sml1 and Sml2) by the presence of thick-bedded sandstone, in beds 3–10 m, in unit Sml1. The member becomes thinner and less sandy toward the north. But in the area on the north of Yamade (Fig. 3) the member consists of crudely bedded sandstone, which is similar in lithology to the basal sandstone bed in the central area.

The Middle Member is 150 m–300 m thick, composed mainly of bedded mudstone, in beds 20–50 cm thick, intercalating a small amount of muddy alternation. The thickness of the member gradually decreases toward the north.

The Upper Member is 200 m–1,400 m thick, composed mainly of muddy alternation, bedded mudstone, partly of thick-bedded sandstone, in beds 3–15 m thick, and sandy alternation. This member is characterized by variable lithology and thickness (Fig. 4). It is thickest in the southern district, and decreases the thickness rapidly to the north and gradually to the west (Fig. 5). The member is subdivided into five lithologic units (units Smu1 to Smu5 in ascending order) in the southeastern part of the area. Lithology of each unit is shown in Fig. 4, and details are given in HISATOMI (1981).

Within units Smu4 and Smu5 or within the upper part of Member Smu, sporadically occurs sandstone which is characterized by scarce quartz and K-feldspar grains, abundant plagioclase grains and acidic volcanic rock fragments. Sandstones in other horizons are distinctively different in the mineral composition (HISATOMI, 1981). Judging from the occurrence of these characteristic sandstones, it is probable that the boundary between the Shimosato and the Shikiya Formations is roughly parallel to the isochronous plane.

The Shikiya Formation is 800 m–1,200 m thick, composed mostly of monotonous mudstone, in beds 5–30 cm thick, and of a small amount of muddy alternation and angular clast-bearing mudstone in the lower part (Fig. 4). This formation can not be subdivided into members. The thickness of the formation gradually decreases toward the north. The detailed descriptions of muddy alternation are given in HISATOMI (1981).

Angular clast-bearing mudstones are developed in the southern part of the area

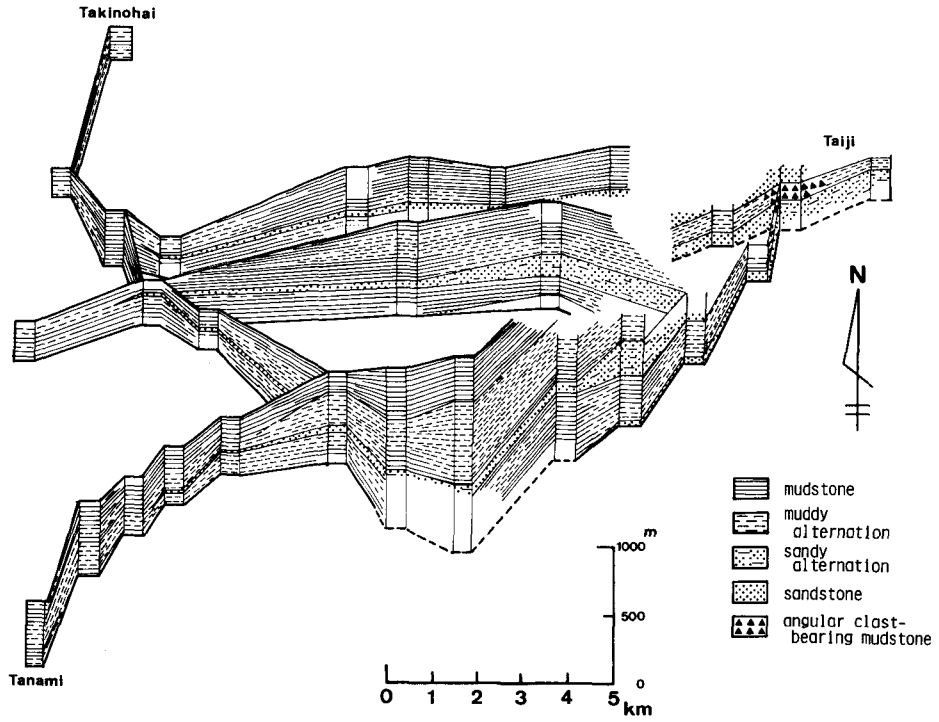

Fig. 5. Panel diagram showing the areal variation of lithology and thickness of Member Smu of the Shimosato Formation. After HISATOMI (1981).

(Fig. 3). They are 2–50 m thick, and consist of granule- to boulder-sized, angular to subangular clasts and muddy matrix.

A small amount of calcareous sandstone and siltstone, and limestone are intercalated in the lower part of the formation (Fig. 4) at Uematsu near Kushimoto. From this limestone, benthonic foraminiferal fossils of *Lepidocyclina* and *Miogypsina* (NISHIMURA and MIYAKE, 1973) and planktonic foraminiferal fossils of *Praeorbulina glomerosa curva*, *Pro. transitoria*, *Globigerinoides japonicus*, *Gds. sicanus* (IKEBE *et al.*, 1975) were reported. From these fossils the geologic age of this horizon is safely assigned to the upper half of Blow's N8. In addition, *Orbulina universa*, of which base datum corresponds to just above the base of Blow's N9, are obtained in the upper part of the Formation (IKEBE *et al.*, 1975).

The Mitsuno Formation is about 1,000 m thick and is distributed in the northernmost part of the area. It is composed of sandy alternation, muddy alternation, sandstone, angular clast-bearing mudstone and a small amount of bedded mudstone. The formation is lithologically subdivided into four members, namely, Members Ma,

Mb, Mc and Md in ascending order. The detailed descriptions of the members are given in HISATOMI (1981), and are briefly shown in Fig. 4.

III. Sedimentological Analyses

The Kumano Group in the study area consists mostly of muddy alternation and mudstone, and the present study is mainly concerned with the muddy sediments in the Shimosato Formation and the lower part of the Shikiya Formation.

The sedimentological study has been focused to the following two purposes. The first one is to reconstruct the morphology of the paleobasin, a part of which has been already reported (HISATOMI, 1981). The second purpose is to consider the transportation mechanisms of thick, fine-grained sedimentary sequences based on the analyses of sedimentary features. For this purpose, the various features of muddy alternation were analyzed at 15 localities along the coastal area where the strata are best exposed (Fig. 6). The localities cover from the lowest part of the Shimosato Formation to the middle part of the Shikiya Formation (Fig. 4). The number of analyzed beds reached about 1,400.

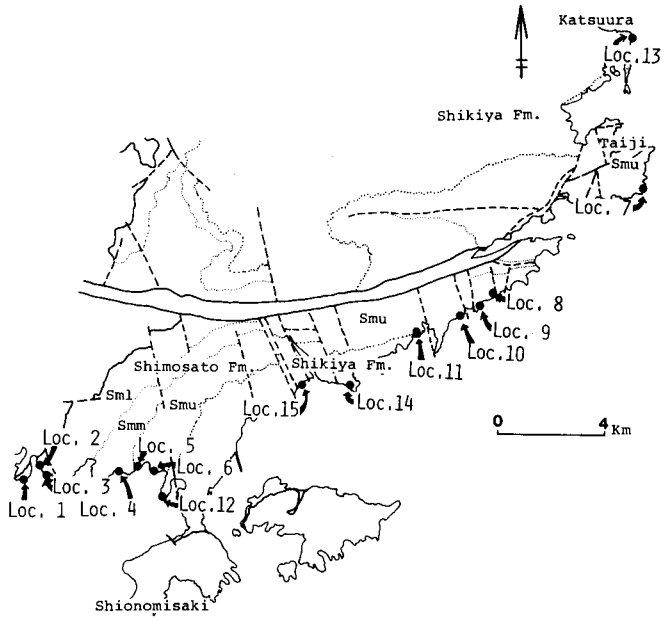

Fig. 6. Localities for the sedimentological analyses. The stratigraphic horizon of each locality is shown in Fig. 4.

1. Muddy alternation of sandstone and mudstone

A. Thickness distribution and mud-sand ratio

The thickness of individual beds*, their sandstone parts and mudstone parts in muddy alternation were measured at fifteen localities mentioned above. The thickness of columns examined is 17.7 m on an average, ranging from 4.8 m to 39.0 m, and the number of beds examined at one locality is 92.9 on an average, ranging from 39 to 140. And then, based on the thickness of sandstone and mudstone parts, the ratio of the overlying mudstone to the underlying sandstone part is calculated.

The bed thickness of muddy alternation in the reported area generally range from 10 to 30 cm, and sometimes attain up to 100 cm or more. In these beds, sandstone parts are mostly 1–10 cm and mudstone parts are mostly 10–25 cm in thickness. The muddy alternation is characterized by its thin bedding and the scarceness of thick sandstone parts.

Table 2. Ranges, median values (Md), mathematical mean values ($\bar{x}$) and other parameters of the thickness distribution of muddy alternations. QD: quartile deviation, SD: standard deviation.

Thickness \ Loc.		1	2	3	4	5	6	7	8	9	10	11	12	13	14	15
Single bed	max.	90.0	154.0	80.0	180.0	200.0	232.0	52.5	270.0	182.0	101.0	120.0	125.0	22.5	34.0	55.0
	min.	1.0	1.0	0.5	0.7	1.0	0.5	1.0	1.0	1.5	1.5	0.5	0.3	4.5	1.7	2.0
Sandstone part	max.	51.0	100.0	16.0	16.0	13.0	41.0	18.0	84.0	92.0	48.0	25.0	27.0	2.0	5.3	4.5
	min.	0.3	0.5	0.2	0.3	0.2	0.5	0.5	0.2	0.3	0.2	0.3	0.2	0.2	0.2	0.3
Mudstone part	max.	87.5	152.0	80.0	179.0	200.0	191.0	50.0	188.0	110.0	92.0	118.5	125.0	20.5	32.6	53.0
	min.	0.2	0.5	0.5	0.4	1.0	0.5	0.3	0.5	1.0	0.5	0.5	0.3	3.0	2.7	0.8
Md	single bed	13.5	16.8	13.7	12.9	17.5	13.5	6.9	14.7	8.7	18.5	11.4	9.9	12.1	10.4	12.3
	sandstone	2.9	3.3	1.0	1.8	1.1	2.0	3.0	2.8	1.4	2.0	0.9	3.3	1.3	1.0	1.5
	mudstone	9.0	11.1	13.2	12.4	17.7	13.0	3.3	12.4	7.9	16.5	10.9	11.0	10.9	9.4	12.4
$\bar{x}$	single bed	18.5	23.2	15.9	25.1	24.3	22.3	9.6	29.8	14.3	23.2	16.4	15.1	12.9	11.5	14.2
	sandstone	5.9	6.5	2.2	3.5	3.0	3.6	3.8	8.6	4.5	4.1	2.0	5.6	1.5	1.3	1.6
	mudstone	13.5	17.8	16.4	24.8	23.2	20.5	6.2	25.7	10.7	19.7	16.3	17.1	11.5	11.0	13.1
QD	single bed	6.6	12.3	9.3	9.2	11.0	11.7	4.0	15.7	3.4	11.7	8.0	8.4	1.3	4.5	5.3
	sandstone	3.2	2.5	1.0	2.0	2.0	1.5	1.1	3.9	1.8	2.0	0.7	3.2	0.3	0.5	0.5
	mudstone	7.1	9.2	9.3	10.7	12.6	11.8	3.2	14.8	3.1	11.0	7.8	8.4	1.4	3.5	5.1
SD	single bed	17.4	22.1	14.5	33.5	27.7	28.2	7.7	37.3	26.1	19.4	17.1	26.0	2.9	6.5	9.3
	sandstone	8.3	8.5	2.9	3.8	3.5	5.6	3.0	15.2	12.9	5.5	3.2	6.1	0.3	0.5	0.5
	mudstone	16.1	20.7	14.9	34.1	28.0	25.1	7.6	33.2	12.2	18.9	17.3	21.2	2.8	6.1	8.9
QD/Md	single bed	0.49	0.73	0.67	0.71	0.62	0.87	0.58	1.07	0.39	0.63	0.70	0.84	0.11	0.43	0.43
	sandstone	1.11	0.76	1.00	1.11	1.75	0.75	0.37	1.38	1.30	1.02	0.77	0.97	0.21	0.54	0.31
	mudstone	0.79	0.83	0.71	0.87	0.71	0.91	0.96	1.19	0.40	0.67	0.72	0.76	0.13	0.37	0.41
SD/$\bar{x}$	single bed	0.94	0.95	0.91	1.33	1.14	1.26	0.80	1.25	1.82	0.84	1.04	1.72	0.22	0.56	0.66
	sandstone	1.40	1.31	1.31	1.08	1.16	1.55	0.79	1.77	2.87	1.33	1.61	1.08	0.32	0.78	0.53
	mudstone	1.20	1.16	0.91	1.37	1.21	1.22	1.22	1.29	1.14	0.96	1.06	1.24	0.24	0.55	0.68

Thickness distribution

The thickness distributions are shown in Table 2 and Fig. 7. None of the cumulative frequency distribution of the mudstone part in log-probability scale is a single straight line, which represents the Gaussian distribution. Also most of the distribution of sandstone parts and individual beds cannot be approximated by a single straight line with some exceptions (e.g. bed thickness at Locs. 7 & 8; thickness of sandstone parts at Locs. 8 & 10).

* In this study, one bed includes a sandstone part and/or a mudstone part, which is bounded by two sharp bedding planes (cf. Fig. 9).

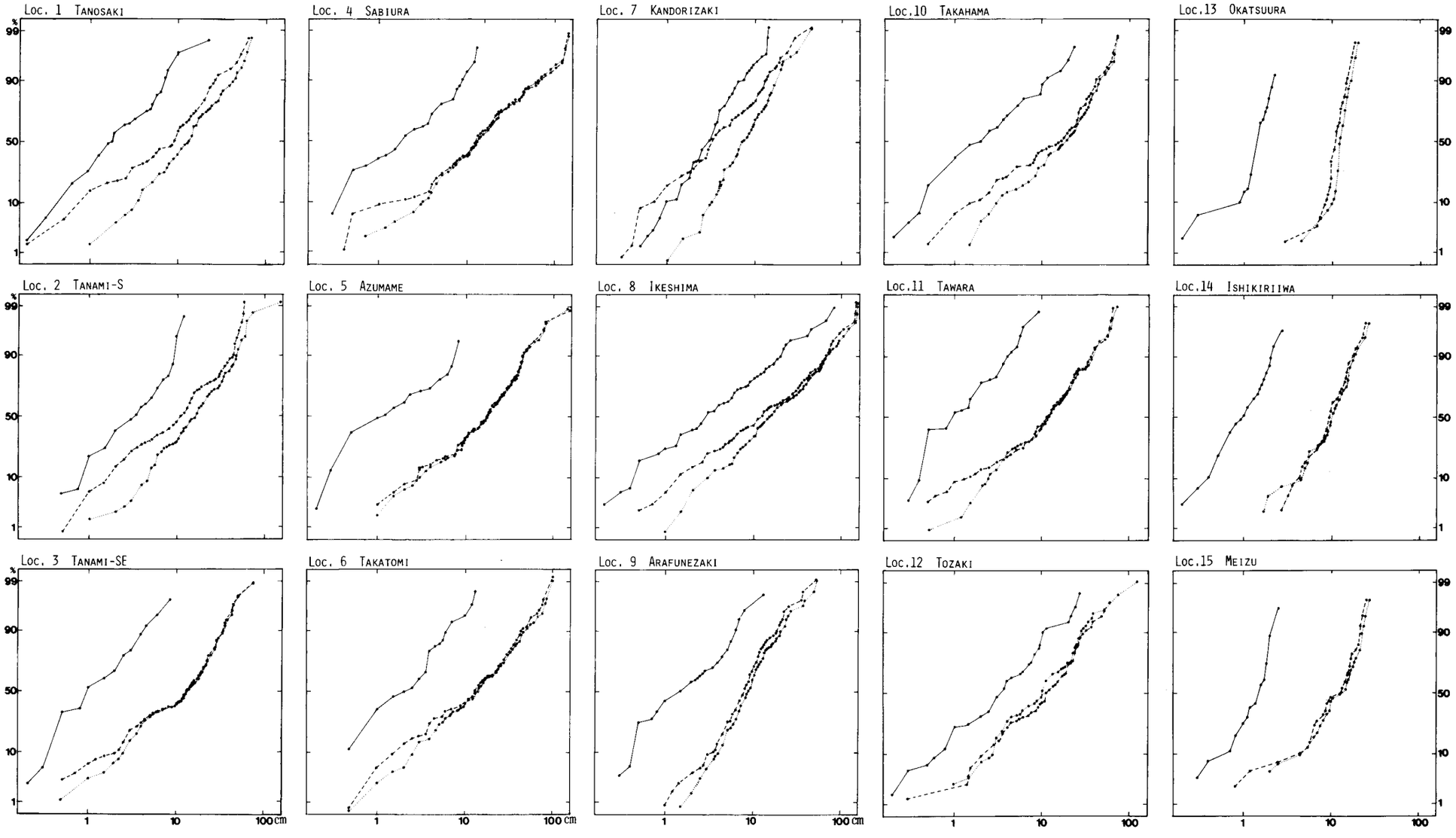

Fig. 7. Cumulative frequency curves of the thickness of sandstone part, mudstone part and individual beds within muddy alternations at fifteen localities. Solid line: thickness of sandstone part. Broken line: thickness of mudstone part. Dotted line: thickness of individual bed.

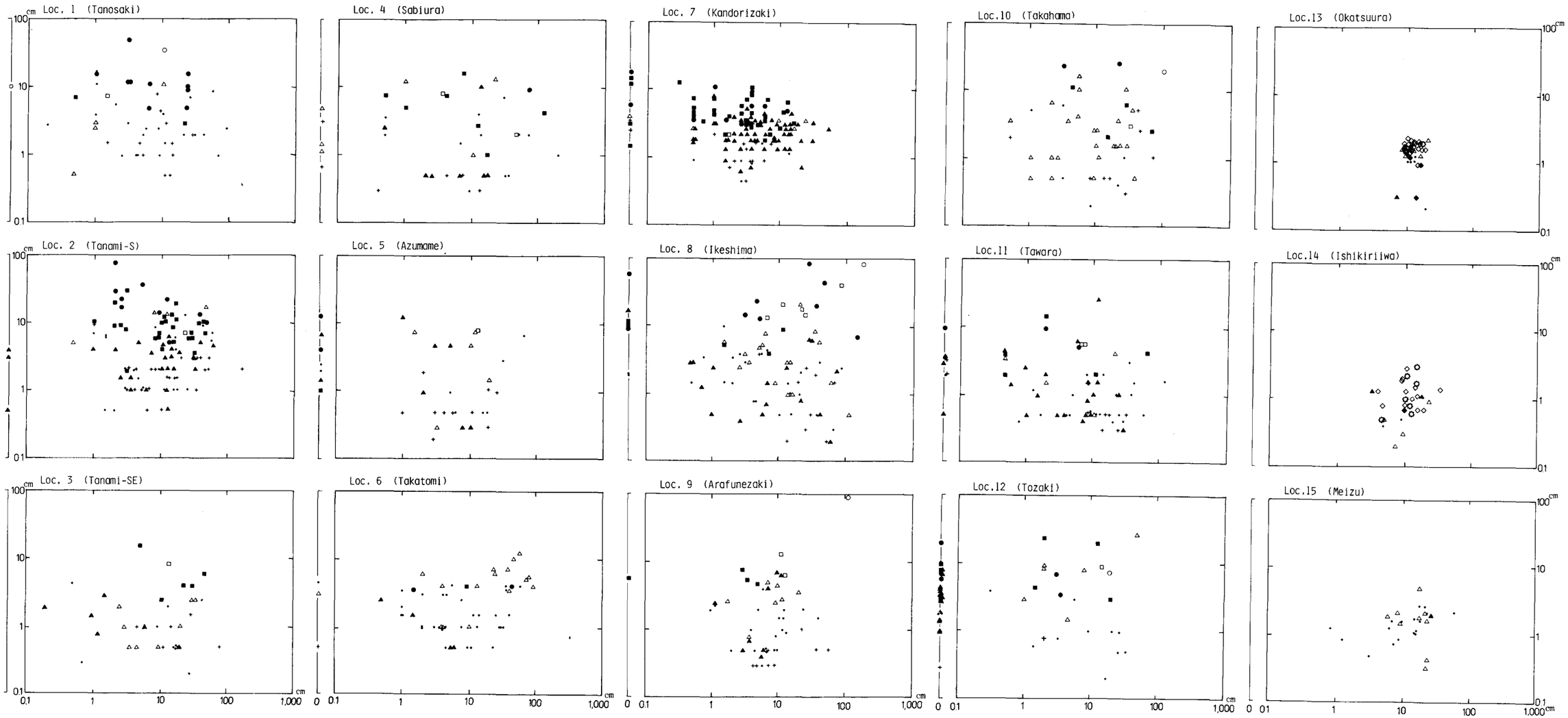

Fig. 8. Variations of the thickness of sandstone part against the thickness of the overlying mudstone part at fifteen localities. Symbols (1–10) represent the kinds of sedimentary divisions developed at the basal part of individual beds. 1 & 2: a-division, 3 & 4: b-division, 5 & 6: x-, c- or w-division, 7: d-division, 8: e-division, 9: s-division, 10: others.

The distribution patterns of fifteen localities can be grouped into two, based on the ratio of the standard deviation over the mean thickness ($SD/\bar{x}$), which represents the relative degree of the concentration around the mean values. The first group, which includes Locs. 13, 14 and 15, is characterized by their small values of $SD/\bar{x}$ of beds as well as of sandstone and mudstone parts. Loc. 7 may also be included into this group, though the degree of the concentration of the distribution is weaker than the above three.

The second group is characterized by the higher values of $SD/\bar{x}$, that is to say, by the larger dispersion of the distribution. In this group, $SD/\bar{x}$ values of sandstone part at Locs. 6, 8, 9 and 11 are especially higher than those at other localities. It is also notable that the $SD/\bar{x}$ values of mudstone parts in localities of this group are relatively constant, ranging from 0.9 to 1.2.

The difference of the two groups is supposed to be derived from the difference in types of sediments, as will be mentioned later.

Mud-sand ratio

Total mud-sand ratio of muddy alternation at each locality ranges from 2 to 25, and is mostly in the range of 4–13. The relation between the thickness of sandstone part and that of the overlying mudstone part is shown in Fig. 8.

It is notable that the ranges of the mud-sand ratio of Locs. 13, 14 and 15 are narrow, compared with those of the other localities, and that range of the ratio at Loc. 7 is also narrow, though its grade is slightly lower than the above three. The narrow distribution of mud-sand ratio at Locs. 13, 14 and 15, is basically consistent with the high concentration of the thickness distribution.

B. Style of bedding

The classification of the styles of bedding of muddy alternation is summarized in Table 3. They can be grouped into two types, that is, graded bedding (type I) and non-graded bedding (type II). It is noteworthy that trough-shaped and wedge-

Table 3. Classification of styles of bedding.

			top surface	bottom surface	bedding	
Graded	(type I)	I-a	gradual	sharp or erosive	even	
		I-b	sharp	sharp or erosive	even or ripple	
Non-graded	(type II)	II-a	sharp	sharp or gradual	even	
		II-b	sharp	sharp	ripple	

shaped sandstone layers are not developed in the study area.

Graded bedding

This type of bedding is further classified into two types (types I–a and I–b) based on the mode of top surfaces of sandstone parts. In the beds of type I–a, top surface of sandstone part is not sharp, and sandstone grades gradually or rapidly into the overlying mudstone. The beds usually show even bedding, and sometimes show the erosional features at the base. Most of the beds of the Kumano Group belong to this type. The vertical change in grain-size of a typical bed is shown in Fig. 9.

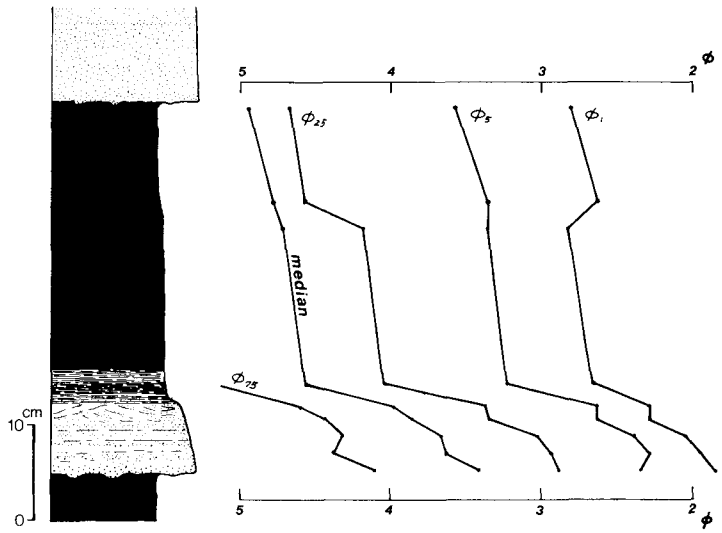

Fig. 9. Bed of type I–a showing the vertical change in grain-size, unit Smu5 of the Shimosato Formation at Shimotawara. The lines indicate one percentile, 5-percentile, 25-percentile, median and 75-percentile from right to left.

On the other hand, sandstone part of type I–b bed is in contact with overlying mudstone part by a sharp surface, and shows both even or ripple beddings (Table 3). Beds which show even bedding in type I–b are well developed at Locs. 2, 3, 6 and 9. Beds which show ripple bedding are developed at Locs. 2 and 12. Type I–b beds are not common in the study area, comparing with type I–a beds.

Non-graded bedding

Most of beds of this type show even bedding, and are called type II–a. Sandstone part of them usually shows sharp top and sharp base. Beds of this type are observed at Locs. 3, 4 and 5. Some beds of type II–a are sharp-topped and gradual-based, and show reverse-grading. They can be observed at Locs. 13 and 14.

The beds having ripple bedding are called type II–b. Sandstone part of them

are thin (2–20 mm thick) usually very fine-grained, and sometimes show the starved-ripple bedding. This type of beds can be observed in the Shikiya Formation at the west of Ishikiriiwa.

C. External sedimentary structures

Ripple marks and sole marks are most popular among the external sedimentary structures. Unfortunately, however, the bottom surfaces of sandstone parts are usually concealed owing to the low dips of strata, usually less than 30°, and it is difficult to observe sole marks.

Sole marks

The most popular scour mark is flute mark, occupying more than 80% of the current marks observed. Ridge-and-furrow mark and current crescent mark are much less common than flute mark.

Flute marks are usually small in size, ranging from 5 to 15 cm in length. They are not crowded, and usually one to several marks can be observed on some one square meter surface.

Most of tool marks are groove mark, occuppying 10% of the total current marks. Prod and bounce marks are rare. Groove marks are generally 1–4 cm in width, and are isolated as in the case of flute mark.

Top mark

Most of top marks are ripple marks, and the rests are current top marks. Ripple marks observed in the area are small scale ripples of ALLEN (1968), and are classified into asymmetrical current ripples and linguoid ripples.

Asymmetrical current ripples are generally 10–20 cm in wave-length, and 1–2 cm in amplitude. They are observed throughout the Kumano Group. They are common in units Smu1 and Smu2 near Taiji. Linguoid ripples are 15–30 cm in wave-length and 1–3 cm in amplitude. They are developed in unit Smu1 at Yamamibana, but are rare in other places and at other horizons.

Current marks generally occur as sole mark. However they are found exceptionally on the top surfaces of sandstone part in muddy alternation at Loc. 13, about 100 m above the base of the Shikiya Formation (Fig. 4). These top marks include flute, prod and ridge-and-furrow marks. Flute marks are 0.5–1.5 cm in length and 0.1–0.4 cm in width. The current mark-bearing sandstone parts are always in sharp contact with the overlying mudstone parts which are 9–15 cm thick and always bioturbated throughout.

Paleocurrent directions indicated by these top marks are distinctly different from the general trend of those deduced from the current sole marks. The significance of these current top marks will be mentioned later in Chapter IV.

D. Internal sedimentary structures

Many kinds of internal sedimentary structures are observed in muddy alternation. Descriptions in this paragraph are mainly based on the observations and analyses in the field, and subsidiarily on the observations of polished surfaces and thin sections, especially of mudstone samples.

Descriptions of sedimentary divisions

The classification of the primary sedimentary structures is shown in Table 4, and the typical occurrences of them are illustrated in Fig. 10.

Table 4. Definition and characteristics of sedimentary divisions. f: fine, m: medium, c: coarse, v: very, lam.: lamination, ss: sandstone, si: siltstone.

Division	Predominating structure	Grain-size	development of grading
a	massive	fss.- css.	well & common
b	parallel lam. (b-type)	fss.- mss.	common
p	parallel lam. (p-type)	vfss.- fss.	commonly reverse-graded
x	cross lam.	vfss.- fss.	rare
c	convolute lam.	vcsi.- fss.	common
w	wavy lam.	vcsi.- fss.	rare
d	parallel lam. (d-type)	vcsi.- fss.	well & common
e	massive	- csi.	rare
s	massive	vcsi.- vfss.	not developed

Massive structure (a-, e- and s-divisions):

The massive structure is classified into two types, namely, massive, graded and massive, non-graded types. The former is restricted in the basal part of sandstone part. This structure is usually developed in the beds whose sandstone part is more than 10 cm thick. Grain-size is usually fine- to coarse-sand size, and grading is well developed. Grains of heavy minerals, such as zircon and garnet, are sometimes concentrated at the lowest part of the structure. Scouring and other erosional structures are often observed. This type of structure is the characteristic structure of BOUMA's a-division* (Fig. 10–2).

Massive, non-graded structure is subdivided into two types in relation to grain-

* The "division" is defined as a part of an individual bed which is distinguished by the predominance of one sedimentary structure in it (BOUMA, 1962; WALKER, 1965).

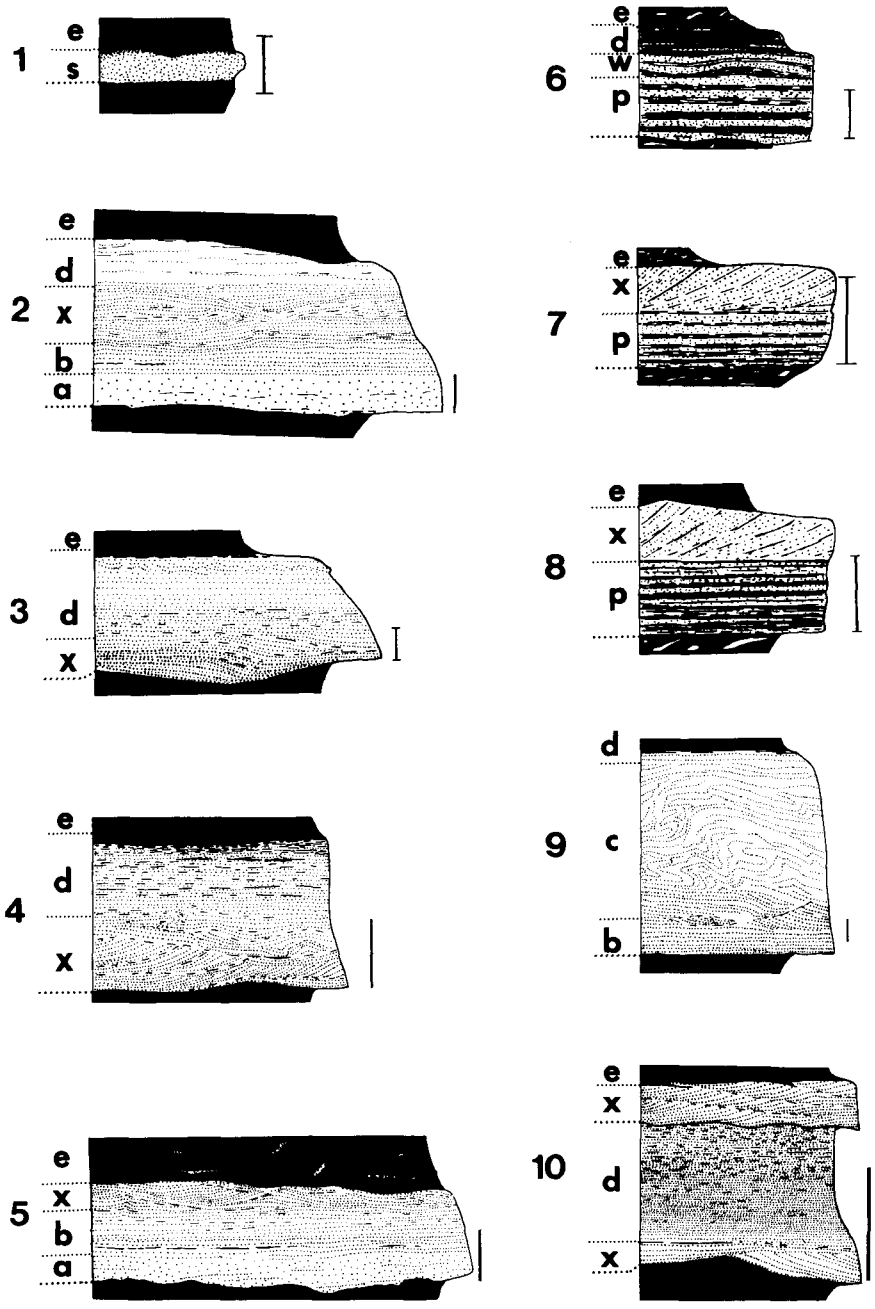

Fig. 10. Sketches of beds in muddy alternation showing the features of sedimentary divisions. Scale bar for 1, 3, 6, 7 and 8 indicates 1 cm, and that for others indicates 5 cm.

size. The first one is represented by bioturbated or non-bioturbated massive mudstone, and occurs as an individual bed or is developed in the upper part of beds. This type of structure characterizes BOUMA's e-division (Figs. 10–1~8, 10–10). The second one is developed as thin layers of very coarse-grained siltstone or very fine-grained sandstone. They are often well sorted, and show no sedimentary structures. The author named such part of beds as s-division (Fig. 10–1).

Parallel lamination (b-, d- and p-divisions):

Parallel laminations represented by horizontal-parallel lamination are classified into the following three types based on the constituents of laminae and the manner of lamination, that is, b-, d- and p-types (Table 4).

The b-type lamination is continuous and horizontal-parallel. It is developed in medium- to fine-grained sandstone. Both coarser and finer laminae consist of framework grains, and grading is commonly developed. This type of structure is usually overlain by cross or convolute laminations, and is the characteristic feature of BOUMA's b-division (Figs. 10–2, –5 and –9).

The d-type lamination is distinguished from b-type lamination by its finer grain-size (usually developed in fine- to very fine-grained sandstone). Coarser laminae consist of framework grains, and finer laminae consist of framework grains and a small amount of clay flakes. This type lamination generally occupies the transitional part from sandstone part to the overlying mudstone part. It often overlies cross or convolute lamination, and sometimes occupies the lowest part of mudstone part. The bed of this type is usually graded and is correlated with BOUMA's d-division (Figs. 10–2, –3, –4, –5, –9 and –10).

The p-type lamination is horizontal-parallel, continuous lamination, and is developed in very fine-grained sandstone or very coarse-grained siltstone. Coarser laminae which consist of framework grains, are infrequently intercalated in finer laminae, which consist of clay flakes and a small amount of framework grains. This type lamination is usually overlain by cross laminated, very fine-grained sandstone (Figs. 10–7 and –8). The p-type lamination is distinguished from b- and d-type laminations by the common presence of upward increase in grain-size of coarse laminae, and by the relatively sharp boundaries between coarser and finer laminae. The author named a part of individual beds characterized by p-type lamination as p-division.

Cross lamination (x-division):

Both cross and convolute laminations characterize the BOUMA's c-division. But the author proposes here to classify BOUMA's c-division into two divisions, namely, x- and c-divisions, each characterized by the predominance of cross and convolute laminations, respectively.

In x-division, ripple-drift cross lamination, ripple cross lamination and fading ripple cross lamination (STOW and SHANMUGAM, 1980) are included. They all belong

to the small scale cross lamination.

Ripple-drift cross lamination is developed alone (Fig. 10–10) in sandstone part, or accompanied with parallel lamination. Ripple cross lamination is concave in shape, showing the erosion in the stoss side (Fig. 10–7). Fading ripple cross lamination is usually observed in very coarse-grained siltstone or very fine-grained sandstone.

Convolute lamination (c-division)

Convolute lamination is generally developed in fine-grained sandstone. In most cases they grade from the underlying b-type lamination (Fig. 10–9).

Wavy lamination (w-division):

Wavy lamination is rarely observed in fine-grained sandstone or very coarse-grained siltstone, and most of them are continuous lamination (Fig. 10–6). The author defined the wavy laminated part of bed as w-division.

Frequency of the occurrence of sedimentary divisions

Among nine sedimentary divisions defined above (Table 4), the most frequent one is e-division, and d- and x-divisions are also common as shown in Fig. 11 and Table 5. These three divisions occupy more than 80% of the total divisions. Con-

Table 5. Frequency of the occurrence of nine sedimentary divisions at fifteen localities. The values marked by star (*) represent the percentage of the division which cannot be classified as any of nine divisions.

	a	b	p	x	c	w	d	e	s
15	-	-	-	8.1	-	2.3	44.2	45.4	-
14	-	-	13.8	26.2	0.7	0.7	24.8	30.0	4.1*
13	-	-	15.5	20.7	-	1.3	29.0	33.6	-
12	2.9	6.9	-	15.0	1.7	2.3	32.4	36.4	2.3
11	1.0	4.8	-	16.2	1.4	1.0	26.7	43.3	5.7
10	1.0	4.3	-	9.5	1.0	1.4	27.0	50.2	5.7
9	2.0	6.1	-	18.2	2.7	2.7	21.6	39.9	6.8
8	3.7	6.0	-	13.3	4.6	2.1	28.4	39.0	2.8
7	2.8	13.4	-	33.8	0.3	-	5.9	39.4	4.4
6	1.3	0.9	-	7.4	0.4	0.9	39.6	48.3	1.3
5	1.2	1.8	-	8.4	0.6	0.6	25.3	53.0	9.0
4	0.6	6.9	0.6	8.8	6.3	-	21.3	50.0	5.6
3	-	4.1	-	15.0	-	1.2	30.6	44.5	4.6
2	3.7	11.5	-	19.6	0.3	2.7	14.9	39.2	8.1
1	8.3	6.3	-	6.9	0.7	0.7	25.0	38.9	13.2

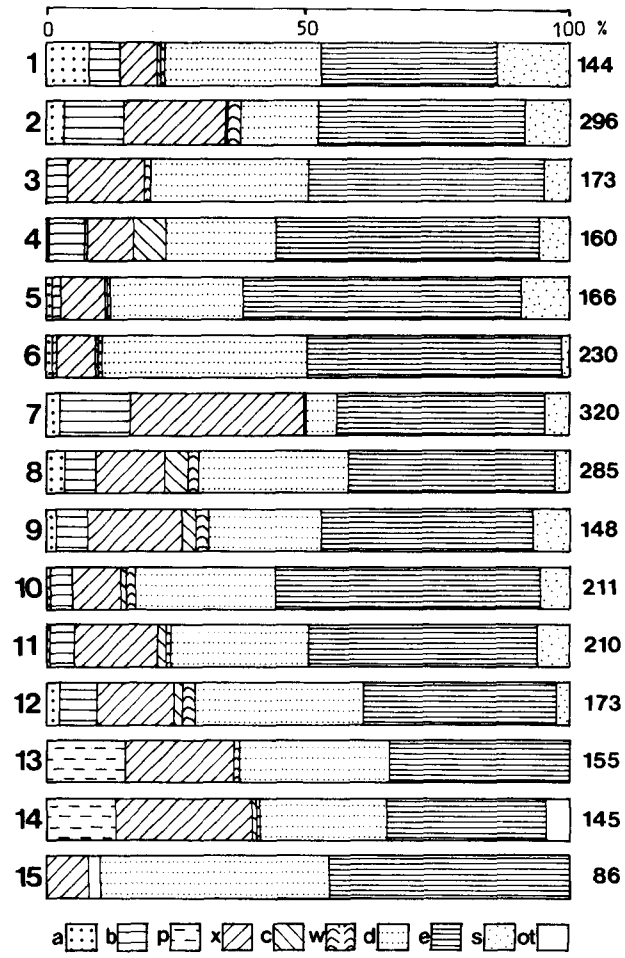

Fig. 11. Frequency of the occurrence of nine sedimentary divisions (a- to s-divisions) at fifteen localities. Numbers in the left side represent localities, and those in the right side represent the total numbers of divisions examined.

sequently, most of sediments are concluded to have been deposited under the condition of the lower flow regime.

On the other hand, a- and b-divisions, showing the upper flow regime sedimentation, occupy only 8% of the total. And s- and p-divisions, which probably show the lower flow regime sedimentation, occupy about 7% of the total.

The relationship among the proportion of a- and/or b-divisions, p- and/or s-divisions, and the other divisions are shown in Fig. 12. Judging from the figure,

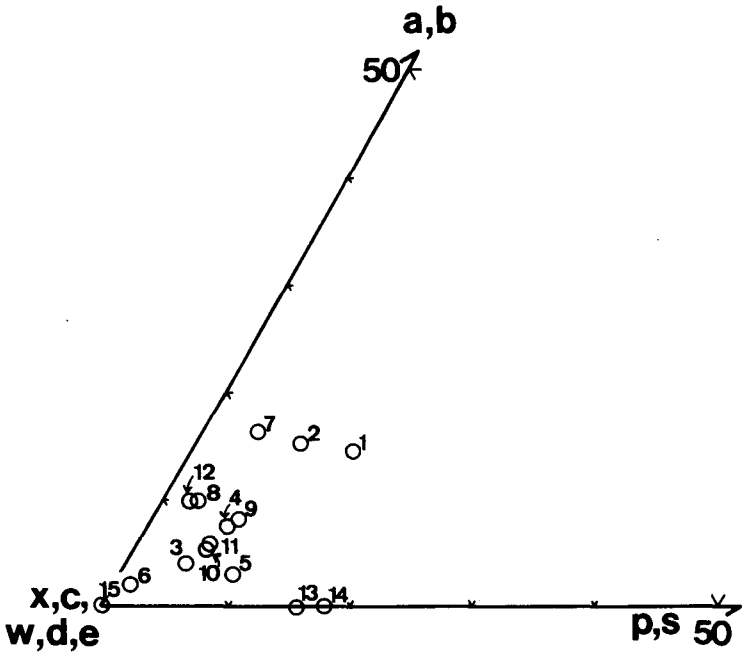

Fig. 12. Triangular diagram showing the relative frequency of a- and/or b-divisions, p- and/or s-divisions, and other divisions.

fifteen localities examined can be classified into three groups based on the relative frequency of the upper and the lower flow regime sedimentary structures. The first one, including Locs. 1, 2 and 7, is characterized by the abundance of a- and b-divisions. The second group, including Locs. 13 and 14, is characterized by the lack of a- and b-divisions. The last group is characterized by the dominance of e-, d- and x-divisions.

The characteristic features of each locality are summarized as follows: (1) At most localities e-, d- and x-divisions are dominant. And a-, b- and s-divisions are relatively small in number but are present at most localities. (2) At Loc. 1, a- and s-divisions are dominant, occupying 8% and 13% of the total divisions, respectively. (3) At Loc. 7, x-division is extremely dominant, while d-division is rare. (4) At Locs. 13, 14 and 15, a-, b- and s-divisions are entirely missing, and instead, p-division is well developed at Locs. 13 and 14 (Table 5). This fact is supposed to be related to the concentrated distribution of thickness (Fig. 7) and the mud-sand ratio (Fig. 8) at those three localities.

Sedimentary structures developed in the basal part of individual beds

The frequency of the occurrence of sedimentary structures developed in the

Table 6. Frequency of the occurrence of sedimentary divisions developed at the basal part of individual beds. The values marked by star (*) represent the division which cannot be classified as any of nine divisions.

	a	b	p	x	c	w	d	e	s
15	-	-	-	17.9	-	5.1	76.9	-	-
14	-	-	46.2	23.1	-	2.6	12.8	-	15.4*
13	-	-	47.1	21.6	-	3.9	27.5	-	-
12	4.9	7.8	-	17.6	-	2.9	38.2	24.5	3.9
11	1.8	7.2	-	23.4	1.8	1.8	36.9	16.2	10.8
10	4.8	9.5	-	30.2	1.6	4.8	17.5	15.9	15.9
9	1.8	6.3	-	13.4	-	2.7	36.6	28.6	10.7
8	8.4	9.2	-	21.4	4.6	3.1	32.8	14.5	6.1
7	6.4	27.9	-	50.7	-	-	4.3	1.4	9.3
6	2.4	0.8	-	12.8	0.8	0.8	56.8	23.2	2.4
5	2.1	2.1	-	11.3	1.0	1.0	35.1	32.0	15.5
4	1.1	11.4	1.1	11.4	5.7	-	22.7	37.5	9.1
3	-	7.3	-	19.8	-	2.1	40.0	22.9	8.3
2	8.5	21.5	-	20.0	-	5.4	21.5	4.6	18.5
1	19.0	3.2	-	7.9	-	-	38.1	1.6	30.2

basal part of individual beds are summarized in Table 6 and Fig. 13. It shows a tendency basically similar to that of the occurrence of total divisions (Table 5).

The beds which start with d-division are most common, and the beds starting with x- and e-divisions are the next. These three types occupy about 70% of the total beds, occurring at nearly all localities. And beds starting with a- and b-divisions occupy only 13.7% of the total beds. The beds starting with p- or s-divisions do not show the characteristics of turbidite, and they occupy about 13% of the total beds. The beds starting with a-, b-, s- or e-divisions do not occur at Locs. 13, 14 and 15. The beds starting with p-division are restricted at Locs. 13 and 14.

The relationship among the beds starting with a- or b-divisions, beds with p- or s-divisions, and others, are shown in Fig. 14. Three groups of localities, which are recognized in Fig. 12, are also recognizable in Fig. 14.

The characteristic features of the localities are as follows: (1) At most localities, except for those listed below, the beds starting with d-, x- and e-divisions are dominant, and the beds with a-, b- and s-divisions are also present. (2) At Loc. 1, the beds starting with a- and s-divisions occupy 20% and 30% of the total beds, respectively. (3) At Loc. 7, the beds starting with b- and x-divisions occupy more than three-fourths of the total, and beds with d-division are rare. (4) At Locs. 13

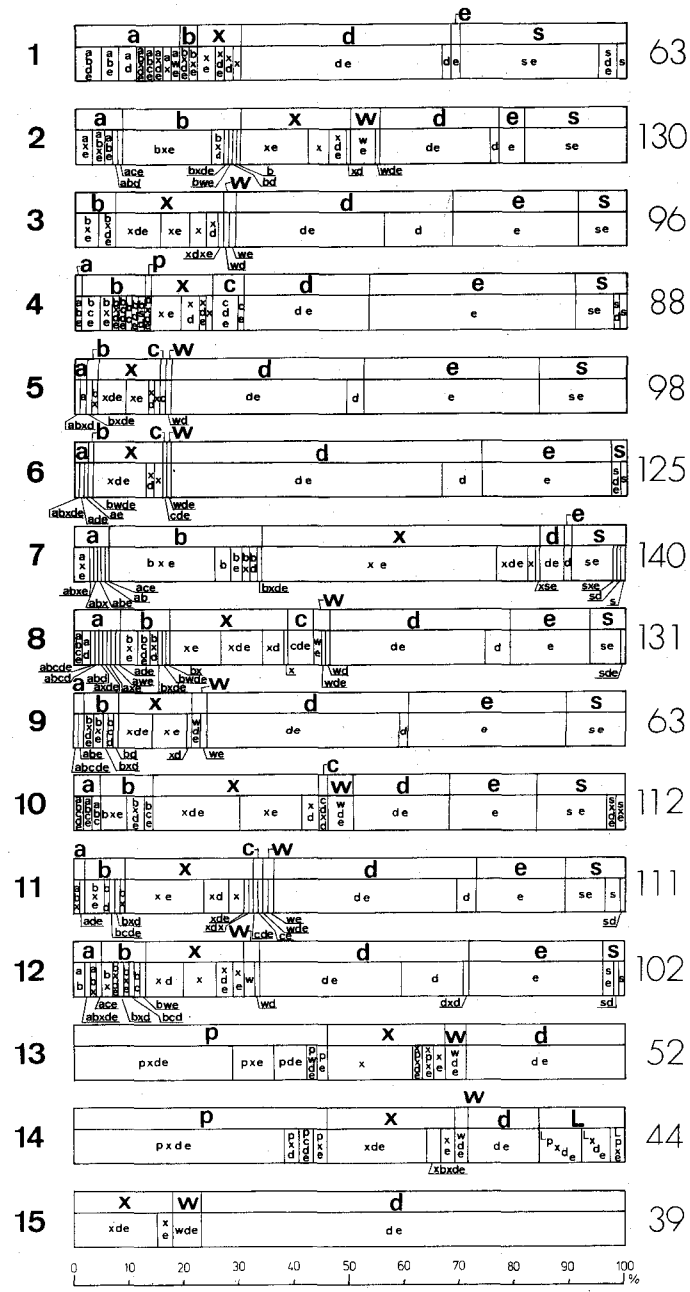

Fig. 13. Frequency of the occurrence of divisions developed at the basal part of individual beds (upper half of each column) and the proportion of bed types (lower half of each column). "L" represents the division which cannot be classified as any of nine divisions. Numerals in the right side indicate the total number of beds examined. Numerals in the left side indicate the locality number.

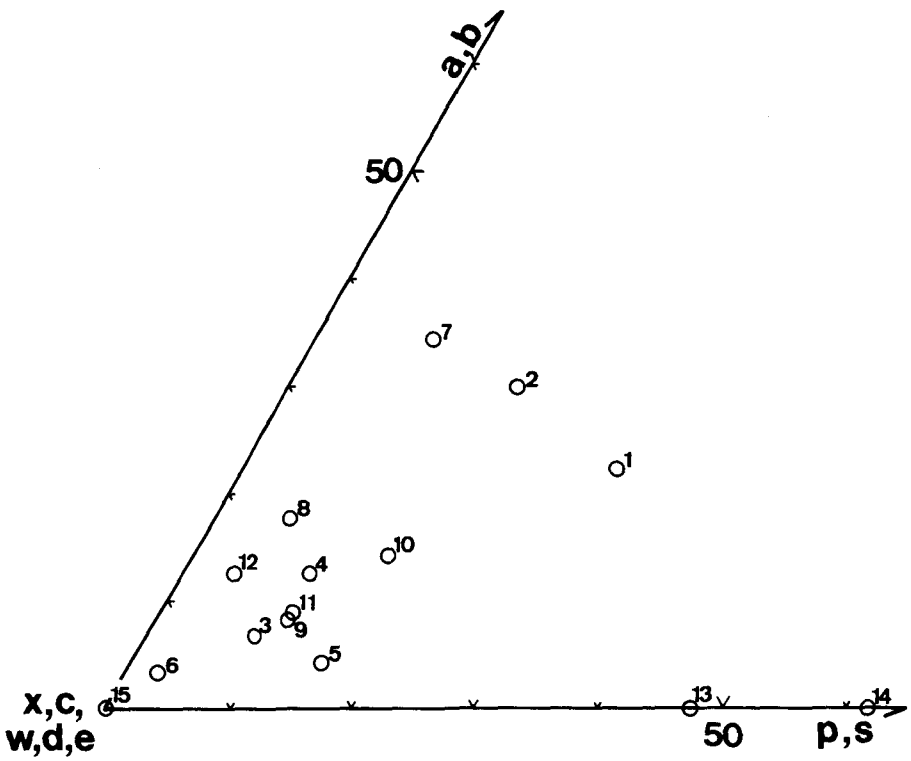

Fig. 14. Triangular diagram showing the relative frequency of divisions developed at the basal part of individual beds in fifteen localities. End members are same with those in Fig. 12.

and 14, beds starting with p-division attain to about 40% of the total. And at Locs. 13, 14 and 15, the beds starting with a-, b-, s- and e-divisions are absent.

Combinations of sedimentary divisions

The successive occurrence of the sedimentary divisions in individual beds are shown in Figs. 13 and 15. Most of beds examined show the BOUMA sequence, and show the base-cut-out sequence of BOUMA (1962) or its variations.

The most popular combinations of divisions are "de", "e", "xe", "xde" and "se" (Fig. 13, lower half of each column). The kinds of the combinations are highly variable among localities, but can be classified into the following five types:

(1) The complete sequence of BOUMA (1962): This type is rare (Fig. 15), and is observed at six localities. An example of this type of beds is shown in Fig. 10–2.

(2) The base-cut-out sequence of BOUMA (1962): This type includes the combinations of "bxde", "bcde", "bwde", "xde", "cde", "wde", "de" and "e", and can be observed in most localties (Fig. 15). This type of beds are exemplified by Figs. 10–3 and –4.

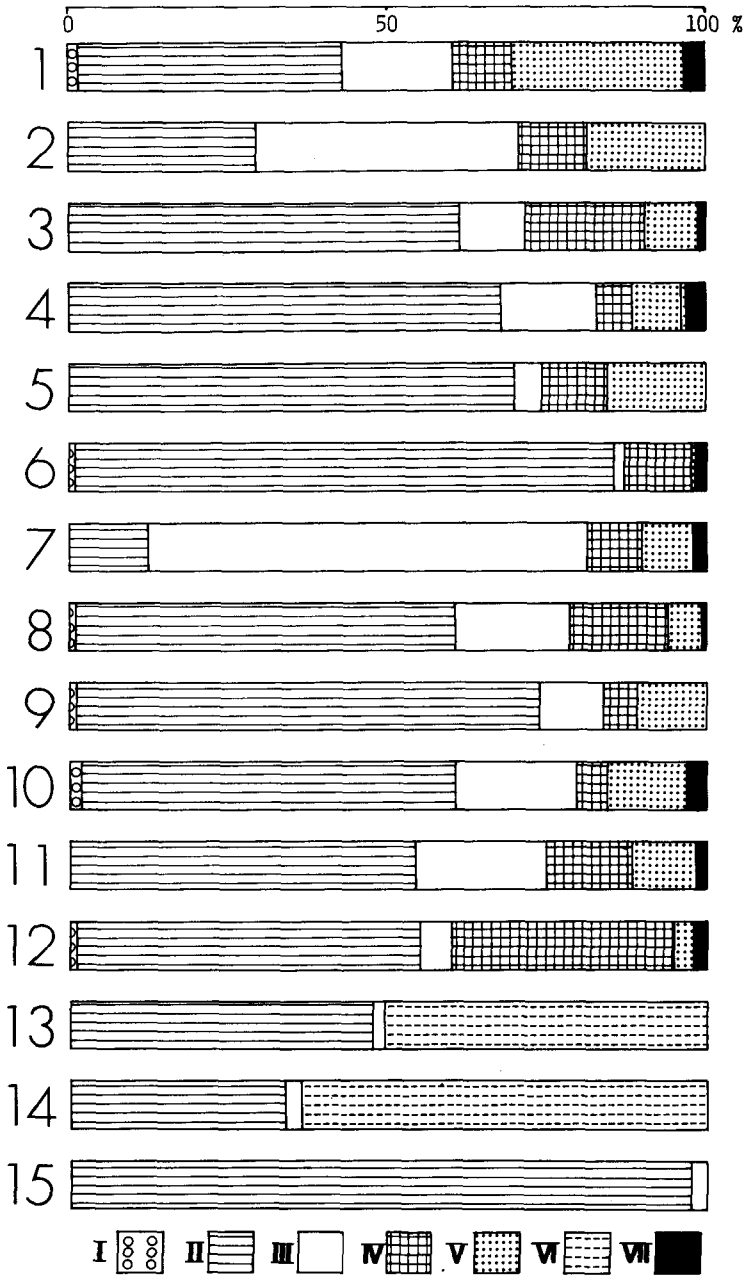

Fig. 15. Proportion of various kinds of the combination of sedimentary divisions in individual beds. I: complete sequence, II: base-cut-out sequence, III: middle-part-depleted sequence, IV: truncated sequence, V & VI: beds which do not show the BOUMA sequence (V: "se" sequence and its variations, VI: "pxde" sequence and its variations), VII: others.

(3) The middle-part-depleted sequence: This type includes both base-cut-out and non base-cut-out sequences. The division depleted in the sequence is usually d-division (Fig. 10–5). It can be observed in all localities, though not so common, occupying 10%–20% of the total. At Locs. 2 and 7, however, it attains to 40% and 70%, respectively.

(4) The truncated sequence of BOUMA (1962): This type includes beds whose middle part and/or basal parts are absent. This type of sequence does not occupy the significant portion of the total beds. Exceptionally, at Loc. 12, it occupies more than one-thirds of the total, but at Locs. 13, 14 and 15, it is not observed. This type of beds are exemplified by Fig. 10–10.

(5) The sequences not showing the BOUMA sequence: This type occupies around 15% of the total or less. At Locs. 1 and 2, the "se" sequence is well developed (Fig. 15), and at Locs. 13 and 14, the "pxde" sequence and its variations are dominant.

The characteristic combination at each locality is as follows: At Loc. 1, the "se" sequence is well developed as well as the base-cut-out sequence. At Locs. 2 and 7, the middle-part-depleted sequence is developed. At Loc. 12, the truncated sequence is exceptionally well developed among fifteen localities. At Locs. 13 and 14, the "pxde" sequence is dominant, occupying more than a half of the total beds. At other localities than ones mentioned above, the most significant type of sequence is the base-cut-out sequence.

Vertical transitions of sedimentary divisions

The Markov chain analysis was used to clarify the mode of the vertical transitions of the nine divisions. The Markov chain analysis has been mainly used for the analysis of the vertical transitions of lithofacies (OSBORNE, 1971; HATTORI, 1976). In this study, however, the analysis was applied to the transition of the sedimentary divisions. Therefore, the symmetric elements (where $i=j$ in matrix $\mathbf{r}ij$) are not necessarily zero. Even if the same kind of sedimentary divisions are in contact with each other, the two cannot be recognized as one continuous hydraulic state, but two states. The method using this kind of matrix is called as "method 2" by MIALL (1973), and is used in this study.

The vertical transitions of divisions at each locality was tested for the first-order Markov property by chi-square test. The significance levels for localities are all more than 99%.

Transition-count matrices are shown in Table 7. In difference matrices shown in in Table 8, one positive value means that the probability of the transition from one state to the next state is much more larger than the probability estimated based on the relative proportion of the state present. And this transition cannot be attributed to the random processes.

Based on the difference matrices, the tendency of each sedimentary division,

Table 7. Transition-count (tally) matrices of the vertical transitions of sedimentary divisions at fifteen localities.

1

	a	b	p	x	c	w	d	e	s	total
a	0	7	-	2	0	1	2	2	0	14
b	0	0	-	3	1	1	4	2	0	10
p	-	-	-	-	-	-	-	-	-	-
x	1	1	-	0	0	0	5	3	0	10
c	0	0	-	0	0	0	0	1	0	1
w	0	0	-	0	0	0	0	1	0	1
d	4	0	-	0	0	0	2	31	0	37
e	9	2	-	4	0	0	20	5	11	51
s	0	0	-	0	0	0	2	10	0	12
										136

2

	a	b	p	x	c	w	d	e	s	total
a	0	6	-	4	1	0	0	1	0	12
b	0	0	-	28	0	1	2	2	0	33
p	-	-	-	-	-	-	-	-	-	-
x	1	1	-	0	0	1	9	47	0	59
c	0	0	-	0	0	0	0	1	0	1
w	0	0	-	0	0	0	1	7	0	8
d	1	1	-	2	0	0	7	30	0	41
e	7	22	-	24	0	7	22	6	22	110
s	0	0	-	0	0	0	0	24	0	24
										288

3

	a	b	p	x	c	w	d	e	s	total
a	-	-	-	-	-	-	-	-	-	-
b	-	0	-	7	-	0	0	0	0	7
p	-	-	-	-	-	-	-	-	-	-
x	-	0	-	0	-	0	17	9	0	26
c	-	-	-	-	-	-	-	-	-	-
w	-	0	-	0	-	0	2	0	0	2
d	-	1	-	6	-	2	5	38	0	52
e	-	6	-	13	-	0	29	20	8	76
s	-	0	-	0	-	0	0	8	0	8
										171

4

	a	b	p	x	c	w	d	e	s	total
a	0	1	0	0	0	-	0	0	0	1
b	0	0	0	4	5	-	1	1	0	11
p	0	0	0	1	0	-	0	0	0	1
x	0	0	0	0	0	-	5	8	0	13
c	0	0	0	0	0	-	4	5	0	9
w	-	-	-	-	-	-	-	-	-	-
d	0	2	0	1	0	-	3	26	1	33
e	1	7	1	7	3	-	18	21	19	77
s	0	0	0	0	0	-	3	18	0	21
										166

5

	a	b	p	x	c	w	d	e	s	total
a	0	1	-	1	0	0	0	0	0	2
b	0	0	-	3	0	0	0	0	0	3
p	-	-	-	-	-	-	-	-	-	-
x	0	0	-	0	0	0	9	5	0	14
c	0	0	-	1	0	0	0	0	0	1
w	0	0	-	0	0	0	1	0	0	1
d	1	0	-	0	0	0	0	38	0	39
e	1	2	-	9	1	1	32	37	5	88
s	0	0	-	0	0	0	0	5	0	5
										153

6

	a	b	p	x	c	w	d	e	s	total
a	0	1	-	0	0	0	1	1	0	3
b	0	1	-	1	0	1	0	0	0	2
p	-	-	-	-	-	-	-	-	-	-
x	1	0	-	0	1	0	16	0	1	19
c	0	0	-	0	0	0	2	0	0	2
w	0	0	-	0	0	0	2	0	0	2
d	0	0	-	5	0	1	8	76	0	90
e	5	1	-	10	1	0	59	31	2	109
s	0	0	-	0	0	0	2	1	0	3
										230

7

	a	b	p	x	c	w	d	e	s	total
a	0	4	-	4	1	0	0	0	0	9
b	0	5	-	21	3	3	2	4	5	43
p	-	-	-	-	-	-	-	-	-	-
x	1	2	-	2	0	0	8	84	2	99
c	0	0	-	0	0	0	0	3	0	3
w	0	0	-	2	0	0	0	1	0	3
d	0	0	-	1	0	0	1	17	0	19
e	9	28	-	63	0	0	7	1	11	119
s	0	1	-	2	0	0	1	14	0	18
										313

8

	a	b	p	x	c	w	d	e	s	total
a	0	5	-	2	0	1	3	0	0	11
b	0	0	-	8	5	2	1	0	0	16
p	-	-	-	-	-	-	-	-	-	-
x	1	0	-	0	1	0	20	13	0	35
c	0	1	-	0	0	0	9	2	0	12
w	0	0	-	0	0	0	3	6	0	9
d	1	2	-	5	1	0	12	69	1	91
e	6	6	-	15	5	6	34	15	8	95
s	0	0	-	0	0	0	2	6	0	8
										277

9

	a	b	p	x	c	w	d	e	s	total
a	0	2	-	0	0	0	0	0	0	2
b	0	0	-	5	2	0	0	0	0	7
p	-	-	-	-	-	-	-	-	-	-
x	0	0	-	0	0	0	9	9	0	18
c	0	0	-	0	0	0	2	0	0	2
w	0	0	-	0	0	0	2	1	0	3
d	0	1	-	2	0	0	4	50	0	57
e	2	3	-	12	0	3	38	30	12	100
s	0	0	-	0	0	0	0	12	0	12
										201

10

	a	b	p	x	c	w	d	e	s	total
a	0	3	-	0	0	0	0	0	0	3
b	0	0	-	5	4	0	0	0	0	9
p	-	-	-	-	-	-	-	-	-	-
x	0	0	-	0	1	0	17	10	0	28
c	0	0	-	0	0	0	1	4	0	5
w	0	0	-	0	0	0	3	-	-	3
d	0	0	-	2	0	0	3	29	0	34
e	2	6	-	18	1	1	10	10	9	57
s	0	0	-	2	0	0	1	6	0	9
										148

11

	a	b	p	x	c	w	d	e	s	total
a	0	1	-	0	0	0	1	0	0	2
b	0	0	-	8	1	0	0	0	0	9
p	-	-	-	-	-	-	-	-	-	-
x	0	0	-	2	0	0	11	20	3	36
c	0	0	-	0	0	0	1	1	0	2
w	0	0	-	0	0	0	1	1	0	2
d	0	0	-	4	0	0	4	47	0	55
e	2	8	-	17	2	2	36	16	9	92
s	0	0	-	3	0	0	1	8	0	12
										210

12

	a	b	p	x	c	w	d	e	s	total
a	0	4	-	0	1	0	0	0	0	5
b	0	0	-	7	2	2	0	0	0	11
p	-	-	-	-	-	-	-	-	-	-
x	0	0	-	1	0	0	19	7	1	28
c	0	0	-	0	0	0	2	1	0	3
w	0	0	-	0	0	0	2	2	0	4
d	2	2	-	9	0	0	9	33	1	56
e	3	6	-	8	0	2	23	22	1	65
s	0	0	-	0	0	0	1	3	0	4
										176

13

	a	b	p	x	c	w	d	e	s	total
a	-	-	-	-	-	-	-	-	-	-
b	-	-	-	-	-	-	-	-	-	-
p	-	-	0	23	-	1	3	1	-	28
x	-	-	2	0	-	0	25	6	-	33
c	-	-	-	-	-	-	-	-	-	-
w	-	-	0	0	-	0	2	0	-	2
d	-	-	0	0	-	0	0	43	-	43
e	-	-	23	12	-	1	12	0	-	48
s	-	-	-	-	-	-	-	-	-	-
										154

14

	a	b	p	x	c	w	d	e	s	s(L)	total
a	-	-	-	-	-	-	-	-	-	-	-
b	-	-	-	-	-	-	-	-	-	-	-
p	-	-	0	21	1	0	0	0	0	0	22
x	-	-	1	-	-	-	29	3	0	0	33
c	-	-	0	0	0	0	1	0	0	0	1
w	-	-	0	0	0	0	1	0	0	0	1
d	-	-	1	0	0	0	0	35	0	0	36
e	-	-	16	10	0	1	4	0	6	0	37
s(L)	-	-	4	2	0	0	0	0	0	0	6
											136

15

	a	b	p	x	c	w	d	e	s	total
a	-	-	-	-	-	-	-	-	-	-
b	-	-	-	-	-	-	-	-	-	-
p	-	-	-	-	-	-	-	-	-	-
x	-	-	-	0	-	0	7	1	-	8
c	-	-	-	-	-	-	-	-	-	-
w	-	-	-	0	-	0	1	0	-	1
d	-	-	-	0	-	0	0	38	-	38
e	-	-	-	7	-	2	30	0	-	39
s	-	-	-	-	-	-	-	-	-	-
										86

Table 8. Difference matrices of the vertical transitions of sedimentary divisions at fifteen localities.

1

	a	b	p	x	c	w	d	e	s
a	-0.103	0.427	-	0.078	-0.007	0.064	-0.115	-0.262	-0.081
b	-0.103	-0.074	-	0.234	0.093	-0.007	0.143	-0.204	-0.081
p	-	-	-	-	-	-	-	-	-
x	-0.003	0.027	-	-0.066	-0.007	-0.007	0.243	-0.104	-0.081
c	-0.003	-0.074	-	-0.066	-0.007	-0.007	-0.257	0.596	-0.081
w	-0.103	-0.074	-	-0.066	-0.007	-0.007	-0.257	0.596	-0.081
d	0.005	-0.074	-	-0.066	-0.007	-0.007	-0.203	0.433	-0.081
e	0.074	-0.034	-	0.012	-0.007	-0.007	0.135	-0.306	0.135
s	-0.103	-0.074	-	-0.066	-0.007	-0.007	-0.091	0.429	-0.081

2

	a	b	p	x	c	w	d	e	s
a	-0.031	0.396	-	0.132	0.080	-0.031	-0.142	-0.326	-0.076
b	-0.031	-0.104	-	0.647	-0.003	-0.001	-0.082	-0.349	-0.076
p	-	-	-	-	-	-	-	-	-
x	-0.014	-0.087	-	-0.201	-0.003	-0.014	0.010	0.387	-0.076
c	-0.031	-0.104	-	-0.201	-0.003	-0.031	-0.142	0.590	-0.076
w	-0.031	-0.104	-	-0.201	-0.003	-0.031	-0.018	0.465	-0.076
d	-0.007	-0.080	-	-0.153	-0.003	-0.031	0.028	0.322	-0.076
e	0.032	0.096	-	0.017	-0.003	0.032	0.057	-0.355	0.124
s	-0.031	-0.104	-	-0.201	-0.003	-0.031	-0.142	0.590	-0.076

3

	a	b	p	x	c	w	d	e	s
a	-	-	-	-	-	-	-	-	-
b	-	-0.041	-	0.848	-	-0.012	-0.310	-0.439	-0.047
p	-	-	-	-	-	-	-	-	-
x	-	-0.041	-	-0.152	-	-0.012	0.344	-0.092	-0.047
c	-	-	-	-	-	-	-	-	-
w	-	-0.041	-	-0.152	-	-0.012	0.690	-0.439	-0.047
d	-	-0.022	-	-0.037	-	0.027	-0.214	0.292	-0.047
e	-	0.038	-	0.019	-	-0.012	0.072	-0.175	0.059
s	-	-0.041	-	-0.152	-	-0.012	-0.310	0.561	-0.047

4

	a	b	p	x	c	w	d	e	s
a	-0.006	0.940	-0.006	-0.078	-0.048	-	-0.205	-0.476	-0.120
b	-0.006	-0.060	-0.006	0.285	0.406	-	-0.114	-0.385	-0.120
p	-0.006	-0.060	-0.006	0.922	-0.048	-	-0.205	-0.476	-0.120
x	-0.006	-0.060	-0.006	-0.078	-0.048	-	0.180	0.140	-0.120
c	-0.006	-0.060	-0.006	-0.078	-0.048	-	0.240	0.080	-0.120
w	-	-	-	-	-	-	-	-	-
d	-0.006	0.000	-0.006	-0.048	-0.048	-	-0.114	0.312	-0.090
e	0.007	0.031	0.007	0.013	-0.009	-	0.030	-0.203	0.126
s	-0.006	-0.060	-0.006	-0.078	-0.048	-	-0.062	0.381	-0.120

5

	a	b	p	x	c	w	d	e	s
a	-0.013	0.480	-	0.408	-0.007	-0.007	-0.275	-0.556	-0.033
b	-0.013	-0.020	-	0.909	-0.007	-0.007	-0.275	-0.556	-0.033
p	-	-	-	-	-	-	-	-	-
x	-0.013	-0.020	-	-0.092	-0.007	-0.007	0.368	-0.199	-0.033
c	-0.013	-0.020	-	0.909	-0.007	-0.007	-0.275	-0.556	-0.033
w	-0.013	-0.020	-	-0.092	-0.007	-0.007	0.725	-0.556	-0.033
d	0.013	-0.020	-	-0.092	-0.007	-0.007	-0.275	0.419	-0.033
e	-0.002	0.003	-	0.011	0.005	0.005	0.089	-0.135	0.024
s	-0.013	-0.020	-	-0.092	-0.007	-0.007	-0.275	0.444	-0.033

6

	a	b	p	x	c	w	d	e	s
a	-0.026	0.325	-	-0.070	-0.009	-0.009	-0.058	-0.141	-0.013
b	-0.026	-0.009	-	0.430	-0.009	0.491	-0.391	-0.474	-0.013
p	-	-	-	-	-	-	-	-	-
x	0.027	-0.009	-	-0.070	0.044	-0.009	0.451	-0.474	0.040
c	-0.026	-0.009	-	-0.070	-0.009	-0.009	0.609	-0.474	-0.013
w	-0.026	-0.009	-	-0.070	-0.009	-0.009	0.609	-0.474	-0.013
d	-0.026	-0.009	-	-0.014	-0.009	0.002	-0.302	0.390	-0.013
e	0.020	0.001	-	0.022	0.005	-0.009	0.150	-0.190	0.005
s	-0.026	-0.009	-	-0.070	-0.009	-0.009	0.275	-0.141	-0.013

7

	a	b	p	x	c	w	d	e	s
a	-0.032	0.317	-	0.141	0.098	-0.010	-0.061	-0.396	-0.058
b	-0.032	-0.012	-	0.185	0.057	0.060	-0.014	-0.303	0.059
p	-	-	-	-	-	-	-	-	-
x	-0.022	-0.108	-	-0.283	-0.013	-0.010	0.020	0.452	-0.037
c	-0.032	-0.128	-	-0.304	-0.013	-0.010	-0.061	0.604	-0.058
w	-0.032	-0.128	-	0.363	-0.013	-0.010	-0.061	-0.063	-0.058
d	-0.032	-0.128	-	-0.251	-0.013	-0.010	-0.008	0.499	-0.058
e	0.044	0.108	-	0.226	-0.013	-0.010	-0.002	-0.388	0.035
s	-0.032	-0.072	-	-0.192	-0.013	-0.010	-0.005	0.382	-0.058

8

	a	b	p	x	c	w	d	e	s
a	-0.029	0.404	-	0.074	-0.043	0.058	-0.031	-0.401	-0.032
b	-0.029	-0.051	-	0.392	0.269	0.093	-0.241	-0.401	-0.032
p	-	-	-	-	-	-	-	-	-
x	-0.000	-0.051	-	-0.108	-0.015	-0.032	0.268	-0.029	-0.032
c	-0.029	0.033	-	-0.108	-0.043	-0.032	0.447	-0.234	-0.032
w	-0.029	-0.051	-	-0.108	-0.043	-0.032	0.030	0.266	-0.032
d	-0.018	-0.028	-	-0.053	-0.032	-0.032	-0.171	0.358	-0.021
e	0.034	0.013	-	0.050	0.009	0.031	0.055	-0.243	0.052
s	-0.029	-0.051	-	-0.108	-0.043	-0.032	-0.053	0.349	-0.032

9

	a	b	p	x	c	w	d	e	s
a	-0.010	0.970	-	-0.095	-0.010	-0.015	-0.274	-0.507	-0.060
b	-0.010	-0.030	-	0.620	0.276	-0.015	-0.274	-0.507	-0.060
p	-	-	-	-	-	-	-	-	-
x	-0.010	-0.030	-	-0.095	-0.010	-0.015	0.226	-0.007	-0.060
c	-0.010	-0.030	-	-0.095	-0.010	-0.015	0.726	-0.507	-0.060
w	-0.010	-0.030	-	-0.095	-0.010	-0.015	0.393	-0.174	-0.060
d	-0.010	-0.012	-	-0.059	-0.010	-0.015	-0.203	0.370	-0.060
e	0.020	0.000	-	0.025	-0.010	0.015	0.106	-0.208	0.060
s	-0.010	-0.030	-	-0.095	-0.010	-0.015	-0.274	0.493	-0.060

10

	a	b	p	x	c	w	d	e	s
a	-0.014	0.939	-	-0.182	-0.041	-0.007	-0.236	-0.399	-0.061
b	-0.014	-0.061	-	0.373	0.404	-0.007	-0.236	-0.399	-0.061
p	-	-	-	-	-	-	-	-	-
x	-0.014	-0.061	-	-0.182	-0.000	-0.007	0.371	-0.042	-0.061
c	-0.014	-0.061	-	-0.182	-0.041	-0.007	-0.036	0.401	-0.061
w	-0.141	-0.061	-	-0.182	-0.041	-0.007	0.764	-0.399	-0.061
d	-0.141	-0.061	-	-0.124	-0.041	-0.007	-0.148	0.454	-0.061
e	0.022	0.044	-	0.133	-0.023	0.011	-0.061	-0.223	0.097
s	-0.014	-0.061	-	0.040	-0.041	-0.007	-0.125	0.268	-0.061

11

	a	b	p	x	c	w	d	e	s
a	-0.010	0.457	-	-0.162	-0.014	-0.010	0.238	-0.443	-0.057
b	-0.010	-0.043	-	0.727	0.097	-0.010	-0.262	-0.443	-0.057
p	-	-	-	-	-	-	-	-	-
x	-0.010	-0.043	-	-0.106	-0.014	-0.010	0.044	0.113	0.026
c	-0.010	-0.043	-	-0.162	-0.014	-0.010	0.238	0.057	-0.057
w	-0.010	-0.043	-	-0.162	-0.014	-0.010	0.238	0.057	-0.057
d	-0.010	-0.043	-	-0.089	-0.014	-0.010	-0.189	0.412	-0.057
e	0.012	0.044	-	0.023	0.007	0.012	0.129	-0.269	0.041
s	-0.010	-0.043	-	0.088	-0.014	-0.010	-0.179	0.224	-0.057

12

	a	b	p	x	c	w	d	e	s
a	-0.028	0.732	-	-0.142	0.183	-0.023	-0.318	-0.386	-0.017
b	-0.028	-0.068	-	0.494	0.165	0.159	-0.318	-0.386	-0.017
p	-	-	-	-	-	-	-	-	-
x	-0.028	-0.068	-	-0.106	-0.017	-0.023	0.360	-0.136	0.019
c	-0.028	-0.068	-	-0.142	-0.017	-0.023	0.348	-0.053	-0.017
w	-0.028	-0.068	-	-0.142	-0.017	-0.023	0.182	0.114	-0.017
d	0.007	-0.032	-	0.019	-0.017	-0.023	-0.157	0.203	0.001
e	0.018	0.024	-	-0.019	-0.017	0.008	0.036	-0.048	-0.002
s	-0.028	-0.068	-	-0.142	-0.017	-0.023	-0.068	0.364	-0.017

13

	a	b	p	x	c	w	d	e	s
a	-	-	-	-	-	-	-	-	-
b	-	-	-	-	-	-	-	-	-
p	-	-	-0.162	0.594	-	0.023	-0.166	-0.289	-
x	-	-	-0.102	-0.227	-	-0.013	0.485	-0.143	-
c	-	-	-	-	-	-	-	-	-
w	-	-	-0.162	-0.227	-	-0.013	0.727	-0.325	-
d	-	-	-0.162	-0.227	-	-0.013	-0.277	0.675	-
e	-	-	0.317	0.023	-	0.008	-0.023	-0.325	-
s	-	-	-	-	-	-	-	-	-

14

	a	b	p	x	c	w	d	e	s(L)
a	-	-	-	-	-	-	-	-	-
b	-	-	-	-	-	-	-	-	-
p	-	-	-0.162	0.712	0.038	-0.007	-0.257	-0.279	-0.044
x	-	-	-0.131	-0.243	-0.007	-0.007	0.621	-0.189	-0.044
c	-	-	-0.162	-0.243	-0.007	-0.007	0.743	-0.279	-0.044
w	-	-	-0.162	-0.243	-0.007	-0.007	0.743	-0.279	-0.044
d	-	-	-0.134	-0.243	-0.007	-0.007	-0.257	0.693	-0.044
e	-	-	0.271	0.028	-0.007	0.020	-0.149	-0.279	0.118
s(L)	-	-	0.505	0.091	-0.007	-0.007	-0.257	-0.279	-0.044

15

	a	b	p	x	c	w	d	e	s
a	-	-	-	-	-	-	-	-	-
b	-	-	-	-	-	-	-	-	-
p	-	-	-	-	-	-	-	-	-
x	-	-	-	-0.081	-	-0.023	0.433	-0.328	-
c	-	-	-	-	-	-	-	-	-
w	-	-	-	-0.081	-	-0.023	0.558	-0.453	-
d	-	-	-	-0.081	-	-0.023	-0.442	0.547	-
e	-	-	-	0.098	-	0.028	0.327	-0.453	-
s	-	-	-	-	-	-	-	-	-

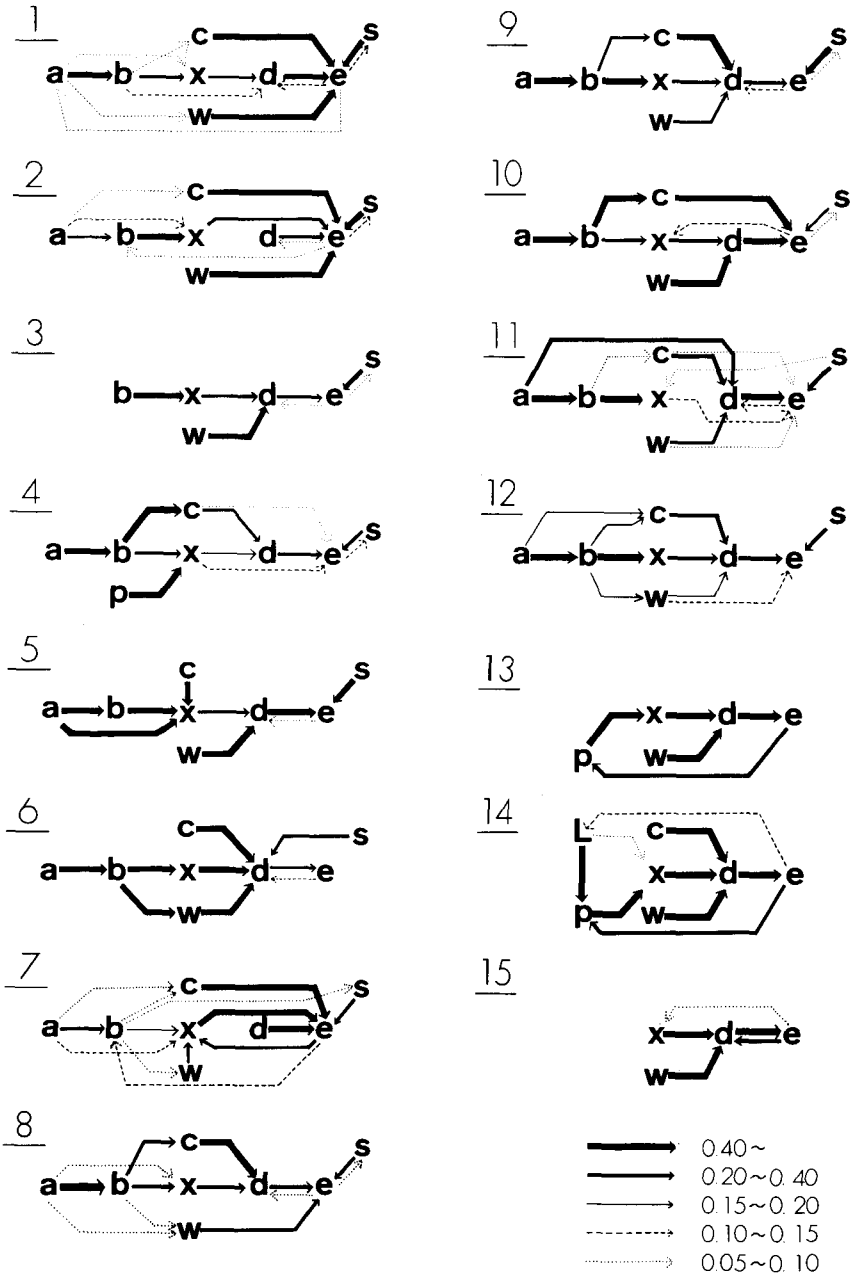

Fig. 16. Transition patterns based on the difference matrices. Values are those in the difference matrices.

which represents a certain hydraulic state, to be followed by what kind of divisions, are summarized in Fig. 16, and also as follows:

(1) From a-division: The transition to b-division is observed with higher values of the difference at all localities where a-division is present. The transitions to x-, c- or w-divisions are also observed in some localities, though the values of the difference are low.

(2) From b-division: The transition to x-division is constantly observed. Together with this, the transitions to c- or w-divisions are also observed at not a few localities.

(3) From p-division: The transition to x-division is strongly indicated with high positive values at Locs. 13 and 14. Other kind of transition is not observed.

(4) From x-, c- and w-divisions: The transitions to d-division are indicated with a little high values at most localities. However, the transitions to e-division are also observed at some localities, such as Locs. 1, 2 and 7.

(5) From d-divisions: The transitions to e-division are constantly observed with high values, and other kinds of transitions are not developed.

(6) From e-division: The transitions to other divisions all show very low values of the difference. The exceptions are the transitions to x-division at Loc. 7, to p-divisions at Locs. 13 and 14, and to d-division at Loc. 15 (Table 8). The transitions to d- or s-divisions are observed in some localities, but the values of the difference are very low.

(7) From s-division: The transitions to e-division constantly show high values at most localities. The transitions to other divisions can be only rarely observed.

Based on the these analyses four dominant patterns of the transitions were recognized as follows:

Transition pattern (i): a→b→x (or c, w)→d→e

This is the most dominant pattern in the studied sections, and are recognized at the majority of localities. This patern corresponds to the typical sequence of turbidite, and also to the complete and the base-cut-out sequences mentioned above (see p. 24).

Transition pattern (ii): a→b→x (or c, w)→e

This pattern is characterized by the lack of d-division. It is observed at Locs. 2, 7 and 11. This pattern is also observed at several other localities, but the values of the difference are lower than those of pattern (i). It is concluded that these two patterns, (i) and (ii), can coexist together. This transition pattern corresponds to the middle-part-depleted sequence and possibly also to the truncated sequence.

Transition pattern (iii): s→e

This pattern of the transition is developed in most localities where s-division is developed.

Transition pattern (iv): p→x→d→e→p→

Only this pattern of the transition show the cyclic nature. It is noteworthy that

this pattern does not coexist with patern (iii) at the same locality.

Besides the four patterns mentioned above, d→e pattern is observed clearly at Locs. 2 and 7, and also at Locs. 1 and 11.

Classification of beds in muddy alternation

The beds in muddy alternation can be classified into four types, namely, types A1, A2, B1 and B2, as shown in Table 9, based on the combinations of sedimentary divisions and the vertical transition patterns of them discussed above. Among these four types, types A1 and A2 beds show the BOUMA sequence, and types B1 and B2 beds do not show the BOUMA sequence.

Table 9. Classification of sediment types of muddy alternation based on the combination of sedimentary divisions and the transition patterns of divisions.

Sediment type		Bouma sequence	Combination of sedimentary divisions	Transition patterns	Typical locality
A	A1	applicable	complete sequence base-cut-out sequence	a→b→x(,c,w)→d→e	Locs. 1, 3, 4, 5, 6, 8, 9 & 10
	A2	applicable	middle-part-depleted sequence truncated sequence	a→b→x(,c,w)→e	Locs. 2, 7 & 11
B	B1	not applicable	"pxde" sequence and its variations	p→x→d→e→p→	Locs. 13, 14 & 15
	B2	not applicable	"se" sequence and its variations	s→e	Locs. 1 - 12

Type A1: This type of beds are represented by the complete sequence and the base-cut-out one. They are dominated at Locs. 1–12, except Locs. 2, 7 and 11. In these localities, the transition pattern (i) is strongly indicated. The range of the distributions of the thickness of sandstone part and the mud-sand ratio are very wide. This type of beds mostly show grading and type I-a bedding.

Type A2: This type of beds are represented by the middle-part-depleted and the truncated sequences. They are observed at Locs. 1–12, though the frequency is lower than type A1 beds. They are dominant at Locs. 2, 7 and 11. At Loc. 7, the distribution of thickness of sandstone part and that of the mud-sand ratio are both relatively narrow in range. The transition pattern (ii) characterizes this type of beds.

Type B1: Beds of this type show the "pxde" sequence and its variations. Transition pattern (iv) characterizes this type of beds. They are developed restrictedly in Locs. 13–15. In these localities, the thickness of sandstone and mudstone parts, and the mud-sand ratio shows the concentrated distribution. This type of beds does not coexist together with beds starting with a- or b-divisions.

Type B2: This type of beds shows the "se" sequence and its variations, and is characterized by the transition pattern (iii). They are observable at Locs. 1–12, coexisting with beds of types A1 and A2.

2. Angular clast-bearing mudstone

The angular clast-bearing mudstones are developed mainly in the southern part

of the study area. They are observed in all formations, but less developed in the Shimosato Formation than in other formations. They are important to reconstruct the paleobasin.

A. Occurrence

Angular clast-bearing mudstones are composed of muddy matrix and clasts, which are scattered randomly in the matrix. They are classified into two types based on the nature of their clasts. The first one (type I) is characterized by the presence of sandstone clasts which show the features of the soft-sediment deformation, and the other by its absence. The color, grain-size and other features of matrices of both types are similar to each other.

Type I

Angular clast-bearing mudstones of this type range from 1 to 50 m in thickness, and are mostly developed in the Mitsuno Formation and partly in Member Smu of the Shimosato Formation and the lower part of the Shikiya Formation (Fig. 3). Those in the Mitsuno Formation can be traced laterally for 2–3 km, and other angular clast-bearing mudstone bodies can be traced for hundred of meters, and then abruptly wedge out laterally.

Type I angular clast-bearing mudstone entirely lack in sedimentary structures. Clasts are mostly angular to subangular, pebble- to cobble-sized (Plate 4–2), and consist of mudstone and very fine- to fine-grained sandstone. Sandstone blocks (max. 10 m or more in diameter) which show slump folds, are sometimes observed.

Type II

This type of angular clast-bearing mudstones are mostly restricted within the lower part of the Shikiya Formation, except for a 0.5–1 m thick body in the basal part of the Shimosato Formation at Tanosaki. Among these, two bodies found at Koza and at the west of Kusu, can be traced laterally for 2–3 km. The rests can be traced for less than several hundred meters and pinch out into mudstones.

Most of type II angular clast-bearing mudstones are structureless and massive (Plate 4–1). Clasts are angular to subangular, pebble- to boulder-sized, and consist of quartzose, fine- to coarse-grained sandstone and mudstone. Clasts of orthoquartzite pebble-bearing conglomerate are sometimes observed. Such a conglomerate is developed in the Muro Group, but cannot be observed in the Kumano Group. By this reason, it is concluded that these clasts were derived from the Muro Group.

The angular clast-bearing mudstone bed at Tanosaki truncates down into muddy alternation. The depth of the truncation attains to about 6 m with the lateral separation of about 50 m.

Among the type II angular clast-bearing mudstone, that developed at Tsuga is distinct in having bedding and some sedimentary structures (Fig. 17). The angular

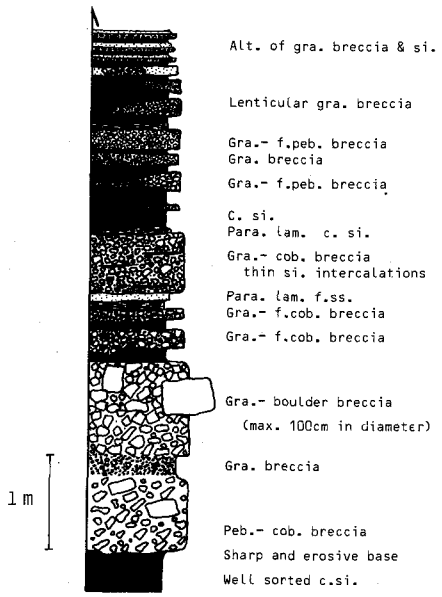

Fig. 17. Columnar section of bedded angular clast-bearing mudstone body developed at Tsuga. Lower part of the Shikiya Formation.

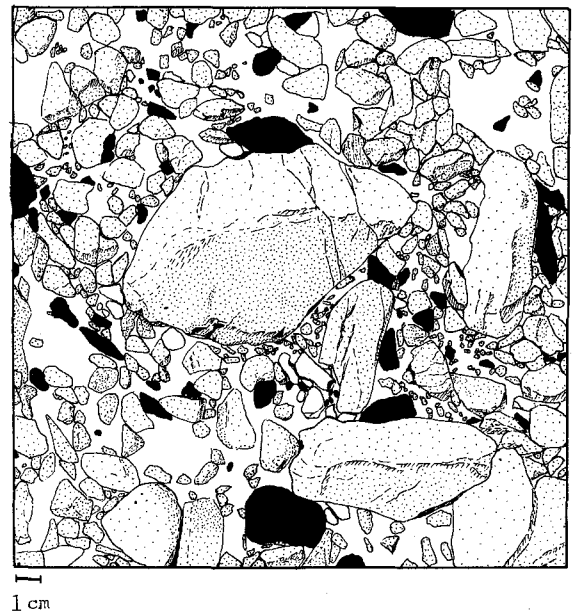

Fig. 18. Sketch showing the occurrence of angular clast-bearing mudstone in the Tsuga body. The horizon is about 1.5 m above the bottom of the body (see Fig. 17).

clast-bearing mudstones are composed of granule- to boulder-sized clasts and muddy matrix. The clasts are closely packed and clast-supported, and the amount of matrix is very small (Fig. 18).

The clast-size of each angular clast-bearing mudstone bed gradually decreases upward in the sequence (Fig. 17), and is overlain by bedded mudstone, typical of the Shikiya Formation.

B. Natures of clasts

Clast-size, roundness and rock-composition were analyzed at three localities, that is, at Tanosaki (type II), at Tsuga (type II) and at Okatsuura (type I). In these analyses, all clasts (larger than 1 cm across) in an area of one square meters are measured.

Clast-size

The median values of clast-size distributions are 3.9, 7.8 and 4.2 cm, respectively (Fig. 19A). However, at all localities, very large clasts, 50–150 cm in diameter, are included (Fig. 19B). Among these bodies, the one at Tsuga shows the Gaussian distribution in clast-size distribution (Fig. 19A, dotted line). And the other two show

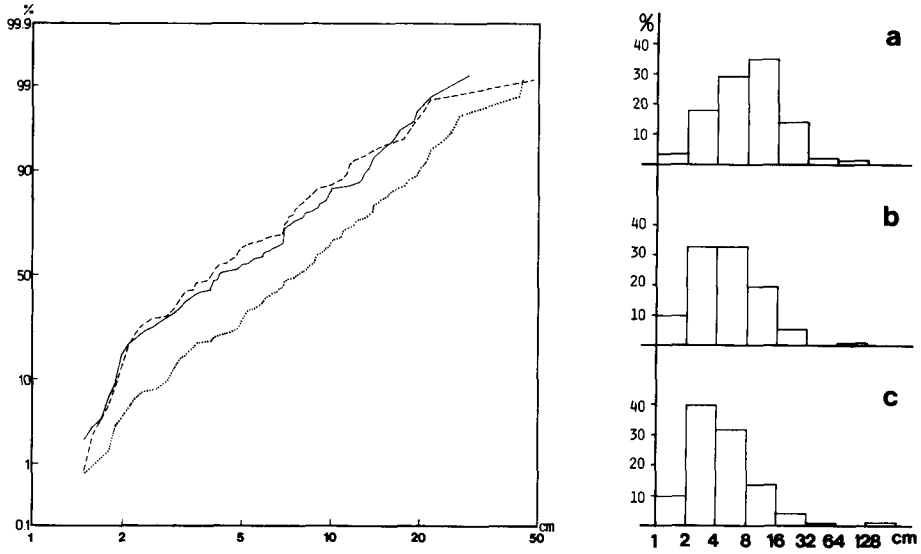

Fig. 19. A: Cumulative frequency curves of the clast-size distribution of angular clast-bearing mudstons. Dotted line: Tsuga, solid line: Okatsuura, broken line: Tanosaki. B: Histograms showing the clast-size distribution of angular clast-bearing mudstone. a: Tsuga, b: Okatsuura, c: Tanosaki.

higher proportion of clast smaller than 2 cm in diameter. It is notable that the gradient of three curves are almost same. This fact and the similarity of the sedimentary occurrences of types I and II, both suggest that two types were transported by similar flow mechanism.

Roundness

The roundness of clasts is characterized by the abundance of angular and subangular clasts and also by the scarcity of rounded clasts. No well-rounded clasts could be found. In angular clast-bearing mudstone at Tsuga, angular clasts are relatively less abundant, and the most of clasts are subangular to subrounded (Fig. 20).

Rock-composition

The rock-compositions of angular clast-bearing mudstones and of roundstone conglomerate are shown in Fig. 21. Type I angular clast-bearing mudstone at Okatsuura consists mostly of mudstone clasts. Contrarily, the other two contain some medium-grained sandstone clasts and quartz rock clasts, although most of clasts are finer in grain-size. The rock-composition of angular clast-bearing mudstones show clear contrast with that of the roundstone conglomerate, which is characterized by the abundance of chert pebbles.

Clast fabric

The clast fabric of angular clast-bearing mudstone were analyzed at three

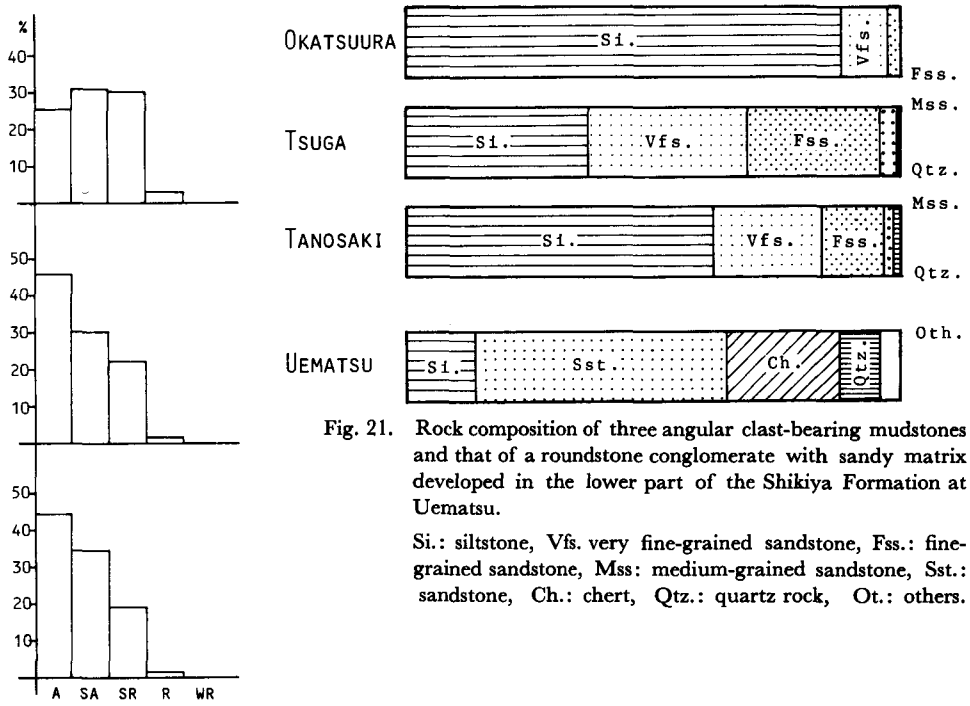

Fig. 21. Rock composition of three angular clast-bearing mudstones and that of a roundstone conglomerate with sandy matrix developed in the lower part of the Shikiya Formation at Uematsu.

Si.: siltstone, Vfs. very fine-grained sandstone, Fss.: fine-grained sandstone, Mss: medium-grained sandstone, Sst.: sandstone, Ch.: chert, Qtz.: quartz rock, Ot.: others.

Fig. 20. Histograms showing the roundness distribution of clasts of angular clast-bearing mudstones. a: Tsuga, b: Okatsuura, c: Tanosaki. A: angular, SA: subangular, SR: subrounded, R: rounded, WR: well rounded.

localities, that is Tanosaki, Tsuga and Ichinono. As the angular clast-bearing mudstone bed at Okatsuura is tectonically complicated, the clast fabric was examined at Ichinono (type I, Member Mb).

The analysis of clast fabrics was done by digging the clasts from the outcrop. Then the direction of a-axes of lod-shaped clasts and the dip and strike of ab-planes of disk-shaped clasts were measured.

The results of the analysis are shown in Fig. 22. The magnitude of mean vectors range from 24.1% to 75.3%. It is concluded that these concentration cannot be formed by random processes based on the Rayleigh test (POTTER and PETTIJOHN, 1977) at more than 95% of confidence.

In all cases, the degree of the concentration of ab-planes (42.9%–75.3% in mean vector magnitude) are better than those of a-axes (24.1%–45.3%). Among these, ab-planes of Tsuga body show fairly good concentration, and at Tsuga the imbrication of clasts can be observed even by naked eyes. At Tanosaki, two projections both show neither cluster nor girdle. At Tsuga, the projection of poles of ab-planes forms a cluster, and that of a-axes resembles a girdle. At Ichinono, the patterns of projections

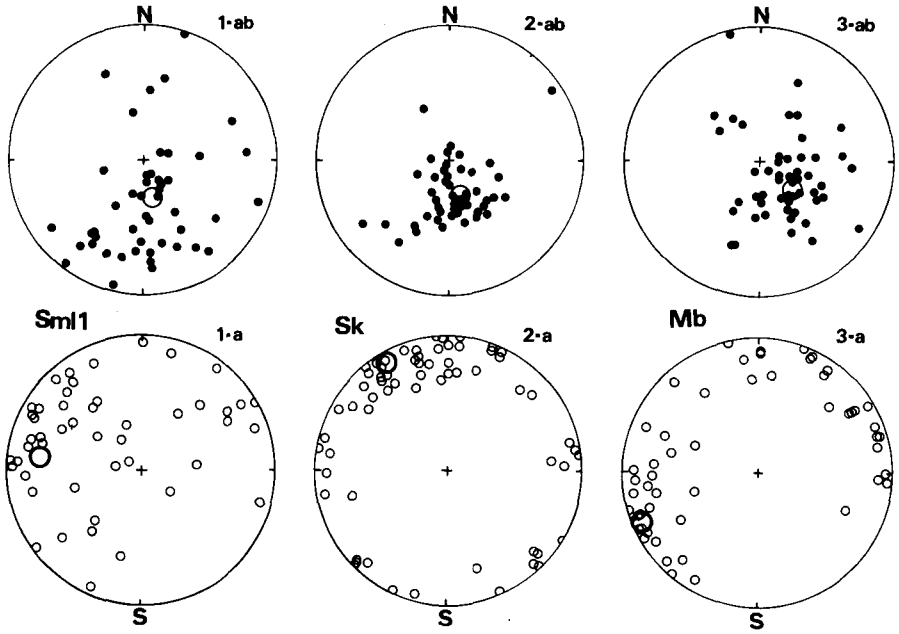

Fig. 22. Equal-area projections of poles of ab-planes and a-axes of clasts in angular clast-bearing mudstones. Lower hemisphere. 1: Tanosaki, 2: Tsuga, 3: Ichinono. Large open circle: vector means. After HISATOMI (1981).

are very similar to those of Tsuga.

The directions of mean vectors mostly trend N–S or NW–SE. The northward or northwestward dipping of a-axes and ab-planes suggest the transportation from the north or northwest. At Tanosaki, the suggested direction of the transportation well coincides with the southerly paleocurrents deduced from flute marks observed at the same locality. At the other two localities, however, paleocurrent directions could not be determined. It is notable that the degrees of the imbrication are quite high, especially on ab-planes (33.7°–46° to the north or northwest).

3. Grain-size and grain-orientation

Grain-size analysis and grain-orientation analysis were done on sandstone and mudstone samples of the Shimosato Formation and the lower part of the Shikiya Formation to clarify the sedimentation mechanisms of sediment.

A. Grain-size analysis

Grain-size analysis of sandstone and mudstone samples was made on 30 thin

sections. The apparent long axes of grains larger than 5 phi were measured on the enlarged screen of a profile projector by the point-count method. The spacing between consecutive points was 0.25 mm for mudstone samples, and 0.50 mm for sandstone samples. The measured values were grouped into every 0.25 phi classes, and were corrected after the FRIEDMAN's equation (FRIEDMAN, 1958). The grain-size parameter, such as median, one-percentile, 25-percentile and 75-percentile*, were read from the cumulative frequency curves. Phi-quartile deviations were calculated from 25- and 75-percentiles.

Table 10. Grain-size parameters of sandstone and mudstone samples. Md: median, Φ1: one percentile, Q1: 25-percentile, Q3: 75-percentile. *: values which were obtained by the extrapolation from the percentages at 4.5 and 4.75 phi.

Sample	Locality	Horizon	Md	Φ1	Q1	Q3
1	Tanosaki	Sml1	4.38	2.97	3.90	5.12*
2	Tanosaki	Sml1	3.01	1.78	2.62	3.69
3	Tanami-S	Sml1	2.25	0.70	1.78	3.01
4	Yamade-N	Sml	2.74	1.50	2.34	3.29
5	Kotachi	Smu1	3.98	2.49	3.47	4.56
6	Kotachi	Smu1	3.35	2.11	2.95	3.98
7	Kotachi	Smu1	3.14	2.08	2.76	3.64
8	Kotachi	Smu1	3.05	0.94	2.42	3.61
9	Kandorizaki	Smu2	2.59	0.73	1.84	3.50
10	Ikeshima	Smu3	2.02	-0.56	1.16	3.00
11	Tenma	Smu	2.09	0.78	1.71	2.65
12	Tawara	Smu5	3.46	2.05	2.98	4.07
13	Tawara	Smu5	3.66	2.14	3.04	4.34
14	Tawara	Smu5	3.69	2.28	3.10	4.28
15	Tawara	Smu5	3.87	2.45	3.42	4.38
16	Tawara	Smu5	3.97	2.41	3.42	4.51
17	Tawara	Smu5	4.47	2.76	4.04	5.06*
18	Tawara	Smu5	4.65	2.93	4.16	5.11*
19	Tawara	Smu5	4.69	2.76	4.04	5.06*
20	Tawara	Smu5	4.82	2.88	4.41	5.27*
21	Tawara	Smu5	2.84	1.37	2.34	3.43
22	Takinohai	Smu	3.23	1.87	2.84	3.84
23	Takinohai	Smu	3.19	1.80	2.74	4.12
24	Nassa	Smu	2.70	0.26	2.13	3.74
25	Tsuga	Sk	4.34	2.79	3.70	5.26*
26	Ishikiriiwa	Sk	3.69	2.38	3.28	4.33
27	Koza-S	Sk	3.87	2.67	3.47	4.51
28	Hashikui	Sk	4.37	2.96	3.88	5.14*
29	Meizu	Sk	4.15	2.57	3.56	4.80
30	Itaya	Mitsuno	1.62	0.37	1.14	2.30

Samples from the Shimosato Formation were mostly collected from d- and b-divisions, and partly from e- and a-divisions. Samples from the Shikiya Formation were collected from p- and d-divisions. The values of grain-size parameters and the cumulative frequency curves are shown in Table 10 and Fig. 23, respectively. It is

* The values of 75-percentile of some samples, which are marked by star in Table 10, were extrapolated from the cumulative frequency curves, because those values are finer than 5 phi.

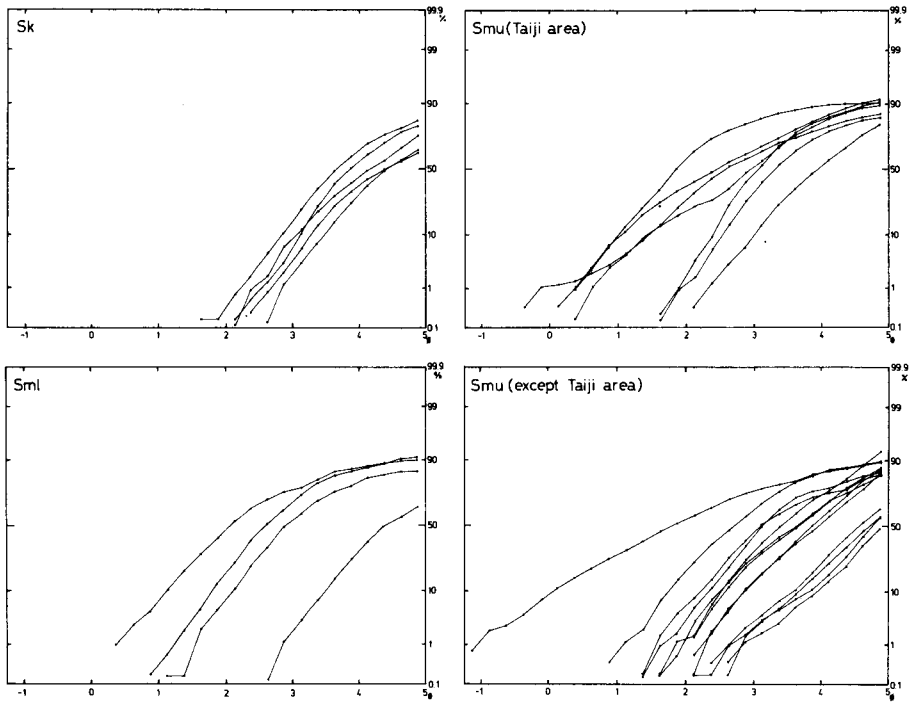

Fig. 23. Cumulative frequency curves of the grain-size distribution of sandstone and mudstone samples. The diagram in upper-right indicates the curves of smaple-5, -6, -7, -8, -9 and -24 in Table 10.

notable that only one-fourths of samples include grains coarser than medium-grained sand.

The cumulative frequency curves of most samples cannot be approximated by a single straight line which indicates the Gaussian distribution, except for five samples. The curves of most samples are divided into two parts. In most cases, the breakages of the two parts are between 3 and 4 phi. The coarser part (left half) of the curve is characterized by a steep gradient. The finer part (right half) of the curve is characterized by gentle gradient.

The characteristics of the grain-size distribution of the samples are summarized as follows:

(1) The abundance of finer-grained fraction (=matrix). This means the poor sorting of the grain-size distribution.

(2) The lack of the coarser-grained (coarser than about 2 phi) fraction and the good sorting of corser part of the distribution. This means the lack of the "surface creep population" of VISHER (1969).

B. Grain-size image

The grain-size image (PASSEGA and BYRAMJEE, 1969), which indicates the behavior of the coarsest fraction in sediments, was made based on the results of the grain-size analysis and those already reported by HISATOMI (1981). The C–M

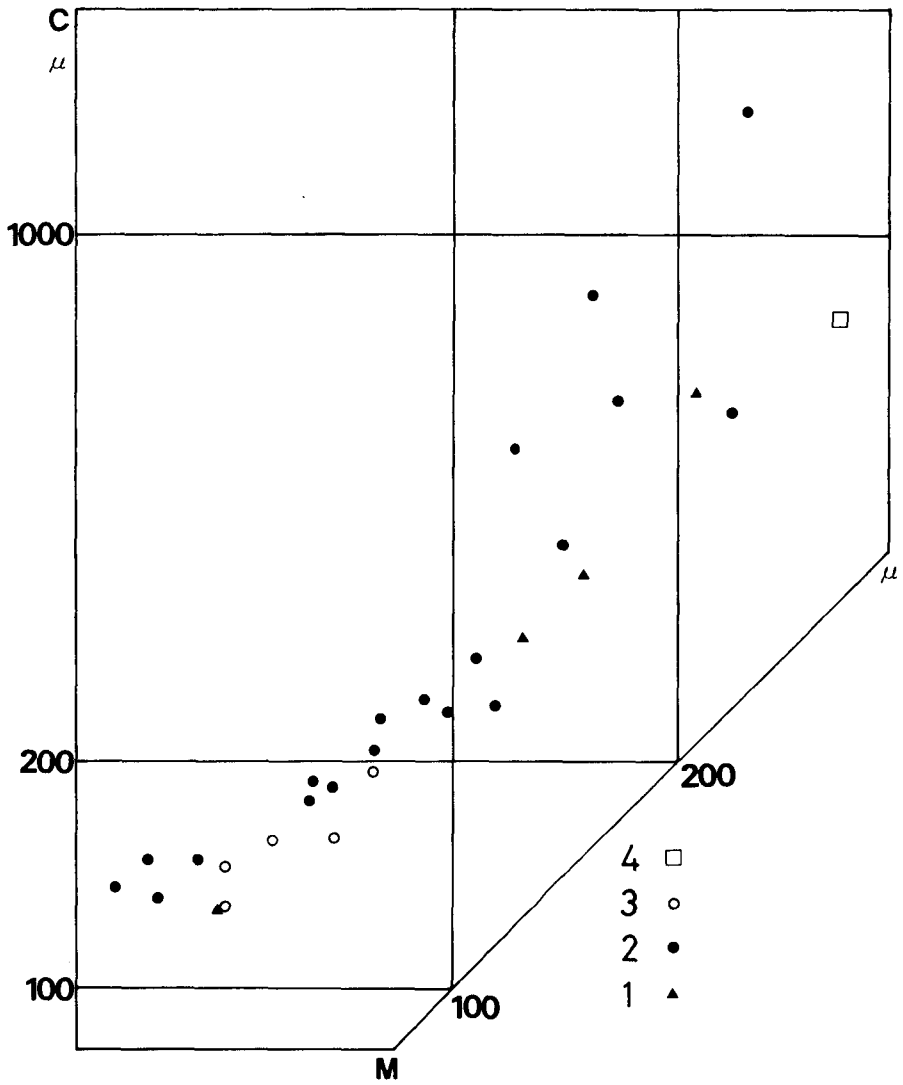

Fig. 24. C–M diagram of samples listed in Table 10. 1: samples from Member Sml, 2: samples from Member Smu, 3: samples from the Shikiya Formation, 4: sample from the Mitsuno Formation.

diagram, which is a constitutent of the grain-size image, is shown in Fig. 24. The characteristics of the grain-size image of the samples are as follows.

In C–M diagram, most of samples are arranged roughly along a straight line nearly parallel to the line C=M. In other words, this C–M pattern is composed almost only of the segment QR, which indicates the deposition from the graded suspension. It is notable that the segment PQ is not shown in this diagram. Adding to this, the one percentiles of samples are mostly less than 1,000 micron. It is concluded that the grain-size image show that these samples were deposited mainly from the graded suspension, and other mechanisms, such as the bottom traction, were not effective to the transportation of sediments.

C. Grain-orientation

The grain-orientation analysis was done on 15 thin sections of sandstone and 9 of mudstone samples. The purpose of the analysis was (i) to analyze the direction of the sediment-supply in the areas where no paleocurrent data are obtained by current marks or other sedimentary features, and (ii) to analyze the fabrics of sandstone. Concerning the first purpose, 9 samples were collected from the parallel laminated siltstone part of bedded mudstones in the Shikiya Formation.

On the analysis, the directions of apparent long axes of elongated grains (a*/b* is larger than 2) were measured under a microscope (100 magnifications) by the point-count method. Intervals of the mesh was set at 0.5 mm. The measured values were grouped into every 10°, and the mean vectors were calculated. The results are shown in Table 11 and also in Fig. 25.

Table 11. Results of the grain-orientation analysis. No: numbers of grains measured, L: magnitude of mean vector, P: confidence values.

Sample	Locality	Horizon	No.	L	P	Azimuth
1	Tanosaki	Sml1	152	21.5	0.0009	N30.8°W
2	Tanosaki	Sml1	162	31.9	0.0000	N 3.8°E
3	Tanosaki	Sml1	246	23.3	0.0000	N 5.9°E
4	Tanosaki	Sml1	213	22.1	0.0000	N11.1°W
5	Arida-SW	Sml2	265	16.7	0.0006	N19.7°W
6	Arida-SW	Sml2	145	40.5	0.0000	N14.6°E
7	Nishiki-N	Smu	110	18.8	0.0203	N44.8°W
8	Tozaki	Sk	113	34.4	0.0000	N 1.4°E
9	Nassa-SW	Sk	203	31.5	0.0000	N85.2°W
10	Yukawa-S	Sk	200	20.9	0.0002	N43.2°E
11	Omizuzaki	Sk	200	20.2	0.0003	N 8.3°W
12	Ishikiriiwa	Sk	152	15.3	0.0285	N70.2°E
13	Hashikui	Sk	168	40.2	0.0000	N22.6°W
14	Hime-S	Sk	200	35.7	0.0000	N18.7°E
15	Hime-E	Sk	160	40.5	0.0000	N79.1°E
16	Koza-S	Sk	150	39.8	0.0000	N82.2°W
17	Igushi-E	Sk	153	28.1	0.0000	N59.9°E

Grain-orientation

As shown in Table 11, the magnitude of mean vectors ranges from 15.3% to 40.5%. These patterns of the orientation can not be assigned to the random processes with more than 97% confidence. The imbrications of grains were not analyzed, because most of samples did not show any imbrications on the preliminary analysis.

Shimosato Formation: Mean vectors of most samples trend N–S or NW–SE in direction, and are both unimodal or bimodal.

Shikiya Formation: Five samples (Sp–9, –10, –15, –16 and –17) show the unimodal pattern, and trend ENE–WSW or NE–SW in direction. These samples stratigraphically correspond to the lower part of the Shikiya Formation. On the other hand, five samples (Sp–8, –11, –12, –13 and –14) show the unimodal or polymodal pattern, and have N–S trend in direction. These five samples were collected around Kushimoto where the coarse-grained facies are developed exceptionally in the Shikiya Formation, and paleocurrent directions from the north are dominated (see next Section).

Vertical change of the grain-orientation

The vertical change of the grain-orientation within a single bed was analyzed on two samples. Four and five thin sections were cut parallel to bedding planes of two fine- to very fine-grained sandstone parts of muddy alternation. Both samples consist of d-division, and show parallel lamination and grading. Fig. 25 shows the rose-diagrams of the grain-orientation of two samples.

As shown in figure, Sample–II shows a relatively distinct vertical change of the orientation patterns. The degree of the concentration* of grain-orientation is the highest in the middle part of the sample (thin section II–3). In the basal part (II–1 and –2), the degree of the concentration is slightly lower than in the middle part, but values of P keep the order of 10^{-2}. In the upper part (II–4 and –5), where the continuous parallel lamination gradually changes into the discontinuous lamination, the degree of the concentration is very low and at the order of 10^{-1}, changing the mode of the orientation to bi- (or poly-)modal pattern. These patterns of the orientation cannot be regarded as showing the reliable concentration. Moreover, the directions of mean vectors show the anticlockwise deviation at 10°–20° from those of the lower part.

On Sample–I, the highest degree of the concentration of the grain-orientation is observed at the middle and the lower middle part (thin sections I–2 and –3). The concentration in the lowest part (I–1) is lower than the above two. In the upper middle part (I–4), the degree of the concentration is 10^{-1}–10^{-2} lower than others.

* This is nearly the same with the magnitude of mean vector. However, because the numbers of measured grains are different for each section, the concentration is more accurately indicated by the significance value P, which is given by $[P=e^{-L/n}]$, where L is the magnitude of mean vector, and n is the number of grains measured (POTTER and PETTIJOHN, 1977).

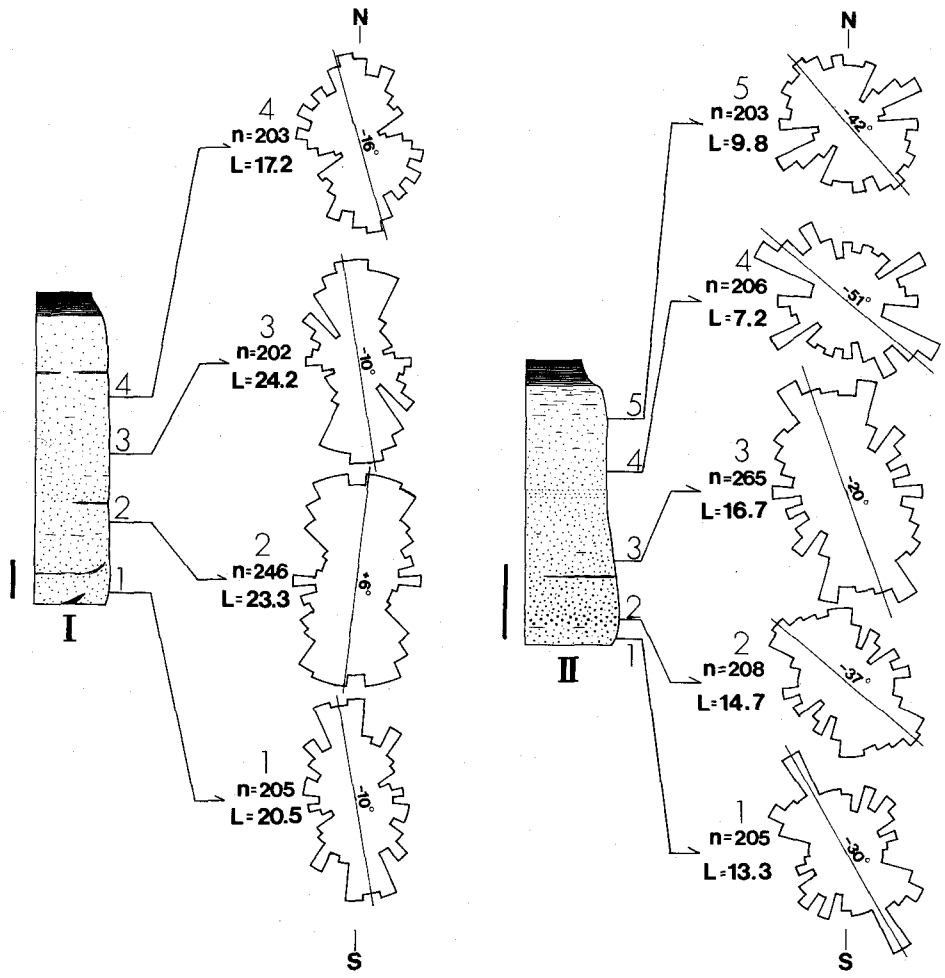

Fig. 25. Rose-diagrams showing the vertical change in the degree of the concentration of the grain-orientation. n: numbers of grains examined, L: magnitude of mean vector. Bars indicate 1 cm. Details are given in text.

Consequently, the mode of Sample–I can be regarded to be concordant with that of Sample–II, though the data of the uppermost part are absent.

It is pointed out that the mean azimuths of the grain-orientation of a single bed are roughly same as those of current marks.

4. Paleocurrent analysis and slump analysis

A. Paleocurrent analysis

Sole marks are poor in the Kumano Group. Moreover, the strata usually incline so gently that sole marks are usually concealed. To obtain more reliable data,

other kinds of the unidirectional features, such as ripple mark, cross lamination, convolute lamination, clast fabric and grain-orientation, were also used for the analysis. The paleocurrent directions after the tilt-correction are shown in Fig. 26A.

As a whole, all sedimentary features used in this study show nearly similar trend of paleocurrent directions, which indicate the sediment-supply from the northwest. The characteristics of paleocurrents in each formation are as follows:

Shimosato Formation

In the lower half of the formation (Members Sml and Smm), paleocurrent directions from the north or the northwest are inferred by all kinds of structures, and the paleocurrents from the northwest are most dominant. Paleocurrents from the east or the northeast and from the south-southeast are also observed, although they are few. The deviation of paleocurrent directions is smaller than that in other horizons.

The preferred directions of grain-orientations are all within the realm of the deviation of paleocurrent directions deduced from other structures mentioned above.

In Member Smu, the paleocurrent directions from the northwest and from the west are dominant, and those from the north are also deduced. The deviation of currents is larger than that in the lower horizons. The wide deviation of the paleocurrent can be assigned to the areal variation and not to the vertical one, as shown in Fig. 26B.

Shikiya Formation

Two kinds of paleocurrent directions are developed, namely, from the north or the northwest, and from the east or the northeast. The former is indicated by current sole marks, ripple mark and convolute lamination, and developed in the southwestern part of the study area (Fig. 26B), where the coarse-grained sediments are well developed, as mentioned already. On the contrary, the latter is observed as current top marks, such as flute and prod marks, and ripple mark mainly in the northeastern part of the area.

The trend of the preferred directions of the grain-orientation is similar to that of paleocurrent directions deduced from sole marks. That is, N–S trending grain-orientations are developed restrictedly in the southwestern part of the reported area. However, ENE–WSW trending grain-orientations can be observed in the lower to the middle part of the formation in the area where the coarse-grained sediments are not developed.

Mitsuno Formation

N–S trending paleocurrent directions are observed. However, the unidirectional features are very poor, presumably due to the shallow marine origin of deposits.

B. Slump analysis

Many slump structures are observed in the area. Most of them are classified as the "recumbent fold-shaped" subtype of YAMAUCHI (1977), and some are as the

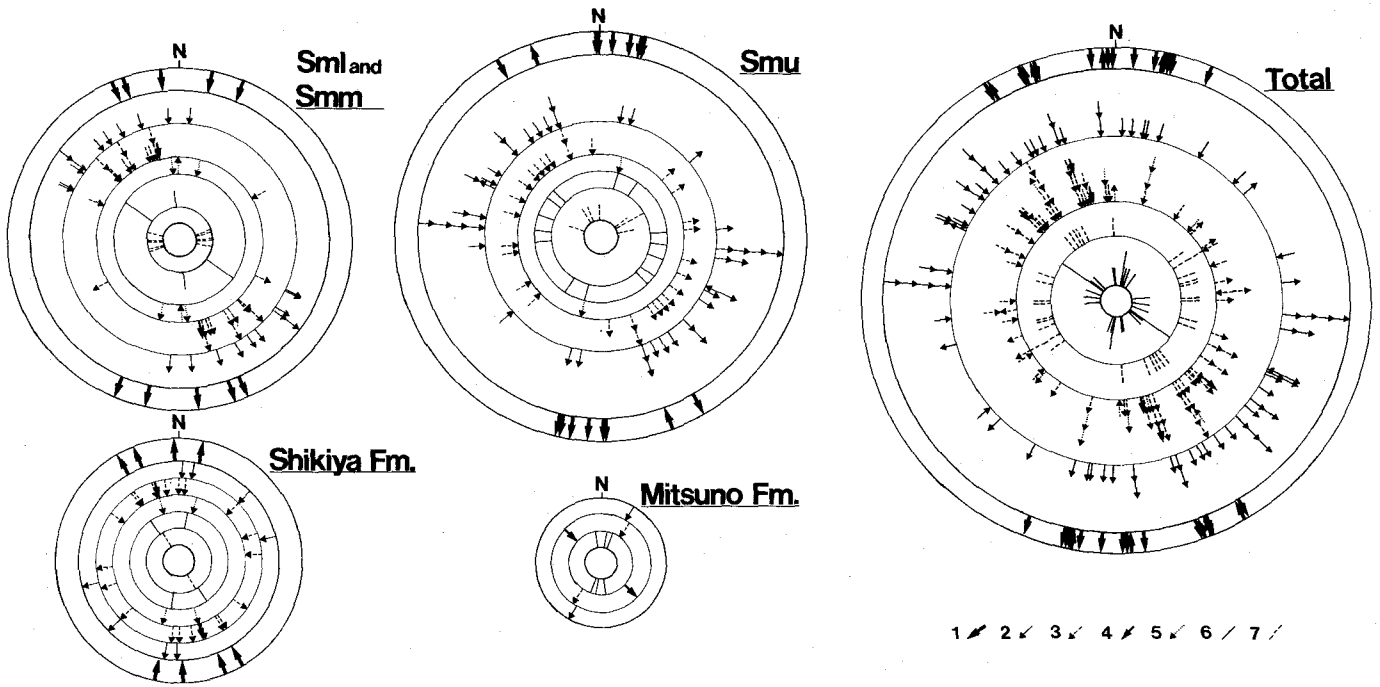

Fig. 26. A: Rose-diagram showing the paleocurrent directions. 1: paleoslope deduced from slump structure, 2: current marks, sense known, 3: ripple mark and cross lamination, 4: clast fabric of angular clast-bearing mudstone, 5: convolute lamination, 6: current marks, sense unknown, 7: parting lineation.

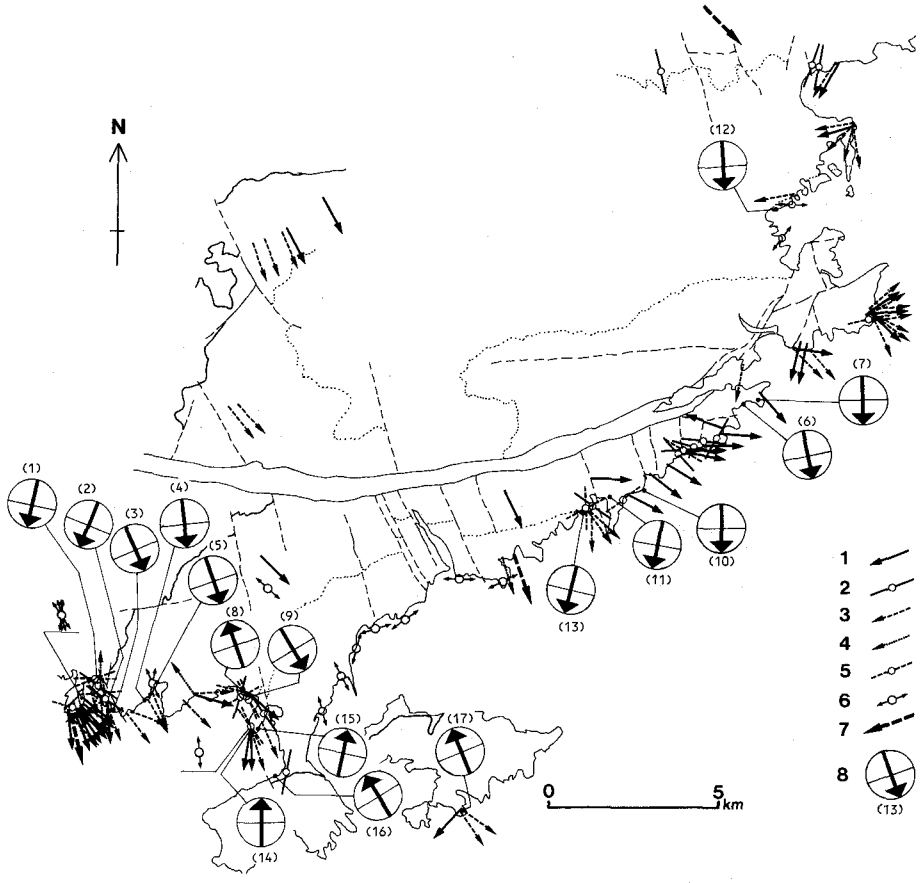

B: Paleocurrent and paleoslope direction. 1: current marks, sense known, 2: current marks, sense unknown, 3: ripple mark and cross lamination, 4: convolute lamination, 5: parting lineation, 6: mean azimuth of the grain-orientation, 7: clast fabric of angular clast-bearing mudstone, 8: paleoslope deduced from slump structures.

"fragment" type. Slump analysis was done on 17 slump sheets of the "recumbent fold-shaped" subtype. The slump sheets range stratigraphically from the lower part of the Shimosato Formation to the middle part of the Shikiya Formation (Fig. 27). The thickness of the sheets analyzed ranges from 0.2 to 40 m. The location of the slump sheets are shown in Fig. 26B.

In each sheet, the directions of hinge lines of the slump folds were measured. In most cases, hinge lines are plotted as cluster on the equal-area projection. Therefore, the directions of the dislocation of sheets were obtained by the mean axis method, and the sense of the dislocation was decided based on the asymmetry of slump folds in the field.

Most of hinge lines of slump sheets trend E–W, and the angle of hinge is low.

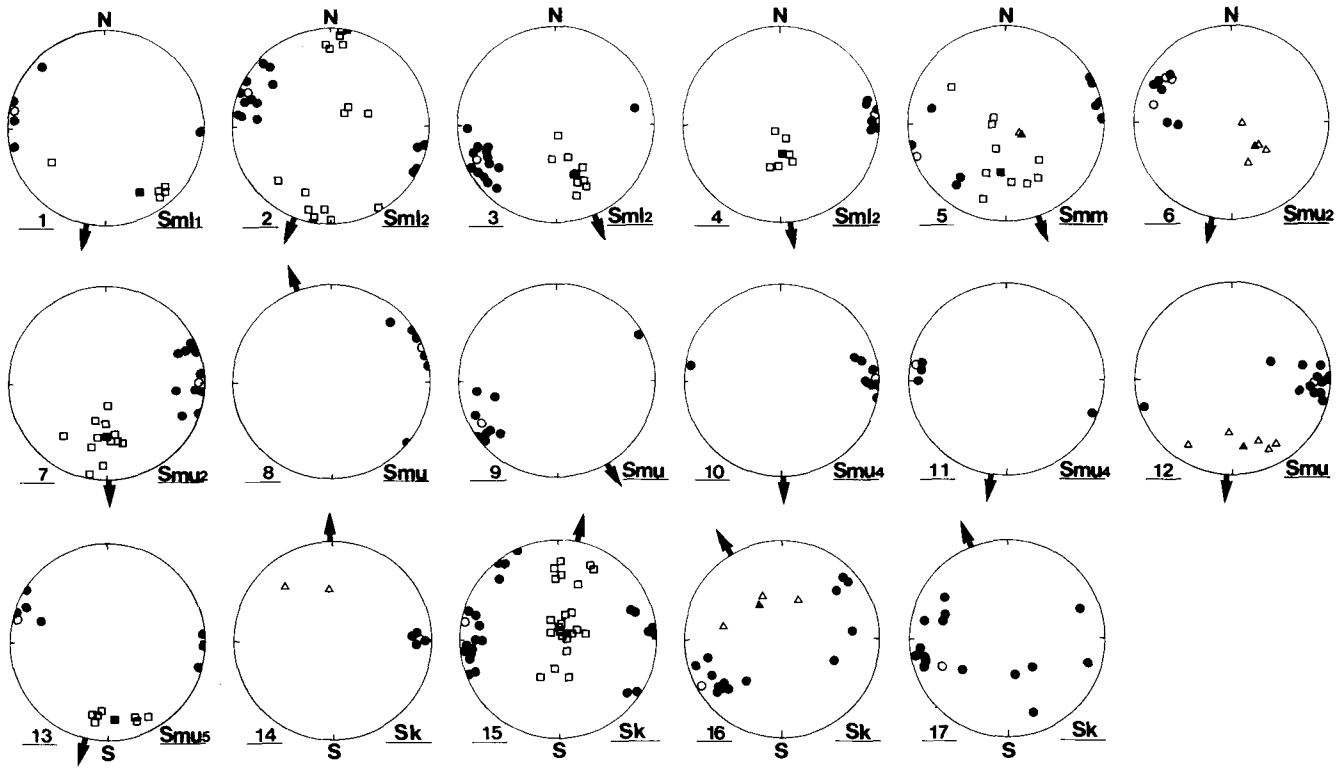

Fig. 27. Equal-area projections of hinge lines (solid circle), poles of axial planes of folds (open square) and poles of thrust planes (open triangle) in slump structures. Lower hemisphere. Open circle, solid square, and solid triangle represent the vector means. Locality of each slump sheet is shown in Fig. 26B.

The trend of the axial planes and slump thrusts are concordant with that of hinge lines (Fig. 27). Two kinds of the dislocation of slump sheets are indicated, namely, from the north and from the south.

In the Shimosato Formation, most of sheets indicate the dislocation from the north. Contrarily, one sheet developed at the southernmost part of the reported area (No. 8 in Fig. 27) indicates the dislocation from the south. The direction of the dislocation ranges from N35°W to N16°E.

In the Shikiya Formation, slump sheets indicate the dislocation from the south. The direction of the dislocation ranges from N36°W to N6°E, and is N16°W on an average. They are areally restricted in the southernmost part of the study area, and stratigraphically lie between the horizon 100 m and 600 m above the base of the formation.

Consequently, the dislocation from the south is restricted in the southernmost part of the area, and in the uppermost part of the Shimostato Formation and the lower part of the Shikiya Formation. On the contrary, the dislocation from the north can be observed extensively in the remaining area.

Based on the slump analysis, the Kumano sedimentary basin can be reconstructed as a southward-inclining slope in general, accompanied with a northward-inclining local slope in the southernmost part of the area (see HISATOMI, 1981).

Detailed descriptions of the slump sheet at Loc. 16 in Fig. 26B, which show northward-facing slope, were given by HISATOMI and MIYAKE (1981).

IV. Discussion

1. Transportation mechanisms and basin analysis

The clastic sediments in muddy alternation were classified into A1, A2, B1 and B2 types in the foregoing chapter (Table 9). In this chapter, the transportation mechanisms and the sedimentary environments will be discussed on the sediments based on the results described in the foregoing chapter.

A. Deposits showing the BOUMA sequence (type A beds)

This type occupies more than 85% of the total beds in number (Fig. 13). Even if excluding the beds consisting only of e-division, this type occupies about 70% of the total, as mentioned in Section III–1. Accordingly, they are the most important constituent of the group.

The sediments of this type are characterized by the following three points. Firstly, as shown in the Markov chain analysis and by the combinations of sedimentary divisions, excepting three beds, the beds of this type are represented by the BOUMA sequence. Secondly, more than 90% of this type beds are sharp-based, and the erosive features are common in the basal parts of beds. Thirdly, the grading is

observable in more than a half of the total beds with the naked eyes. These three characteristics are the essential ones of turbidite (BOUMA, 1962; SANDERS, 1965). Therefore, it is safely concluded that this type sediments were formed by turbidity currents.

The turbiditic origin of type A1 beds are also supported by the features in the grain-size distribution. Higher proportion of finer-grained materials (Fig. 23) and the coexistence of them with sand grains, both show that the grains did not suffer sorting so strongly during the transportation, and that grains and matrices were transported mixedly in turbulent flows.

This fact is also endorsed by the fact that the beds starting with a- or b-divisions are few at all localities analyzed (Fig. 13). Consequently, the ABC index (WALKER, 1967) of the sequences are very low (max. 20.6), suggesting that most of the beds of this type were deposited in lower flow regime.

Judging from those natures mentioned above, the turbiditic deposits in the area corresponds to the "classical distal turbidite" of WALKER and MUTTI (1973).

As mentioned already, the C–M diagram (Fig. 22) shows that most grains are considered to have deposited from graded suspension. PQ segment, which suggests the transportation of the coarsest fraction by "suspension and rolling*" of PASSEGA and BYRAMJEE (1969), is not developed in the diagram.

It is also supported by the cumulative frequency plots of the grain-size distribution (Fig. 23). The coarsest part cannot be distinguished from the major part. Theoretically, in flows of the same velocity, coarser grains are transported as the bed-load by rolling or saltation, rather than by suspension, and the gradient of curves should be more gentle, if grains transported as the bed-load were mixed with grains transported by suspension. By this reason, the transportation mechanism of the coarsest grains in each sample is safely assigned to have been suspension without the effective contribution of the bed-load transportation.

Another characteristic in grain-size distribution is the general absence of coarse grains. This tendency can be recognized throughout the study area, suggesting that turbidity currents were not so high in density.

The generation processes of turbidity currents have been discussed mainly based on the experimental studies (MIDDLETON, 1966a, b; HAMPTON, 1972). HAMPTON (1972) discussed the generation processes of turbidity current from debris flow. According to him, materials in debris flow were mixed with the surrounding water by erosion of materials from the front of flow and by the ejection of water into the flow. Consequently, turbidity currents are formed as a dilute turbulent cloud above and behind the debris flow.

---

* PASSEGA and BYRAMJEE (1969) did not mention about the role of saltation, however, "rolling" of them must include saltation.

The generation of turbidity current from denser gravity flow has been presented in the submarine fan models (WALKER and MUTTI, 1973; RICCI-LUCCHI, 1975; WALKER, 1978). In these models, the "classical distal turbidites" are regraded as the deposits in the area in outer fan or in basin plain. They are considered to have been deposited from dilute flows resulted from the deposition of coarser-grained sediments in the proximal area.

However, the dilution process stated above cannot be applied to turbidity currents in the case of the Kumano Group, because, firstly, there are no sandy or conglomeratic sediments in the proximal area of the study area, and secondly, the deposits which show the characteristics of grain flow and sandy debris flow deposits are not developed, and thirdly, the facies association of the submarine fan complex is not developed (HISATOMI, 1981).

As mentioned later, angular clast-bearing mudstones are supposed to have been formed by debris flow. However, sandy deposits are not accompanied with them. Moreover, even if the water is mixed into these debris flow, turbidites of such grain-size as described in Section III–3 cannot be formed, because angular clast-bearing mudstone lack in sand grains.

Accordingly, the clastic sediments of type A is considered to have been transported by the low density flow from its birth to deposition, and its supporting force of grains was formed only by the turbulence of flow. This kind of gravity flow can be called the "turbidity current *sensu stricto*".

Taking into account of the fact that there were no fan-channel complex in the Kumano Group, it can be concluded that the turbidity currents in the study area did not form a submarine fan-channel complex and that they flowed down on a slope not as channelized flows but as sheet-flows.

The site of the generation of the turbidity current is supposed to have been on the upper part of the continental slope adjacent to the margin of the continental shelf, as will be discussed later. This generation site is the most characteristic feature of turbidity currents of the Kumano Group.

The difference of the origin of types A1 and A2

Type A2 beds are distinguished from type A1 by the lack of division(s) in the middle part of bed. Among type A2 beds, about 85% of the total beds lack in d-division (upper parallel laminated division). As mentioned already, type A2 beds are predominant at Locs. 2, 7 and 11, occupying the majority of the sequence. They are variable in proportion in the other localities.

The lack of divisions can be explained by two processes. The one is due to the erosion by the other kind of flows after the initial deposition of turbidites, and the other one is resulted from non-deposition of the division. To consider the lack of d-division, it is necessary to clarify the deposition process of d-division. This has been discussed by many authors (PIPER, 1972; JACKSON, 1976), but has not been clarified fully.

It is highly possible that fine- to very fine-grained sandstone parts of turbidite lack in d-division at the initial deposition as stated below. According to MIDDLETON and SOUTHARD (1978), plane beds of lower flow regime tend to be not formed, and small scale ripples are formed, when the grain-size is finer than 0.7–0.8 mm. And for such grain-size, grains are not moved by the lower mean velocity (Fig. 28) which cannot form the small scale ripples. Among type A2 beds, there are beds which lack in b- or x- (, c- or w-) divisions, though not common. The lack of b- or x-divisions cannot be explained by erosion after deposition, because x- and/or d-divisions overlie them. So it is possible that the lack of divisions were generated by non-deposition of divisions.

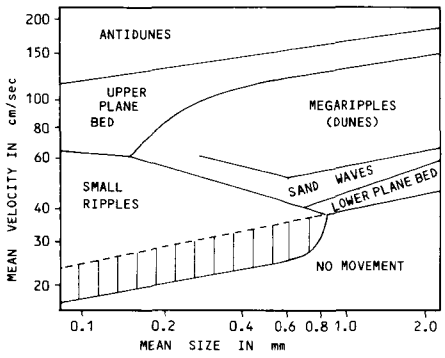

Fig. 28. Hydralic criteria for bed forms, based on the condition of mean velocity and mean grain-size. After MIDDLETON and SOUTHARD (1978).

However, the author prefers the erosion theory for the lack of d-division at Locs. 2, 7 and 11, judging from the following facts:

(1) The presence of E–W trending paleocurrent directions which oblique to the paleocurrent direction from the north or the northwest deduced from current sole marks in Loc. 2.

(2) The dominance of ripple marks on the top surfaces of sandstone part and the abundance of the sharp-topped sandstone parts in Loc. 7.

(3) The presence of E–W trending small scouring structure in bedded mudstone in unit Smu5 adjacent to Loc. 11 (Plate 3–3). This cannot be explained by the scouring of turbidity currents, because there are no sandy, coraser deposits there.

B. Deposits not showing the BOUMA sequence (Type B beds)

Type B beds occur at all localities, occupying less than 20% of the total beds in number at most localities, but at Locs. 1, 13 and 14, they occupy more than 30% of the total beds. Because type B1 and B2 beds do not coexist in one section, they are considered to be different in origin, and the two types will be discussed separately.

Type B1

Type B1 beds occur restrictedly in the lower to middle part of the Shikiya Formation (Locs. 13 and 14). The most significant features of type B1 which are distinct from types A1 and A2, are that the bottom surface of sandstone part is

generally gradual, and that the grain-size of coarser laminae increases upward in each sandstone part, suggesting the gradual increase of flow velocity. The reverse grading is commonly developed at the basal part of beds of conglomerate transported by dense gravity flows as mentioned by MIDDLETON and HAMPTON (1976). However, in fine-grained gravity flow deposits, reverse grading is usually not developed.

Type B1 beds are also characterized by their sharp top surfaces of sandstone part. The sharp top surfaces of sandstone part of type B1 can be formed by two processes. The one is the erosion and reworking of fine clastics at the upper part of sandstone part. And the other one is the rapid waning of flow containing a small amount of suspended fines.

Around 20 cm/s of flow velocity is needed at minimum to retransport very fine- to fine-grained sand, and in this case, small scale ripples will be formed as bedforms. The examples of this process can be observed at Loc. 7.

On the contrary, top surfaces of sandstone parts of type B1 beds are usually horizontal. The presence of reverse grading and the scarceness of ripples at the top surface of sandstone part implies that this type beds record the gradual decrease of flow velocity.

The fundamental difference of type B1 beds from type A beds suggests that type B1 beds are not turbiditic in origin. Type B1 beds were possibly formed by the flow of the normal bottom current fluctuating in flow velocity.

The paleocurrents from the east deduced from current top marks at Loc. 13, is nearly at right angle to the general trend (from N or NW) of sediment-supply by turbidity current, and is nearly parallel to the strike of the paleoslope deduced from slump structures. The both facts support the conclusion that the flow was not the gravity-induced flow.

As mentioned in Charpter III, the transition pattern of sedimentary divisions of type B1 forms a closed chain such as "p→x→d→e→p→". This tendency shows the distinctive contrast to that of type A, which does not form closed chains and is turminated at e-division. Transition pattern of type A can be well explained by the deposition from turbidity currents. On the other hand, closed chains of type B1 can be reasonably explained as in the followings.

In type B1 beds, e-division was deposited under the condition of the very low flow velocity, judging from the fine grain-size and the absence of sedimentary structures. Following to this state, p-division and then x-division were formed when the velocity of the flowing water gradually increased. Then, the flow velocity rapidly decreased, and d-division and then again e-division are formed. Consequently, the transition pattern formed a closed chain.

The bioturbation is strongly developed in all of e-division in type B1 beds (Plate 2–4). This feature is different from e-divisions in type A beds. This also supports the non-turbiditic origin of e-divisions in type B1 beds.

The ancient contourites have been reported in flysch sequences in the world (BOUMA, 1972; STOW and LOVELL, 1979). Type Bl beds are different from the features of these ancient contourites in relatively high proportion of matrix, degrees of sorting, the existence of the vertical order of sedimentary structures and so on (see Chapter Ⅲ). Therefore, it is concluded that the possibility of the ancient contourites for type Bl beds is very low.

According to SCHNEIDER *et al.* (1967), the sediment-laden ocean bottom currents, which is a kind of the contour current, is the fastest in the lower part of the continental rise (−3,500 m to −5,000 m in depth), and the velocity of this current ranges from 2 to 20 cm/s. The velocity of the ocean bottom current as fast as 22 cm/s was measured at the site (−5,000 m in depth) near Samoan Passage in Central Pacific (HOLLISTER *et al.*, 1974). These flow velocity is enough to produce type Bl beds. However, the paleodepth of the Kumano basin is estimated at upper bathyal depth, based on the benthonic fossils (MIZUNO, 1953; IKEBE *et al.*, 1975). This is also negative to consider type Bl beds as contourites.

The existence of subsurface cold water currents or the subsurface compensation currents of the surface water current in the Miocene sedimentary basins in Japan was discussed by CHINZEI (1982). Recently, TAIRA and TERAMOTO (1983) directly measured the velocity of the subsurface water current beneath the Kuroshio current at the continental slope area to the south of Shionomisaki. According to them, the the southwestward current with a velocity of maximum 20 cm/s was measured periodically. Then, it is highly possible that there existed the subsurface water current which was capable to transport very fine- to fine-sand grains periodically in Miocene age. The author prefers this explanation as the generating precess of type Bl beds, although the detailed and direct measurements of the water current system in the modern oceans are needed.

*Type B*2

Type B2 ("se" type) beds occur at various horizons except for Locs. 13, 14 and 15. They lack any sedimentary structures such as grading and laminations. They are distinguished from the "ae" type beds of turbidites by their fine grain-size and the lack of grading. So, this type beds cannot be regarded as "Tae" beds of BOUMA (1962).

The sedimentary structures developed in turbidite siltstone beds have been studied by PIPER (1972), STOW and SHANMUGAM (1980) and other authors. STOW and SHANMUGAM (1980) proposed a model for the sequence of internal sedimentary structures in turbidite silt-mud beds. According to them, massive part is not developed in siltstone layers, and developed only in the upper finer-grained mudstone part (this roughly corresponds to e-division). So, there are no supporting evidences of low density turbidite for type B2 beds.

Judging from fine grain-size, thin bed thickness and the lack of sedimentary

structures, it is probable that type B2 beds were formed under the lower energy levels, that is, the low-velocity water current, presumably bottom currents, but the flow mechanism cannot be concluded at present.

C. Angular clast-bearing mudstone

As mentioned already, angular clast-bearing mudstones do not occupy the significant volume of the Kumano Group. But they are very important to reconstruct the paleogeography of the Kumano basin.

As described in Chapter III, angular clast-bearing mudstones occur lenticularly and have limited distributions. The muddy conglomerates and pebbly mudstones of this kind have been reported in the various orogenic belts and have been assigned to be submarine debris flow deposits. Their flow mechanisms, however, had not long been clarified (CROWELL, 1957; DOTT, 1963). Recently, the supporting force of clasts in submarine debris flows have been assigned to the viscous strength of the clay-water mixture (JOHNSON, 1970; MIDDLETON and HAMPTON, 1976).

MIDDLETON and HAMPTON (1976) and HAMPTON (1975) provided the concept of the "bouldery submarine debris flow" based on the experimental studies and the comparison with subaerial debris flows. In the submarine debris flows, according to them, clays and water combine together to act as a single fluid, and the cohesion of fluid of clay-water mixture provide the major amount of support of clasts. The bouldery debris flow deposit is characterized by massive structure and floated solid clasts within muddy matrix. They are the essential features of angular clast-bearing mudstones in the Kumano Group. It is probable that angular clast-bearing mudstones are submarine debris flow deposits.

The abundance of muddy matrix, the matrix-supported clasts and the angularity of clasts show that clasts were not rounded during the dislocation of flows. These facts clearly shows that the dispersive pressure provided by the clast collision were not effective for the supporting force of clasts, and also suggest the debris flow origin of them.

The internal clast fabric of debris flow deposits has long been regarded as random due to high viscous resistance and cohesion of muddy matrix. Recently, however, the preferred orientation and imbrication have been revealed on angular clast-bearing mudstone of the Paleogene strata by detailed observations (HISATOMI *et al.*, 1980).

Angular clast-bearing mudstones in the study area also show the preferred orientation and imbrication of clasts as mentioned in Chapter III (Fig. 22). This fact implies that the solid clasts were able to move or rotate during the dislocation of debris flow against the viscosity and the cohesion of clay-water mitxures. This means the relatively low viscosity and cohesion of the clay-water mixture.

The competency of the clay-water mixture increases with the decrease of the

density difference between fluid and solid clasts, and also with the increase of the cohesion of fluid. Therefore, if the density of clast is low, the same competency can be provided by lower cohesion.

In the case of type I angular clast-bearing mudstone, clasts consist of mudstone and sandstone, some of which show the soft-sediment deformation (see Section III–2). It is suggested that the clasts were semi-consolidated and their density was relatively low. So, the debris flows could transport the clasts, though muddy matrix contained a considerable proportion of water and the cohesion of the clay-water mixture was relatively low.

It is concluded that the debris flow, which transported these angular clast-bearing mudstones to the study area, were relatively low in density, and the main supporting force of clasts was provided by the buoyancy as well as the cohesion of clay-water mixture. Type II angular clast-bearing mudstones are considered to be of similar origin, although the density of clasts cannot be estimated.

Angular clast-bearing mudstone body at Tsuga shows the distinctive features from others. It is clast-supported, and is poor in muddy matrix, and clasts are rounded in some degree. These facts indicate that the dispersive pressure of the clast collision provided at least a part of support of clasts. Judging from the strongly developed orientation and imbrication, and the stratification, calsts and matrix were under the condition of strong horizontal shear during the dislocation.

Submarine debris flow is a non-Newtonian fluid, and they have cohesion and internal friction. Therefore, the morphological hollow like channel is needed to maintain the flow. The existence of the morphological hollows are also suggested by the occurrence of Tanosaki body and also by the lenticular shape of angular clast-bearing mudstone bodies. It is supposed that debris flows flowed down with gullies or channels existed on the slope of the Kumano basin.

2. Reconstruction of the paleobasin

In this section, the author attempts to reconstruct the morphology and the sedimentary environments of the Kumano basin based on the sedimentological evidences described already. Firstly, the morphology of the basin will be discussed, and then the nature of flows, which was intimately related to the basin morphology.

A. Paleogeography

Paleogeography of the Kumano Group in the study area

The paleogeomorphology of the study area was reconstructed schematically as shown in Fig. 29 (HISATOMI, 1981). In the late Early Miocene, the area was situated on an E–W trending, southward-facing slope. The clastic sediments were deposited and dammed up in a slope-basin area, which was formed by an E–W trending upheaval zone stretching through the Shionomisaki area. The reconstruction of the

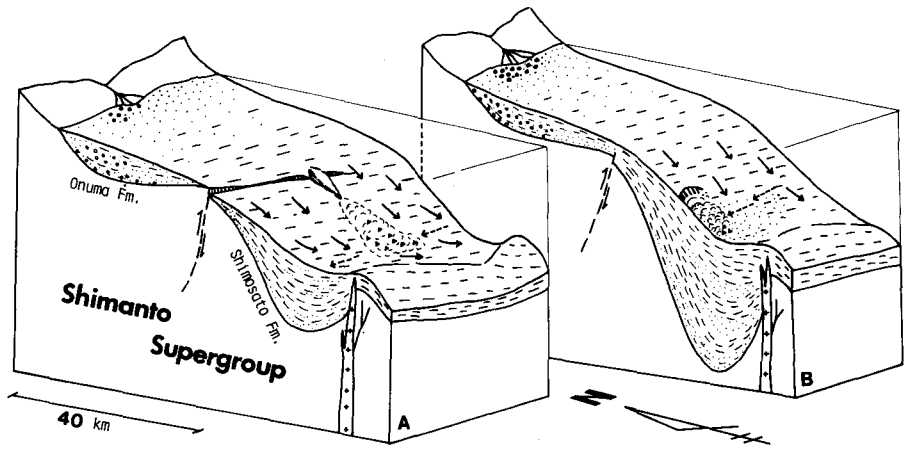

Fig. 29. Schematic reconstruction of the Kumano sedimentary basin at the end of the sedimentation of the Shimosato Formation. Solid arrows and broken arrows represent turbidity current and bottom water current, respectively. Modified from HISATOMI (1981).

basin was mainly based on the following evidences (HISATOMI, 1981).

(1) Most of paleocurrent directions deduced from current marks, ripple marks etc., indicate the supply from the north or northwest.

(2) Paleoslope deduced from slump analysis shows that the paleoslope dips to the south in the most part of the study area, and that the northward inclination is confined in the southernmost part of the area.

(3) The characteristic features of the slope or base-of-slope environments such as the constant paleocurrent direction, the development of slump structures and angular clast-bearing mudstone (STANLEY and UNRUG, 1972) are developed in the southernmost part of the study area.

The nature of the upheaval zone was discussed in detail especially on the genetic relation with the activity of the Shionomisaki Igneous Complex by HISATOMI and MIYAKE (1981) and this zone was named the "Shionomisaki Magmatism-Upheaval Zone (Shionomisaki Zone)".

The extension of the Shionomisaki Zone cannot be decided directly. Howerver, the strikes of northward-facing paleoslopes deduced from five slump sheets range from N57°E to N85°W, averaging in N74°E. Therefore, the Shionomisaki Zone is supposed to have had the trend of roughly ENE–WSW.

The bottom of the depression adjacent to the northern flank of the Shionomisaki Zone was narrow, unlike a wide depositional plain of the Kumano Deep Sea Terrace in the modern continental slope off Southwest Japan, because the paleocurrent directions from the north and dislocation of slump sheets are found very close to the

Shionomisaki Zone*.

Paleogeography of the Kumano Group

The depositional site of the Kumano Group in the study area which is situated in the southern area was a southward-facing slope in bathyal depth. On the other hand, the deposits in the northern and the central areas are supposed to have been formed in the shallow environments (CHIJIWA and TOMITA, 1981). In the followings, the relation in paleogeography of the above two will be discussed.

The Shikiya Formation and its northern equivalent, the Koguchi Formation, are distributed throughout the distribution area of the Kumano Group. On the contrary, the Shimosato Formation is limited in the southern area, and is not developed in the central area. In the northern area, the Onuma Formation is developed below the Koguchi Formation. The relation of the Shimosato and the Onuma Formation is schematically shown in Fig. 30.

The Onuma Formation is rich in coarse-grained sediments, such as conglomerate and sandstone, and is about 600 m thick (see Section II–1). According to SAEKI and KOTO (1972), the coarse sediments of the formation are supposed to have been de-

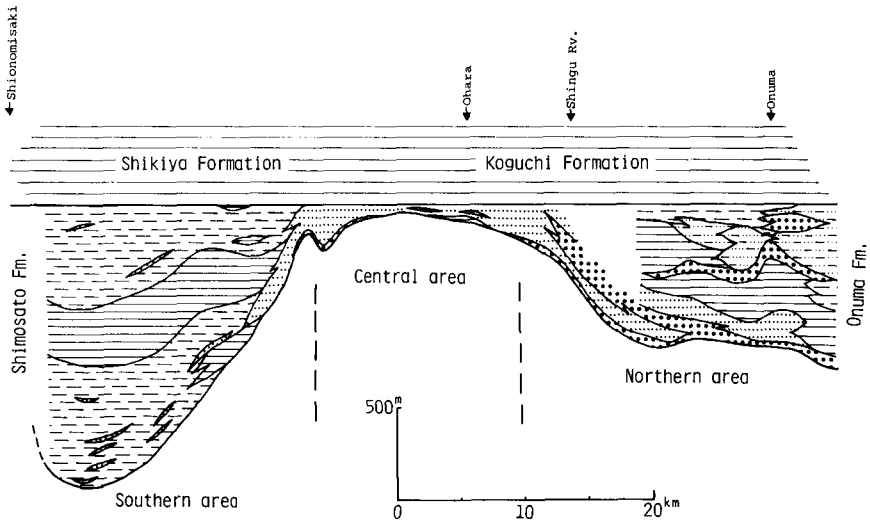

Fig. 30. Generalized stritigraphic profile of the Shimosato and the Onuma Formations in NNE–SSW section. In the central area, basal conglomerate-sandstone beds, which are included in the Koguchi Formation, are treated as the equivalent strata of the former two formations. Data from TATEISHI *et al.* (1979), SUZUKI *et al.* (1979), Report of METAL MINING AGENCY (1979) and HISATOMI (1981).

* Judging from the facts that the equivalent marine strata of the Kumano Group are developed in the present continetal slope area (OKUDA *et al.*, 1979) and in the area to the south of Nankai Trough (KARIG *et al.*, 1975), the upheaval zone was supposed to have been situated on the general southward-facing slope which reached to the deep sea area (see HISATOMI, 1981, P. 171), and analogous to the Outer Ridge of the present arc-trench system of Southwest Japan.

posited in the shallow sea. The neritic origin of the formation is also proved by benthonic molluscan fossils (MIZUNO, 1953). Contrarily, the paleodepth of the Shimosato Formation is estimated to have been deeper than 200 m based on the benthonic foraminiferal fossils (IKEBE *et al.*, 1975).

If the Shimosato Formation had been deposited in shelf environments shallower than 200 m, the angle of the slope should have been less than 3–4/1,000 (about 0.2°) using the distance of 60 km. This assumption is not acceptable. That is, the gradient of the slope, on which the Shimosato Formation was deposited, should have been steeper, judging from the frequent development of slump sheets and the existence of debris flow deposits. Thus, it is more reasonable to consider that the Onuma Formation is the neritic deposits, and the Shimosato Formation is its bathyal equivalent deposited on a slope.

In the central area, only the basal conglomerate-sandstone bed of 50 m thick underlies the mudstone of the Koguchi Formation. The central area must have been the area between the neritic and the bathyal environments. It is suitable to suppose the shelf edge as the site of the deposition where the thickness of deposits are very thin between the shelf and slope areas.

The Shimosato Formation and its equivalents are thinnest near the line between Oyadani and Ugui shown in Fig. 1. Thus, this line roughly marks the shelf edge. The occurrence of fossil bivalves of bathyneritic and hemibathyal facies at Narumigama (Fig. 1), which is about 5 km to the east-southeast of Oyadani, supports this conclusion.

The northern area of the Kumano Group was a subsiding area during the sedimentation, because there are thick neritic deposits. To take this into account, the shelf break area was a relatively upheaving area forming a basement-high, and was trapping the coarse clastics of the Onuma Formation.

In conclusion, the paleogeography and the environments of the Kumano Group discussed above is summarized as follows.

In the northern area of the present distribution of the Kumano Group, coarse clastic sediments were deposited in the neritic environments, being trapped by a basement-high of the shelf edge. In the southern area, clastics were deposited in a slope area between the basement-high of the shelf edge and the Shionomisaki upheaval zone of the trench-slope-break or the Outer Ridge. Terrigenous clastics spilt over the shelf break and flowed down on the slope and were dammed up by the Shionomisaki Zone to form a thick sequence of muddy sediments.

In the area to the south of the Shionomisaki Zone, "T formation", which is referred to as the equivalent strata of the Kumano Group, is developed in and beneath the present continental slope (OKUDA *et al.*, 1979). Thickness of the "T formation" is estimated at around 800 m. Judging from this, terrigenous clastics are supposed to have partly spilt over the Shionomisaki Zone, and deposited to the south of this

zone, though their volume was relatively small.

B. Sedimentation process on the slope

Here, the details of sediment flows on the paleoslope are discussed to reconstruct the sedimentation processes in the Kumano sedimentary basin.

Turbidity current

Judging from the paleocurrent system and paleoslopes described in Section III–4, most of turbidity currents, which deposited type A sediments, flowed down on the slope normally or obliquely to the strike of the slope. These clastic sediments must have been derived from the shelf area to the north. Two different processes can explain the spillover process of the terrigenous clastics from the shelf area to the bathyal slope area, that is, (1) entrapment of bed-load moving on shelf by a submarine canyon incised into the shelf (In this case, clastics are transported into submarine fan area, bypassing the shelf edge), (2) accumulation of clastic sediments at the shelf edge by a shelf sand stream (SOUTHARD and STANLEY, 1976), and consequent downflowing of clastics into the slope area by sediment gravity flows. In this case, clastics are transported across the shelf edge.

As mentioned in Sections III–3 and IV–1, turbidity currents of the Kumano Group are characterized by the absence of the non-Newtonian nature of flows. Furthermore, HISATOMI (1981) emphasized that the development of the submarine fan-cahnnel complex could not be expected for the Kumano Group in the study area on the basis of the lithology, the association of sedimentary facies and the paleocurrent system.

The possibility (1) is easily rejected from these facts and thus spillover of the clastics into the slope area must be accomplished by process (2). The most suitable mechanism of the dislocation of sediments on the shelf is the effect of the storm-agitation which affects deeper part of the ocean water than the fair-whether wave action.

In this manner, fine-grained sediments were transported to the shelf edge, and they flowed down from their temporal sites of deposition into the slope area as turbidity currents. So, the generation sites of turbidity currents are concluded to have been at the shelf break area or its neighbouring area on the slope, and they did not flow through the submarine canyons.

The characteristic natures of turbidity currents of the Kumano Group — the absence of non-Newtonian nature, the wide variation of the combination of sedimentary divisions, the general lack of coarser grains and so on — must be deeply connected with the generation process, the generation sites and their forms like sheet-flow deposits. It shows a clear contrast to the fan-turbidites exemplified by many sandy flysch sequences in the world.

Subsurface water current

As stated in Chapter III, the paleocurrent directions of the subsurface water currents are nearly parallel to the strike of the paleoslope. And the thickness of sandstone part of each bed is very thin, and grains are mostly fine. These facts suggest that the capacity of the transportation of these water currents were small. Therefore, it is difficult to regard these water currents as the main transportation currents of clastics from shallower shelf region into the deeper region. Probably the clastic materials were transported down on the slope also by turbidity currents, and then water currents retransported them along the strike of the paleoslope.

The existence of subsurface water current in Miocene age is discussed by CHINZEI (1982). According to him, subsurface cold water currents (Oyashio Senryu) were present during the early Middle Miocene (Fig. 31). This was proposed mainly based on the occurrence of the offshore water association of fossil bivalves such as *Portlandia tokunagai, P. watasei, Malletia inermis* etc. These fossils have been reported in the late Early to Middle Miocene Ichishi and the Morozaki Groups, both distributed to the northeast of the Kumano Group. And *Portlandia tokunagai* and other bivalve fossils of eurythermal cold water facies have been reported from the Kumano Group by MIZUNO (1953, 1957).

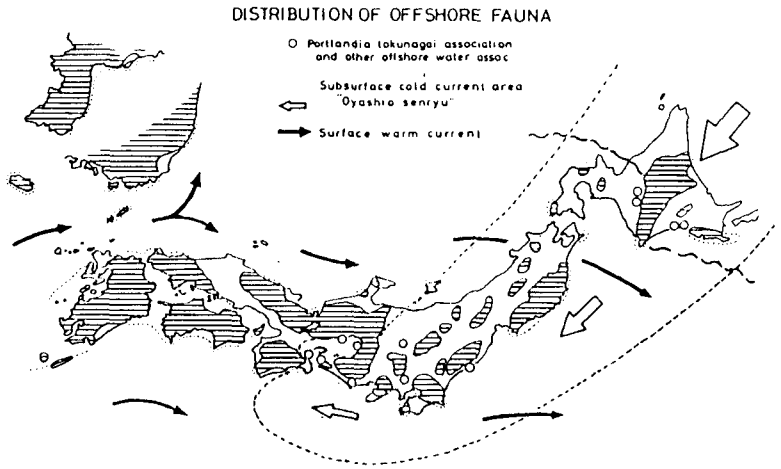

Fig. 31. Distribution of offshore fauna and the supposed "Oyashio Senryu" in the Nishikurosawa Age (late Early to early Middle Miocene). After CHINZEI (1982).

Moreover, the direction of the supposed subsurface water current is similar to the paleocurrent directions of type B1. Accordingly, it is possible that the subsurface cold water was flowing into the Kumano basin.

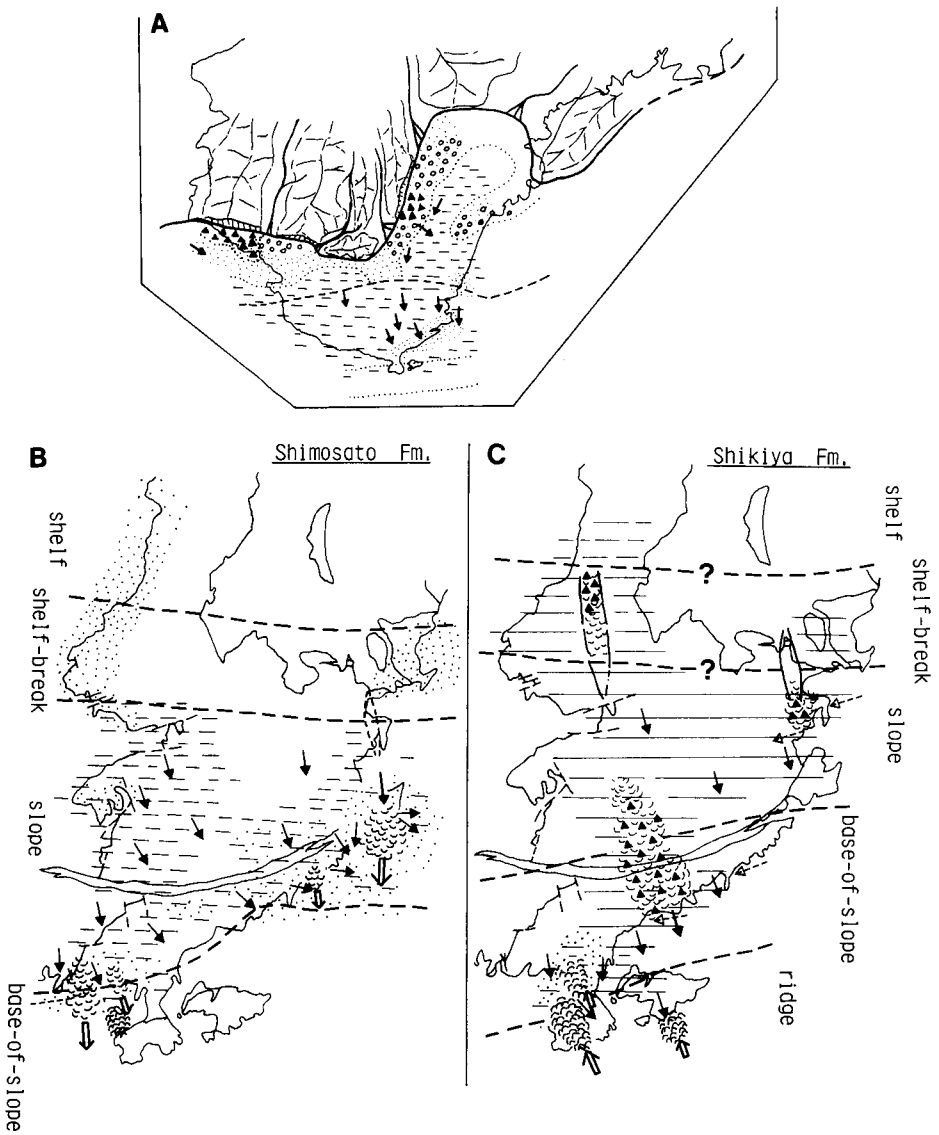

Fig. 32. A: Paleogeography of the southern part of the Kii Peninsula in the Early to Middle Miocene. The reconstruction of the Tanabe basin is based on the unpublished data of Tanabe RESEARCH Group.
B & C: Paleogeographic reconstruction of the Kumano sedimentary basin in the southern area at the stage of the Shimosato (B) and the Shikiya (C) Formations. Solid arrows and broken arrows represent turbidity current and bottom water current, respcetively.

The velocity of the subsurface cold water current called Oyashio Senryu is not apparent, but is supposed to have been rather small. However, the velocity of the subsurface water current flowed into the Kumano basin probably increased after the Bernoulli's Law in the basal part of the slope where the narrow depressional morphology was formed between the southward facing slope and the Shionomisaki Zone, as mentioned already. So it is reasonable to consider that type B1 beds may have been formed by the ancient subsurface cold water current.

Debris flow

As mentioned in Chapter III, clasts in type II angular clast-bearing mudstones, being derived from the Muro Group, are angular in shape and large in size (max. 4 m in length). In the lower part of the Shikiya Formation, in which most of these angular clast-bearing mudstones are developed, monotonous mudstone is developed throughout the distribution area of the Kumano Group. If the clasts have been derived from the land area to the far north, they would have been transported for tens of kilometers across the shelf where monotonous muds were distributed throughout. This assumption is not acceptable. Instead, it is probable that angular clasts were formed at the exposures of the basement rocks uplifted above the sea bottom by active faults around the shelf edge, where the substrata were very thin (Fig. 30). Clasts are supposed to have rushed into the surrounding muds by rock-falls, and have mixed together, forming debris flows, then they flowed down on the slope adjoining to the south. By this process, angular and boulder-sized clasts derived from the Muro Group could be supplied into the study area.

The generation of debris flows might be in close relation with the activity of the upheaval of the basement-high at the shelf edge and also with the brisk subsidence of the Shimosato Formation.

The paleogeography and the sedimentary processes of the Kumano Group in the study area are illustrated schematically in Fig. 32.

V Summary

The Kumano Group in the study area consists mostly of thick piles of fine-grained clastic rocks, such as muddy alternation, bedded mudstone, and angular clast-bearing mudstone. Most of the materials are concluded to have been transported by a low density turbidity current on the basis of the following evidences.

(1) The individual beds of muddy alternation are usually thin and mud-sand ratio is large. Among two types of bedding, namely, the graded type and the non-graded type, the former is much more predominant than the latter, and sole marks are found at various horizons.

(2) Nine sedimentary divisions are recognized in the individual beds. The combination of divisions show that most of the beds have BOUMA sequence of turbidites.

(3) Most clastic grains were transported in the state of graded suspension as judged from the CM diagram, and the high admixture of muddy particles and sandy particles is suggested by the grain-size distribution on log-probability curve.

Concerning the basin morphology in the study area, the Kumano Group have been supposedly formed on the slope and slope-basin bordered on the south by the upheaval zone. This is deduced from the following evidences.

(1) The southward paleocurrent governed the most part of the area and the eastward paleocurrent was limited to the narrow zone trending E–W in the southern marginal area.

(2) The structural analysis on slump folds and debris-flow deposits indicate the southward-inclining paleoslope in the main part, and the northward-inclining slope is supposed only in the southernmost part where the syndepositional magmatic activity took place.

The geomorphological setting of the whole Kumano basin is considered to be comparable to the present fore-arc setting in Southwest Japan by the reasons of the following facts.

(1) The Kumano Group in the northern part is characterized by shelf-facies lithology and fossils, and that of the southern part were deposited on the slope and slope-basin as clarified in the present study.

(2) The Kumano Group in the central part between the northern and southern parts is much thinner in thickness than that of the other two areas. This may reflect the upheaval of the shelf-edge area.

The low-density turbidity current which transported the fine clastic materials was generated at the shelf-edge or shelf-slope transition area, and not a diluted current from high-density current, considering the fact that there is no channel and submarine-fan sediments throughout the Kumano basin.

Some beds have characteristic sedimentary structures made by tractional current flowing to the west. They were the products of the cold-water bottom currents as deduced from paleontological evidences in the Early Miocene age.

Acknowledgements

The author wishes to thank the members of the Research Group on Geosyncline and Sedimentation of Department of Geology and Mineralogy of Kyoto University. The author cordially thanks Prof. Keiji Nakazawa of Kyoto Univ. for his helpful guidance. Special thanks are due to Dr. Takao Tokuoka of Shimane Univ., Dr. Tsunemasa Shiki of Kyoto Univ., and Prof. Tetsuro Harata of Wakayama Univ. for their suggestions and encouragements. Special gratitude is also due to Dr. Yasuyuki Miyake of Kyoto Univ. for his kind advice and discussions. The author thanks Messers. Hisao Tsutsumi and Kinzo Yoshida of Kyoto Univ. for their preparing

many thin-sections to examine grain-size and grain fabrics.

References

ARAMAKI, S. and HADA, S. (1965)*: Geology of the central and southern parts of the igneous complex (Kumano Acidic Rocks) in the southeastern Kii Peninsula. *Jour. Geol. Soc. Japan,* **71**, pp. 494–512.

ALLEN, J. R. L. (1968): *Current Ripples.* North-Holland Publ. Co., Amsterdam, 433 p.

BOUMA, A. H. (1962): *Sedimentology of some flysch depoists — A graphic approach to facies interpretation.* Elsevier Sci. Publ. Co., Amsterdam, 168 p.

——— (1972): Fossil contourites in Lower Niesenflysch, Switzerland. *Jour. Sedi. Petrol.,* **42**, pp. 917–921.

CHIJIWA, K. and TOMITA, S. (1981): Stratigraphic notes on the Kumano Group (A study of the Tertiary formations of the Kumano Coalfield in the Kii Peninsula, Southwest Japan, Part 1). *Memoirs Fac. Sci., Kyushu Univ., (D),* **24**, pp. 155–178.

CHINZEI, K. (1982)**: The oceanic-biostratigraphy in the Nishikurosawa Stage viewed from the bivalvian fossil assemblage. *Problems on the Nishikurosawa Age* (Pre-prints for 89th Annual Meeting of Geol. Soc. Japan), pp. 70–71.

CROWELL, J. C. (1957): Origin of pebbly mudstones. *Bull. Geol. Soc. Amer.,* **68**, pp. 993–1010.

DOTT, R. H. Jr. (1963): Dynamics of subaqueous gravity depositional processes. *Amer. Assoc. Petrol. Geologists, Bull.,* **47**, pp. 104–128.

FRIEDMAN, G. M. (1958): Determination of sieve-size distribution from thin-section data for sedimentary petrological studies. *Jour. Geol.,* **66**, pp. 394–416.

HAMPTON, M. A. (1972): The role of subaqueous debris flow in generating turbidity currents. *Jour. Sedi. Petrol.,* **42**, pp. 775–793.

——— (1975): Competence of fine-grained debris flow. *Jour. Sedi. Petrol.,* **45**, pp. 834–844.

HATENASHI RESEARCH GROUP (1980)*: The Otonashigawa Belt of the Shimanto Terrain in the Kii Peninsula —The stratigraphy and geologic structure—. *Memoirs Fac. Educ., Wakayama Univ., Nat. Sci.,* **29**, pp. 33–70.

HATTORI, I. (1976): Entropy in Markov chains and discrimination of cyclic patterns in lithologic successions. *Math. Geol.,* **8**, pp. 477–497.

HILDE, T. W. C., WAGEMAN, J. M. and HAMMOND, W. T. (1969): The structure of Tosa terrace and Nankai Trough off Southwest Japan. *Deep-sea Res.,* **16**, pp. 67–75.

HIROKAWA, O. and MIZUNO, A. (1965)*: *Explanatory text of the geological map of Japan "Kushimoto" (scale* 1/50,000). Geol. Surv. Japan, 25 p.

HISATOMI, K. (1981)*: Geology and sedimentology of the Kumano Group in the southeastern part of the Kumano Basin, Kii Peninsula. *Jour. Geol. Soc. Japan,* **87**, pp. 157–174.

———, ISHIGAMI, T., NAKAYA, S., SAKAMOTO, T., SUZUKI, H. and TATEISHI, M. (1980)*: Sedimentation of the "Sarashikubi beds" (olistostrome beds) in the Muro Group, Southwest Japan. *Earth Sci.,* **34**, pp. 73–91.

——— and MIYAKE, Y. (1981)*: Upheaval movement and igneous activity in the Shionomisaki area, Kii Peninsula, Southwest Japan. *Jour. Geol. Soc. Japan,* **87**, pp. 629–639.

HOLLISTER C. D., JOHNSON, D. A. and LONSDALE, P. E. (1974): Current-controlled abyssal sedimentation: Samoan Passage, equatorial West Pacific. *Jour. Geol.,* **82**, pp. 275–300.

IKEBE, N., CHIJI, M. and MOROZUMI, Y. (1975)*: *Lepidocyclina* horizon in the Miocene Kumano Group in reference to planktonic foraminiferal biostratigraphy. *Bull. Osaka Museum of Natural History,* **29**, pp. 81–89.

JACKSON, R. G. (1976): Sedimentological and fluid-dynamic implications of the turbulent bursting phenomenon in geophysical flows. *Jour. Fluid Mech.,* **77**, part 3, pp. 531–560.

JOHNSON, A. M. (1970): *Physical Processes in Geology.* Freeman Sci. Publ. Co., San Francisco, 577 p.

KARIG, D. E. *et al.* (1975): *Initial Reports of the Deep Sea Drilling Project, Vol.* 31. U. S. Government Printing Office, Washington D. C., 927p.

KAWANO, Y. and UEDA, Y. (1964)*: K–Ar dating on the igneous rocks in Japan. I. *Jour. Japan Assoc. Min. Petrol. Econ. Geol.*, **51**, pp. 127–148.

KISHU SHIMANTO RESEARCH GROUP (1975)*: The development of the Shimanto geosyncline. *Monograph Assoc. Geol. Collabor. Japan*, **19**, pp. 143–156.

MATSUSHITA, S. (1971)**: *Regional geology of Japan, "Kinki district"*. Asakura Publ. Co., Tokyo, 289p.

METAL MINING AGENCY (1979)**: *Reports of the geological survey of the Nachi district"*. Metal Mining Agency, 74p.

MIALL, A. D. (1973): Markov chain analysis applied to an ancient alluvial plain succession. *Sedimentology*, **20**, pp. 347–364.

MIDDLETON, G. V. (1966a): Experiments on density and turbidity currents, I. Motion of the head. *Can. Jour. Earth Sci.*, **3**, pp. 523–546.

——— (1966b): Experiments on density and turbidity currents, II. Uniform flow of density currents. *Ibid.*, **3**, pp. 627–637.

——— and HAMPTON, M. A. (1976): Subaqueous sediment transport and deposition by sediment gravity flows. *In* D. J. STANLEY and D. J. P. SWIFT (ed.), *Marine sediment transport and evironmental management*, Wiley Intersci. Publ., New York, pp. 197–218.

——— and Southard, J. B. (1978): Mechanics of sediment movement. *Soc. Econ. Paleont. Mineral., Short Cource notes*, **3**, 246p.

MIYAKE, Y. (1981)*: Geology and Petrology of the Shionomisaki Igneous Complex, Wakayama Prefecture, Japan. *Jour. Geol. Soc. Japan*, **87**, pp. 383–403.

MIZUNO, A. (1953): Notes on the Miocene molluscs from the Kumano Group in the southeastern *Kii* Peninsula, Japan, with descriptions of three new species. *Trans. Proc. Paleont. Soc. Japan, N.S.*, **9**, pp. 9–18.

——— (1957)*: *Explanatory text of the geological map of Japan "Nachi" (scale* 1/50,000). Geol. Surv. Japan, 37p.

——— and Imai, K. (1964)*: *Explanatory text of the geologic map of Japan "Tanami" (scale* 1/50,000). Geol. Surv. Japan, 27p.

MURAYAMA, M. (1954)*: *Explanatory text of the Geologic map of Japan "Shingu and Atawa" (scale* 1/50,000). Geol. surv. Japan, 27p.

NISHIMURA, A. and MIYAKE, Y. (1973)**: Occurrence of Lepidocyclina, Miogypsina from the Kumano Group. *Postprint for the Symposium on the Shimanto Geosyncline*, pp. 37–38.

OKUDA, Y., KUMAGAI, M. and TAMAKI, K. (1979)*: Tectonic development of the continental slope and its peripheral area off Southwest Japan in relation to sedimentary sequence in sedimentary basins. *Jour. Japan Assoc. Petrol. Technologists*, **44**, pp. 279–290.

OSBORNE, R. H. (1971): The American Upper Ordovician standard XIV: Markov analysis of typical Cincinnatian sedimentation, Hamilton County, Ohio. *Jour. Sedi. Petrol.*, **41**, pp. 444–449.

PASSEGA, R. and BYRAMJEE, R. (1969): Grain-size image of clastic deposits, *Sedimentology*, **13**, pp. 233–252.

PIPER D. J. W. (1972): Turbidite origin of some laminated mudstone. *Geol. Mag.*, **109**, pp. 115–126.

POTTER, P. E. and PETTIJOHN, F. J. (1977): *Paleocurrents and basin analysis, Second Ed.* Springer-Verlag, New York, 460p.

RICCI-LUCCHI, F. (1975): Depositional cycles in two turbidite formations of northern Apennines (Italy). *Jour. Sedi. Petrol.*, **45**, pp. 3–43.

SAEKI, H. and KOTO, J. (1972)*: Geology and ore deposits of the central Kii Peninsula. *Jour. Soc. Mining Geol. Japan*, **22**, pp. 437–447.

SANDERS, J. E. (1965): Primary sedimentary structures formed by turbidity currents and related resedimentation mechanisms. *In* G. V. MIDDLETON (ed.), *Primary sedimentary structures and their hydrodynamic interpretation*, Soc. Econ. Paleont. Mineral., Spec. Publ., **12**, pp. 192–219.

SASAKI, Y. (1981MS)**: On foraminiferal fossils from the Asso Mudstone Beds, Tanabe Group in the area from Mori Harbour to the northern bank of Tonda River in Tanabe City, Wakayama Prefecture. Unpublished graduate thesis, Wakayama Univ., 34 p.

SCHNEIDER, E. D., FOX, P. J., HOLLISTER, C. D., NEEDHAM, H. D. and HEEZEN, B. C. (1967): Further evidence of contour currents in the western North Atlantic. *Earth Planet. Sci. Letters*, **2**, pp. 351–359.

SHIBATA, H. (1962): Chemical composition of Japanese granitic rocks in regard to petrographic provinces, part X — petrographic provinces. *Sci. Rep. Tokyo Kyoiku Diagaku, Ser. G*, **8**, pp. 33–47.

SHINAGAWA, Y. (1958MS): Cenozoic rocks in Tanabe district. unpublished master thesis, Kyot Univ., 97 p.

SOUTHARD, J. B. and STANLEY, D. J. (1976): Shelf-break processes and sedimentarion, *In* D. J. Stanley and D. J. P. Swift (ed.), *Marine sediment transport and environmental management*, pp. 351–378.

STANLEY, D. J. and UNRUG, R. (1972): Submarine channel deposits, fluxoturbidites and other indicators of slope and base-of-slope environments in modern and ancient marine basins, *In* J. K. RIGBY and K. HAMBLIN (ed.), *Recognition of ancient sedimentary environments*, Soc. Econ. Paleont. Mineral., Spec. Publ., **16**, pp. 287–340.

STOW, D. A. V. and LOVELL, J. P. B. (1979): Contourites: Their recognition in modern and ancient sediments. *Earth Sci. Rev.*, **14**, pp. 251–291.

——— and SHANMUGAM, G. (1980): Sequence of structures in fine-grained turbidites: comparison of recent deep-sea and ancient flysch sediments. *Sedi. Geol.*, **25**, pp. 23–42.

SUZUKI, H., HARATA, T., ISHIGAMI, T., KUMON, F., SAKAMOTO, T., TATEISHI, M., TOKUOKA, T. and INOUCHI, Y. (1979)*: *Geology of the Kurisugawa district.* Quadrangle series, scale 1/50,000, Geol. Surv. Japan, 54 p.

TAIRA, K. and TERAMOTO, T. (1983)**: Long-period-measurement of deep flows in the eastern part of Izu-Ogasawara Trench. *Special Project Research, The Ocaen Chracteristics and their Changes, News Letter*, **10**, pp. 3–9.

TANAI, T. and MIZUNO, A. (1954)*: Geological structure in the vicinity of the Kumano Coal Field in southeastern Kii Peninsula. *Jour. Geol. Soc. Japan*, **60**, pp. 28–39.

TATEISHI, M., BESSHO, T., HARATA, T., HISATOMI, K., INOUCHI, Y., ISHIGAMI, T., KUMON, F., NAKAYA, S., SAKAMOTO, T., SUZUKI, H. and TOKUOKA, T. (1979)*: *Geology of the Esumi district*, Quadrangle seires, scale 1/50,000, Geol. Surv. Japan, 65 p.

TERAI, K. and TANABE RESEARCH GROUP (1982)**: Study on the Tanabe Group, Kii Peninsula (part 1) —Stratigraphy and geologic structure—, *Abstract for 89th Annu. Meet., Geol. Soc. Japan*, p. 184.

TOKUOKA, T., HARATA, T., INOUCHI, Y., ISHIGAMI, T., KIMURA, K., KUMON, F., NAKAJO, K., NAKAYA, S., SAKAMOTO, T., SUZUKI, H. and TANIGUCHI, J. (1981)*: *Geology of Ryujin district.* Quadrangle series, scale 1/50,000, Geol. Surv. Japan, 69 p.

VISHER, G. S. (1969): Grain-size distributions and depositional processes. *Jour. Sedi. Petrol.*, **39**, pp. 1074–1106.

WALKER, R. G. (1965): The origin and significance of the internal sedimentary structures of turbidites. *Proc. Yorkshire Geol. Soc.*, **35**, pp. 1–32.

——— (1967): Turbidite sedimentary structures and their relationship to proximal and distal depositional environments. *Jour. Sedi. Petrol.*, **37**, pp. 25–43.

——— (1978): Deep-water sandstone facies and ancient submarine fans: models for explanation for stratigraphic traps. *Bull. Petrol. Geol.*, **62**, pp. 932–966.

——— and MUTTI, E. (1973): Turbidite facies and facies associations. *Soc. Econ. Paleont. Mineral., Pacific Sect., Short Course Notes*, pp. 119–157.

YAMAUCHI, S. (1977):*: On the slump structures in the Miocene series of the Chichibu basin, central Japan. Part I, Morphology. *Jour. Geol. Soc. Japan.* **83**, pp. 475–489.

*: In Japanese with English abstract.

**: In Japanese.

Arafunezaki	荒船崎	Arida	有田	Azumame	東雨
Hashikui	橋杭	Hidakagawa	日高川	Hime	姫
Ichinono	市野々	Igushi	伊串	Ikeshima	池島
Ishikiriiwa	石切岩	Itaya	板屋	Kandorizaki	梶取崎
Kii	紀伊	Koguchi	小口	Kotachi	河立
Koza	古座	Kumano	熊野	Kushimoto	串本
Meizu	目津	Miminohana	耳ノ鼻	Mitsuno	三津野
Muro	牟婁	Narumigawa	成見川	Nassa	夏山
Nishiki	二色	Okatsuura	大勝浦	Onuma	大沼
Otonashigawa	音無川	Oyadani	親谷	Sabiura	錆浦
Shikiya	敷屋	Shimanto	四万十	Shimosato	下里
Shimotawara	下田原	Shionomisaki	潮岬	Taiji	太地
Takahama	高浜	Takatomi	高富	Takinohai	滝ノ拝
Tanabe	田辺	Tanami	田並	Tanosaki	田の崎
Tawara	田原	Tenma	天満	Tozaki	砥崎
Tsuga	津荷	Uematsu	植松	Ugui	宇久井
Yamade	山手	Yamamibana	山見鼻	Yukawa	湯川

Explanations of Plates

Plate–1

1. Bedded mudstone and muddy alternation. Clastic dikes are intruded into bedded mudstone. Lower part of unit Sml1 of Member Sml, at Tanosaki.
2. Muddy alternation. The thickness of a sandstone part at upper right is about 40 cm. Middle part of unit Sml1 of Member Sml, at Tanosaki.
3. Muddy alternation. Note the sharp top surfaces of sandstone parts. Unit Smu2 of Member Smu, at the south of Kandorizaki.
4. Bedded mudstone intercalating thin sandstone parts. Member Smu of the Shimosato Formation, at the south of Takatomi.

Plate–2

1. Muddy alternation. Member Smu of the Shimosato Formation, at the northeast of Takinohai.
2. A slump sheet (No. 7 in Fig. 27) developed in muddy alternation. Unit Smu 2 of Member Smu, at Miminohana.
3. Bedded mudstone intercalating thin sandstone parts. Lowest part of the Shikiya Formation, at the north of Tozaki.
4. Muddy alternation. Lower part of the Shikiya Formation, at Okatsuura (Loc. 13 in Chapter III).

Plate–3

1. A bed showing the "abde" sequence of sedimentary divisions. The thickness of the sandstone part is 11 cm. Unit Sml1 of Member Sml, at Tanosaki.
2. A sandstone part showing the ripple-drift cross lamination. Lowest part of the Shikiya Formation, at Tozaki.
3. A small scale channel structure developed in bedded mudstone. Unit Smu 5 of Member Smu, at the southeast of Shimotawara.
4. Ripple cross lamination developed in a thin sandstone part. Lower part of the Shikiya Formation, at Ishikiriiwa.

Plate–4

1. Occurrence of angular clast-bearing mudstone. Lower part of unit Sml1, at Tanosaki.
2. Occurrence of angular clast-bearing mudstone. Lower part of the Shikiya Formation, at Okatsuura.
3. Occurrence of the lower massive part of the angular clast-bearing mudstone body developed at Tsuga. Lower part of the Shikiya Formation.
4. Interbedded angular clast-bearing mudstone part, sandstone part and mudstone part. Upper part of the angular clast-bearing mudstone body at Tsuga.

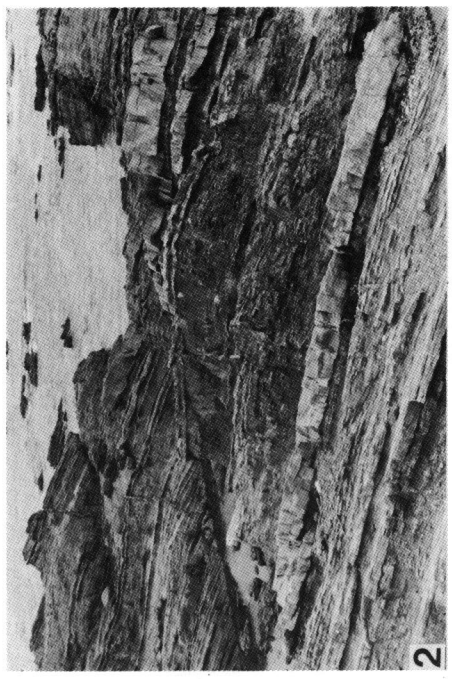

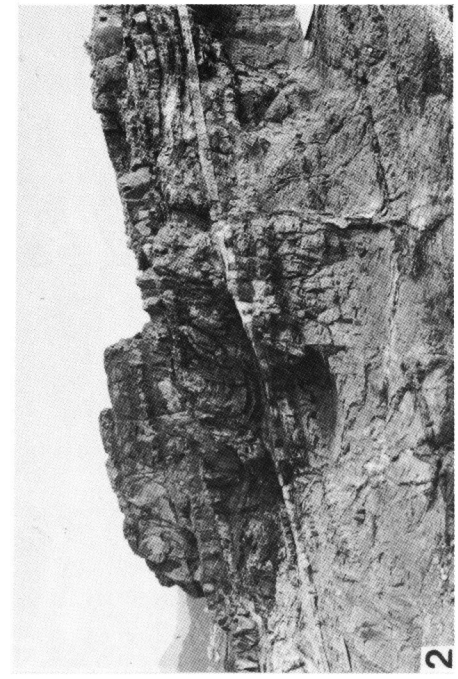
2


4

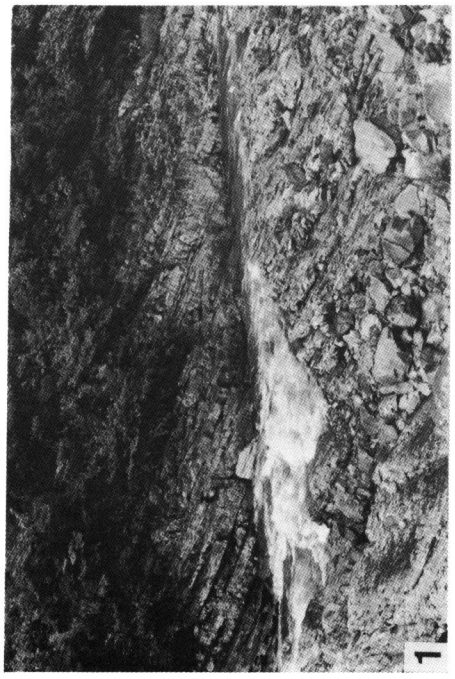
1


3

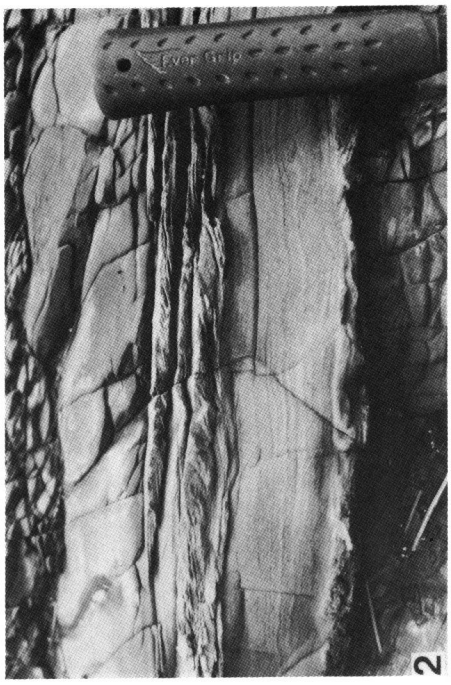
2


4


1

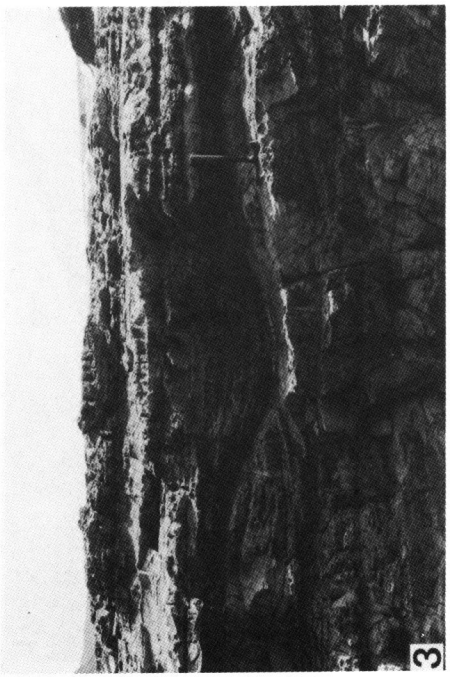
3

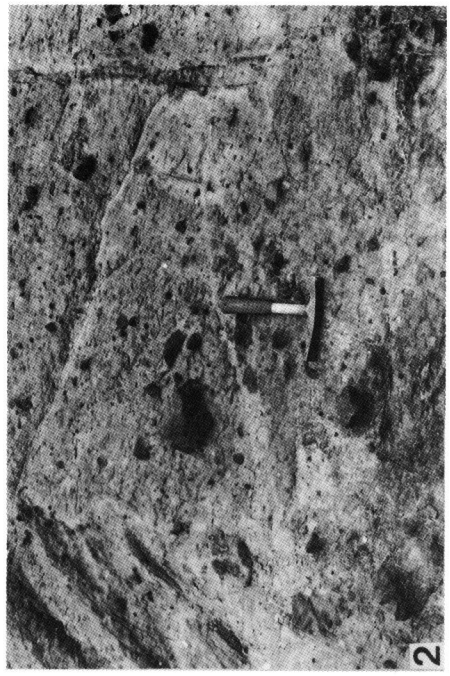
2

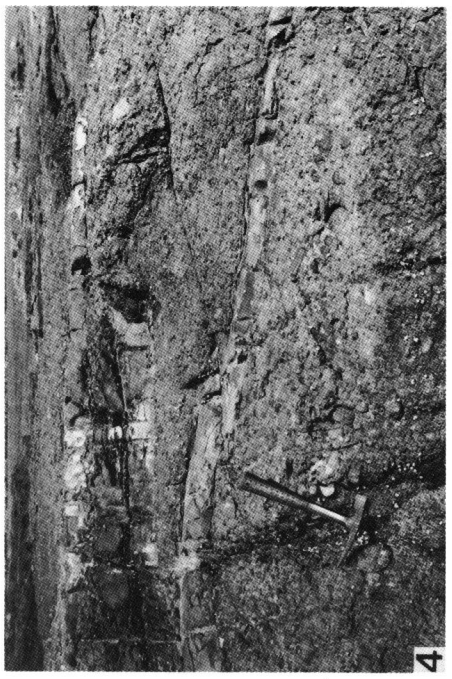
4


1


3